ANALYSIS OF REMAINING LIFE FOR RUNWAY 17R-35L AND TAXIWAY L AT DALLAS/FORT WORTH INTERNATIONAL AIRPORT

Michael T. McNerney, B. Frank McCullough, Kenneth H. Stokoe, W. James Wilde, James Bay, and James Lee

Research Report Number ARC-702

VOLUME II FINAL REPORT

Prepared in cooperation with the

CENTER FOR TRANSPORTATION RESEARCH
Bureau of Engineering Research
THE UNIVERSITY OF TEXAS AT AUSTIN

by the

AVIATION RESEARCH CENTER
A Division of the Center for Transportation Research
The University of Texas at Austin
3208 Red River, Suite 200
Austin, Texas 78705-2605
Phone: 512/232-3140 • FAX: 512/232-3151

August 1997

PREFACE

This report is the second of three volumes of the report prepared by The University of Texas at Austin, Center for Transportation Research to document the research project to evaluate the remaining life of the primary runway and adjacent taxiway at Dallas Fort Worth International Airport. Volume I, Executive Summary is a stand alone document to describe the testing developed and results of the field and laboratory testing undertaken for this research project. The Executive Summary also provides the conclusions reached that there is a concrete fatigue problem evident in the keel section of both the runway and taxiway. Volume II, Final Report is the complete description of the findings of the research study. Volume III, Data Appendices is a complete listing of the data gathered during this study. In addition, to the printed reports, a MicroStation CAD file was delivered to the Airport with all nearly all the distress data and deflection profiles provided in a geographic format.

TABLE OF CONTENTS

CHAPTER 5. FIELD TESTING—ANALYSIS AND RESULTS

CHAPTER 6. LABORATORY TESTING—ANALYSIS AND RESULTS

CHAPTER 7. CONCLUSIONS ON REMAINING LIFE OF RUNWAY 17R/35L AND TAXIWAY L

CHAPTER 1. INTRODUCTION AND BACKGROUND

This report is the second of three volumes of the report prepared by The University of Texas at Austin, Center for Transportation Research to document the research project to evaluate the remaining life of the primary runway and adjacent taxiway at Dallas/Fort Worth International Airport. Volume I, Executive Summary is a stand alone document to describe the testing developed and results of the field and laboratory testing undertaken for this research project. The Executive Summary also provides the conclusions reached that there is a concrete fatigue problem evident in the keel section of both the runway and taxiway. Volume II, Final Report is the complete description of the findings of the research study. Volume III, Data Appendices is a complete listing of the data gathered during this study. In addition, to the printed reports, a MicroStation CAD file was delivered to the Airport with all nearly all the distress data and deflection profiles provided in a geographically correct format.

DESCRIPTION OF THE PROBLEM

Dallas/Fort Worth (DFW) International Airport is the second busiest airport in the world with over 800,000 aircraft operations annually on the six runways that were operation when this study began. DFW began operational service in 1974 as a origin-destination airport serving the DFW metropolitan area. After airline deregulation, DFW became a large hub airport for American, Delta and Braniff Airlines. The initial runway design was for a 20-year life based upon the projected aircraft origin and destination operations growth pattern. In addition to the fact that these runways have already exceeded their 20-year design life, aircraft operations on them have far exceeded design projections due to hubbing operations.

The problem is that the cost of rehabilitating a runway is a significant investment both in direct cost of reconstruction and indirect costs as a result of aircraft delays. Therefore, the precise forecasting of when a runway will require reconstruction can result in a significant savings by delaying the reconstruction as long as possible without accumulating unexpected runway shutdowns and major maintenance problems.

Another central tenet of the problem is that the science of defining and forecasting pavement failure is not an exact science and that the variability of pavement materials can make precise forecasting extremely difficult. Traditional methods of forecasting the time for reconstructing airfield pavements have relied upon a system developed for the United States Air Force for justifying the prioritization of maintenance budgets among different Air Force Bases. The Pavement Condition Index (PCI) was developed for the Air Force and later endorsed by the FAA as a repeatable method of measuring surface distress of airfield pavements. The PAVER and

MicroPAVER software endorsed by the FAA is based upon a principle of pavement life as measured in the decline of the PCI over time. Essentially, the prevailing theory is that when PCI reaches a terminal value of 50 to 70 it is time to reconstruct the runway.

The premise of this research project is that the PCI simply measures surface distress which is only one of five potential failure mechanisms possible at the DFW airport. Research by the FAA in pavement technology has lagged far behind the research in pavement technology in the highway sector. The problem which this research study attempts to solve is to use new pavement technology to forecast the remaining life of Runway 17R and Taxiway L for all five potential failure modes (surface profile roughness, surface condition, subsurface deterioration, concrete fatigue, and joint deterioration)

BACKGROUND INFORMATION

In 1988, the DFW airport contracted with Harding Lawson Associates to develop a pavement management system and conduct a 100 percent survey of the existing pavement conditions for the airside pavements. The study concluded in 1990 and provided a Pavement Condition Index for all airfield pavements. The major distress noted in the pavement survey was predominately low severity patching. Based upon this high density of patching distress, they predicted that the primary runways and taxiways would require full width reconstruction by 1995.

AVIATION RESEARCH CENTER OF THE UNIVERSITY OF TEXAS AT AUSTIN

The University of Texas at Austin established the Center for Transportation Research (CTR) in 1963 and has been a national leader in highway pavement technology and research. Dr. B. Frank McCullough has been a professor at the University since 1969 and has been the Director of CTR Research since 1986. Dr. McCullough has specialized in highway and airport pavement research and was a consultant in the design of the original DFW runway and taxiway pavements.

In 1995 The Aviation Research Center was formed as a division of the Center for Transportation Research specializing in airport research. The Aviation Research Center (ARC) has research projects with Dallas Fort Worth International Airport, the Federal Aviation Administration, Department of Energy, and TxDOT Aviation Division. The Center also conducts annual short courses in Airport Pavements, Airport Noise, Airport Planning and Airport Modeling.

COOPERATIVE RESEARCH AGREEMENT

The Center for Transportation Research has had a cooperative research agreement with the Texas Department of Transportation for many years which resulted an excellent working relationship and multiple research projects totaling over $6 million per year. A cooperative research

agreement was developed between the Dallas Fort Worth International Airport Board and The University of Texas at Austin to serve as the Master Agreement for future research projects. DFW Airport suggested this study as the first research project under this cooperative research agreement. A research proposal was submitted to the DFW Airport in November 1994 and a project was awarded in June 1995. Dr. Michael McNerney served as the principal investigator for the University of Texas and Mr. Darryl Boyd served as the Project Director for DFW Airport.

RESEARCH OBJECTIVES

The objectives of this research project are to analyze the past pavement evaluation data and current pavement condition to determine from testing when Taxiway L and Runway 17R-35L are most probably required to be removed from active service and have reconstruction started. After the most probable failure modes are identified, the pavement life predictors are evaluated, and the deterioration rates computed, a comprehensive analysis of the probabilities of failure will be conducted. The end result will be prediction of the remaining pavement life.

Although not included in this project, a logical follow on to this project would be to determine the best rehabilitation, maintenance, and reconstruction strategies for these and other airport pavements taking into account the failure analysis and the cost of disruption to aircraft traffic.

PROJECT SCOPE

The scope of this project is limited to an 11,400-ft. section of Runway 17R-35L (this does not include recent 2000-ft. extension) and 11,700 ft. of Taxiway L (formerly K in the Harding Lawson Study). This research project conducted an analysis of the data in the pavement condition database maintained at DFW. Both statistical and analytical analyses of the data were proposed. The statistical analysis by itself and in combination with the analytical analysis are used to develop functional and structural performance relations for the various pavement sections represented in the database. Analyses will be conducted to determine the effect of multi-wheel loads on the pavements. Subsequently, an analysis can be made to determine the performance predicted for the material, thickness, loads and volumes of traffic that have been applied to the various pavement sections.

An essential part of this study involved conducting both destructive and non-destructive testing. A testing plan was developed by the CTR (Center for Transportation Research) team and submitted to the DFW team for review and approval. The field testing program was conducted to verify past test results, provide data to document changes, and make available data from new tests. The testing conducted included the following:

- Rolling Dynamic Deflectometer (non-destructive)
- Heavy Falling Weight Deflectometer (HWD) testing (non-destructive)
- Core extraction from the pavements (destructive)
- Cross-hole Seismic Analysis in some core holes
- Shelby Tube extraction of subsurface materials
- Measurement of Runway Profile for roughness analysis (non-destructive)
- Distress survey with PCI (Pavement Condition Index) Survey review

One new test that was conducted was the Rolling Dynamic Deflectometer. Equipment for this test includes a large truck that functions as a reaction mass. The system applies a surcharge of up to 60,000 lb. on a dual tire, single axle load configuration. Up to a 30,000 lb. peak dynamic load can be cycled within the range of the 60,000 lb. surcharge. With the load applied, the truck travels at one ft. per second and a continuous pavement deflection profile is recorded.

Thickness is a significant factor in pavement evaluation and performance. The most direct way of determining pavement thickness is to measure cores taken from the pavement. Cores were obtained in both strong and weak areas as indicated by the deflection profile. The cores were tested for indirect tensile strength and fatigue from both in and out of traffic areas.

Non-destructive tests were conducted using the heavy weight deflectometer (HWD). Pavement condition surveys were conducted to verify distress identifications and recent video distress surveys. Additional limited sample surveys were conducted to identify the level of fatigue cracking present on the runway and taxiway.

CHAPTER 2. ANALYSIS OF EXISTING PAVEMENT DATA

REVIEW OF PAVEMENT CONDITION SURVEY DATA

During 1990, Harding Lawson conducted a pavement condition index survey of runways and taxiways of DFW Airport. Provided to CTR were the MicroStation CAD files of the Runway 17R and Taxiway L, the Harding Lawson report with appendices and a photocopy of the data sheets used to record the distresses on each concrete slab. Also provided to CTR was access to the videotapes of the distresses recorded in a video equipped van in 1994 by a consultant. The video system provides a 12 ft. path longitudinally down the runway/taxiway and requires special equipment to locate a specific section of the runway or taxiway.

Joint Spalling

At the DFW airport there is a considerable amount of spalling along the longitudinal joints. Most of this distress was observed to be less than 2 ft. in length and very shallow. The typical maintenance repair procedure is to saw out a 2 ft. by 3-inch area a few inches deep and replace with patching materials as shown in Figure 2.1.

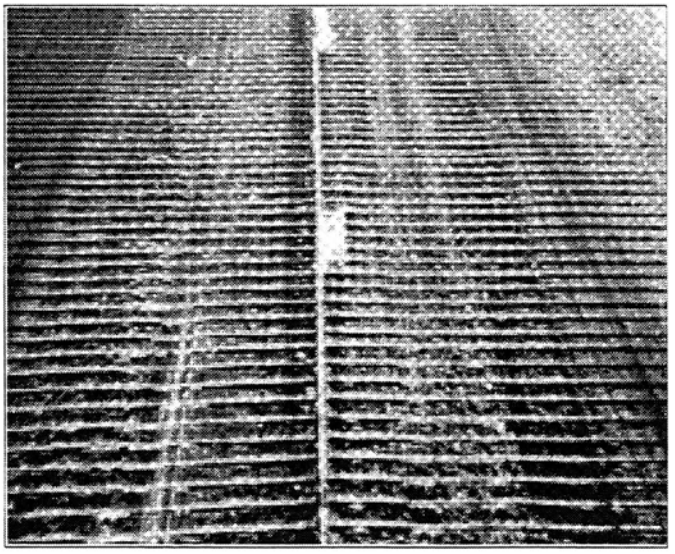

Figure 2.1 Patching of Joint Spalling

The FAA Advisory Circular AC150/5380-6 and ASTM D5340-93 both indicate that joint spalls of under 2 ft. in length are not counted as distress if the spall is not broken into pieces. If the broken pieces are removed leaving frayed edges less than 2 ft. in length, according to the PCI method there is no distress. If the pieces are still in place or the spall is greater than 2 ft. in length, it is counted as a joint spall.

However, if the joint spall is repaired with a patch, it becomes patching distress, even if it is less than 2 ft. in length. This leads to an anomaly in the PCI method, whereby a good

maintenance practice of patching actually increases the level of distress on the pavement as calculated by the PCI method. The actual deduction for patching and joint spalling depends upon the percent of slabs in the sample (% density) which have the distress and level of severity. The values of each are given below:

Low Severity Joint Spalling	50% density	11 point deduct value
	100% density	14 point deduct value
Low Severity Small Patching	50% density	7 point deduct value
	100% density	10 point deduct value

Corner Spalling

On Runway 17R at the DFW Airport there was an pattern of corner patching observed to be associated with doweled joints. The pattern reflected a 50 ft. spacing at each doweled joint, generally skipping each sawed joint between the doweled joint. Most of the observed patches were along the longitudinal joint 50 ft. offset from the runway centerline in an area traditionally considered to be out of the trafficked area. The observed corner patching is usually less than 2 ft. square in two adjacent slabs as shown in Figure 2.2. The maintenance engineer reports that the depth of repair usually extends down to the steel reinforcement.

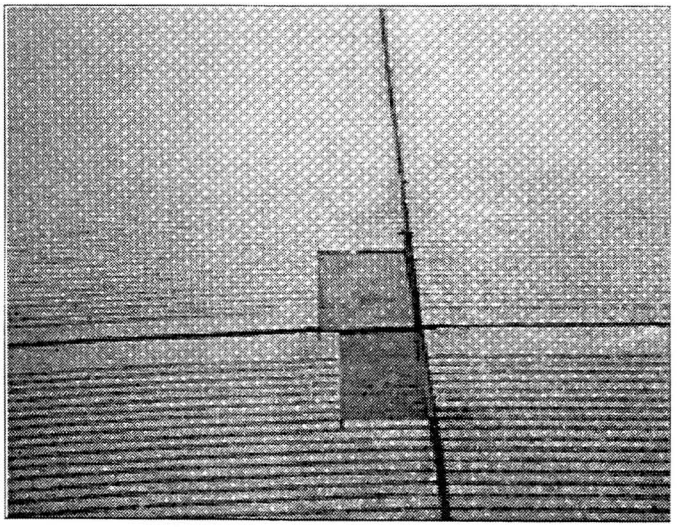

Figure 2.2 Patching of corner spalling.

Using the FAA and ASTM criteria for corner spalling :

Corner Spalling	50% density	13 point deduct value
	100% density	19 point deduct value

Pumping

Pumping distress was only observed in one area on Taxiway L which also had a resulting severe cracking due to loss of subgrade support. The Harding Lawson Associates study reported more pumping than was observed by the research team. (6 slabs on RW17R and 108 slabs on Taxiway L)

Pumping Distress	20% density	19 point deduct value
	50% density	38 point deduct value
	100% density	52 point deduct value

Small Patching (< 5 square ft.) and Patching/Utility Cut

Low severity small patching was the overwhelming observed distress in the Harding Lawson Associates report on Runway 17R and Taxiway L. However, once the patching was reviewed from videotapes and mapped, there was evidence that nearly all the patching was a result of joint and corner spall repair. There were probably only two or three cases of patching on Taxiway L or Runway 17R other than at the corners or joints. The Harding Lawson Associates report only recorded about a dozen or less slabs with large patching but approximately 25 percent of all slabs were recorded as having small patching (nearly always low severity).

Low Severity Small Patching:	50% density	7.5 point deduct value
	100% density	10 point deduct value
Medium Severity Small Patching	50% density	17 point deduct value
	100% density	22 point deduct value
Low Severity Patching	50% density	18 point deduct value
	100% density	22 point deduct value
Medium severity patching	50% density	38 point deduct value
	100% density	49 point deduct value

Longitudinal, Transverse or Diagonal Cracking

All longitudinal, transverse and diagonal cracking is considered a low severity unless it has a crack width of 1/8th - inch (3mm) or in the case where the slab is broken into three or more pieces by the low severity cracking. All filled cracking is considered low severity regardless of crack width. Hairline cracking of less than a few ft. are considered only as shrinkage cracking under the FAA and ASTM guideline.

At the DFW airport most observed cracking was less than 2mm in width. Much of the reported cracking observed by the research team was hairline cracks. Our recording process ignored cracks of less than 1 ft. in length. The PCI method uses the following deduct values:

Low Severity Cracking	50% density	20 point deduct value
	100% density	22 point deduct value
Medium Severity Cracking	50% density	45 point deduct value
	100 % density	58 point deduct value

Shrinkage Cracking

Hairline cracks of less than a few ft. are considered as shrinkage cracks and have the following deduct values:

Shrinkage cracking	50% density	7.5 point deduct value
	100% density	13 point deduct value

Joint Seal Damage

Joint seal damage was evident only on Runway 17R and not on Taxiway L. The damage was usually associated with trafficked areas near the centerline of transverse joints. This damage was not wide spread but was visible in several areas of the runway. The joints on Runway 17R were resealed in the last 2-3 years.

Construction History

Taxiway L as constructed in 1974 and evaluated by UT is 11,700 ft. long. It is 100 ft. wide. It was constructed in 50 ft. paving lanes with a longitudinal sawed joint at 25 ft.. In most cases on the Taxiway the 25 x 50 ft. slabs were left to crack on their own, some were saw cut into 25 x 25 ft. slabs. Some slabs remain uncracked at 25 x 50 ft.. From field measurement taken by the research team, it is assumed that there are 6 slab locations that are 37.5 ft. in length and 459 slab locations that are 25 ft. in length. The taxiway is 4 slabs wide for a total of 1860 slabs in Taxiway L (not including the 2000 ft. extension that was added in 1994).

Runway 17R was also constructed in 1974 and as evaluated by the researchers is 11,387.5 ft. long and 200 ft. wide. It was constructed in four 50-ft. paving lanes with a sawed longitudinal joint at the 25 ft. location. The construction joint at the centerline of the runway is both keyed and doweled. The two construction joints 50 ft. off the centerline are keyed but not doweled. Longitudinally, as a general rule at each 50 ft. location there is a doweled transverse joint and a sawed transverse joint in between each doweled joint. Along the length of the runway evaluated by the researchers, there are 9 slabs that are 37.5 ft. in length and 442 slabs that are 25 ft. in length for a total of 3608 slabs. Runway 17R was extended in 1994 to a total length of 13,400 ft..

Fatigue Cracking

FAA Advisory Circular AC150/5380-6 and the ASTM D5340-93 procedure are essentially exactly the same in the identification of distresses. AC150/5380-6 precedes ASTM adoption of the Pavement condition index survey as a standard. The significant difference is that ASTM corrects a deficiency in the FAA method of how multiple deducts points are aggregated and adjusted.

Neither the FAA or ASTM method specifically identifies fatigue cracking as a distress. In both methods all cracking in rigid pavements must either be one of the following:

- shrinkage cracking
- longitudinal, transverse or diagonal cracking
- durability (D) cracking

The majority of the cracking observed at the DFW airport on Runway 17R and Taxiway L was definitely fatigue related cracking. The cracking was normally only visible in the slabs within 25 ft. of the runway or taxiway centerline (those slabs receiving aircraft loading). The cracking was predominately in the longitudinal direction (parallel to aircraft traffic) and most visible in the aircraft wheel paths. The cracking was most pronounced either in the center of the slab or beginning near the transverse joint proceeding toward the center of the slab as shown in Figure 2.3. Although much of the cracking consided of hairline cracking and not visible by video survey, some was up to $1/8^{th}$ inch in width and more easily observed. The cracking does not follow the pattern of durability cracking which is classified as parallel to or "D" shaped along the transverse joints. Neither does the cracking follow the pattern of shrinkage cracking because slabs poured as one slab and sawed longitudinally into two slabs show cracking only on slabs with frequent aircraft loading.

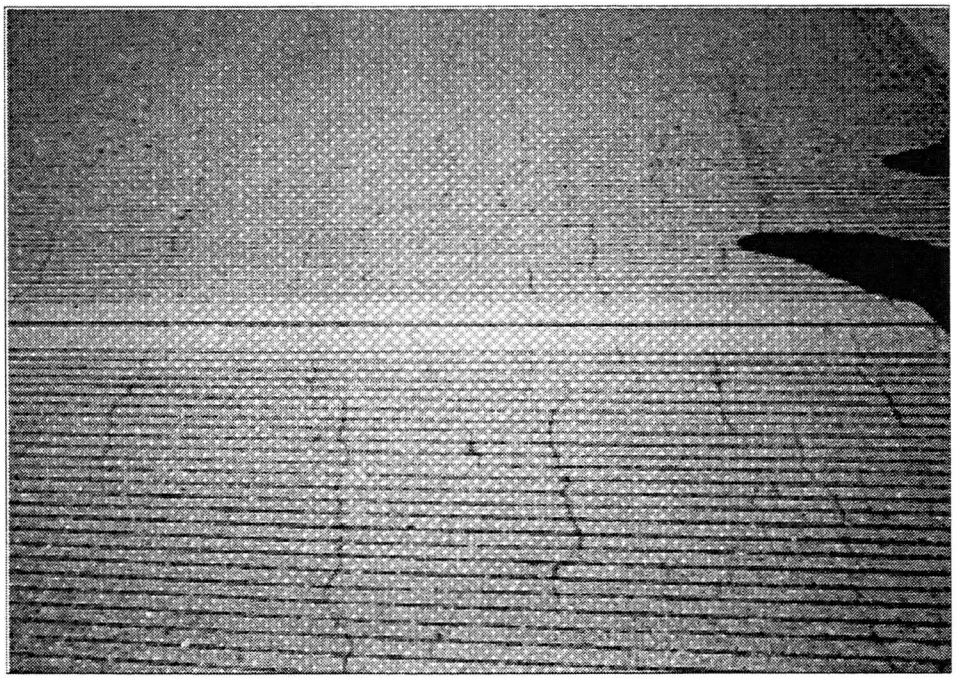

Figure 2.3 Fatigue cracking.

The observed cracking on the runway and taxiway is primarily a load related phenomena. The cracking for the most part was not observed or reported in much detail in the Harding Lawson Associates report.

	Harding Lawson Associates Report (100% survey)		UT Report (extrapolation)	
	Keel Section	Entire Width	Keel Section	Entire Width
Taxiway L Cracking	7.3%	6%	88%	50%
Taxiway L Patching	25%	30%		
Runway 17R Cracking	1.8%	0.4%	92%	26%
Runway 17R Patching	35%	29%		

	Runway 17R Keel Section	Runway 17R	Taxiway L Keel Section	Taxiway L
Total Number of Slabs	902	3608	930	1860
Patching Distress - 66 & 67	314	1051	229	558
Linear Cracking Distress - 63		4		3
Shrinkage Cracking - 73		12		113
Total Cracking 63 & 73	14	16	68	116
Pumping Distress - 69		6		108

CHAPTER 3. TRAFFIC DATA—ANALYSIS AND FORECASTS

CURRENT AND FUTURE TRAFFIC ANALYSIS

Historical traffic data is necessary to evaluate current runway pavement deterioration and to generate a correlation between cumulative runway traffic and current runway fatigue. Future traffic forecasts are necessary to evaluate remaining pavement life.

From 1991-1994, traffic data was obtained from the FAA Airport Activity Statistics. For 1995, traffic data was obtained from the DFW Airport Planning Department. Pre-1991 traffic data was obtained using assumptions from the Harding Lawson Pavement Evaluation Report. Traffic forecasts were projected based on traffic growth from 1991 to 1995. Current and forecast traffic data is shown by Table 3.1.

DETERMINATION OF EQUIVALENT ANNUAL DEPARTURES BY THE DESIGN AIRCRAFT

The design aircraft is the aircraft which requires the greatest pavement thickness. The MD-11 exerts the highest stress on the airport pavement, thus requiring the greatest pavement thickness. Since the MD-11 becomes the design aircraft, it is necessary to convert all traffic at DFW into MD-11 equivalents. Converting traffic into MD-11 equivalents was done using the method demonstrated with *Determination of Equivalent Annual Departures by the Design Aircraft*, in FAA Advisory Circular AC 150/5320-6D. This method first requires grouping all aircraft into the same landing gear configuration by multiplying the number of departures of an aircraft type by its gear conversion ratio:

Convert From	To	Conversion Ratio
single	dual wheel	0.8
single	dual tandem	0.5
dual	dual tandem	0.6
double dual tandem	dual tandem	1.0
dual tandem	single	2.0
dual tandem	dual	1.7
dual	single	1.3
double dual	dual	1.7

After grouping all aircraft into the same gear configuration, the conversion to equivalent annual departures is determined by the following formula:

$$\log R_1 = \log R_2 * \left(\frac{W_2}{W_1}\right)^{1/2}$$

TABLE 3.1. DFW AIRCRAFT OPERATIONS 1991-2015 (JETS ONLY)

				Departures						
Year		1991	1992	1993	1994	1995	2000	2005	2010	2015
Runway	H/L Split									
13L	0.50%	1335	1385	1460	1460	1525	1750	1975	2200	2425
17L	0.50%	1335	1385	1460	1460	1525	1750	1975	2200	2425
17R	36.90%	98523	102213	107748	107748	112545	129150	145755	162360	178965
18L	32.40%	86508	89748	94608	94608	98820	113400	127980	142560	157140
18R	4.70%	12549	13019	13724	13724	14335	16450	18565	20680	22795
13R	0.00%	0	0	0	0	0	0	0	0	0
31R	0.00%	0	0	0	0	0	0	0	0	0
35R	0.50%	1335	1385	1460	1460	1525	1750	1975	2200	2425
35L	11.50%	30705	31855	33580	33580	35075	40250	45425	50600	55775
36L	0.30%	801	831	876	876	915	1050	1185	1320	1455
36R	10%	26700	27700	29200	29200	30500	35000	39500	44000	48500
31L	2.70%	7209	7479	7884	7884	8235	9450	10665	11880	13095
Total	100.00%	267000	277000	292000	292000	305000	350000	395000	440000	485000
				Arrivals						
Runway	H/L Split									
13L	0.00%	0	0	0	0	0	0	0	0	0
17L	34.50%	92115	95565	100740	100740	105225	120750	136275	151800	167325
17R	0.00%	0	0	0	0	0	0	0	0	0
18L	0.00%	0	0	0	0	0	0	0	0	0
18R	25.20%	67284	69804	73584	73584	76860	88200	99540	110880	122220
13R	15.30%	40851	42381	44676	44676	46665	53550	60435	67320	74205
31R	3.20%	8544	8864	9344	9344	9760	11200	12640	14080	15520
35R	9.30%	24831	25761	27156	27156	28365	32550	36735	40920	45105
35L	0.00%	0	0	0	0	0	0	0	0	0
36L	12.50%	33375	34625	36500	36500	38125	43750	49375	55000	60625
36R	0%	0	0	0	0	0	0	0	0	0
31L	0.00%	0	0	0	0	0	0	0	0	0
Total	100.00%	267000	277000	292000	292000	305000	350000	395000	440000	485000

where:

R_1 = equivalent annual departures by design aircraft

R_2 = annual departures expressed in design aircraft landing gear

W_1 = wheel load of design aircraft

W_2 = wheel load of aircraft in question

As before, 95% of the gross weight is assumed to be carried by the main landing gear. This method of computing annual equivalent departures works excellently for narrowbody aircraft. Widebody aircraft require special attention. Since widebody aircraft have significantly different gear assembly spacing than other aircraft, this method of computing equivalent annual departures is not very accurate when widebody aircraft are included. Therefore, each widebody must be treated as a 300,000 pound dual tandem aircraft.

Table 3.2 shows the MD-11 Equivalent Departures for the airport in 1994, without using the widebody assumption. Table 3.3 shows the equivalent departures with the widebody assumption on W_1 only. Table 3.4 shows the equivalent departures with the assumption both on W_1 and W_2. Results vary tenfold between Tables 3.2 and 3.3. Results also vary slightly between Tables 3.3 and 3.4. The widebody assumption used in the Advisory Circular is unclear and yields varying results, depending on how the assumption is applied. Under this assumption, all widebody aircraft exert the same stress on runway pavement, which is questionable. Since the 727 is the aircraft that creates the next highest amount of stress, we have chosen it as our design aircraft, as it involves fewer widebody assumptions. Table 3.5 shows the equivalent 727 departures for the airport in 1994.

CUMULATIVE TRAFFIC ANALYSIS

The Harding Lawson Report assumes that 37% of all traffic operations occur on Runway 17R and 12% on Runway 35L. Our predictions also used the same assumption. This unway is used for departures only, consequently it is not necessary to conver arrivals to equivalent departures. According to the Harding Lawson report, 6.5 million MD-11 equivalent departures occurred at the airport before 1991; 2.4 million equivalent departures were on Runway 17R/35L. To convert equivalent MD-11 departures to equivalent B-727 departures a conversion factor of one B-727 departure to four MD-11 departures was used. Therefore, prior to 1991, 568,750 727 equivalent departures occurred on Runway 17R and 177,066 on 35L. After calculating and adding the 727 equivalent departures for years 1991-1995, it was found that a cumulative total of 730,492 equivalent departures of 727s have occurred on Runway 17R and 227,420 on 35L in 1995. As expected, the greatest number of departures (load) occur on the north end of 17R/35L. For determining the number of departures on each section of the runway, it was determined that most of the aircraft operating at DFW rotate before

TABLE 3.2. MD-11 EQUIVALENT DEPARTURES, WITHOUT WIDEBODY ASSUMPTION

Aircraft	**flights per day	Annual Dep.	MTOW	Gear Type	W2	W1	R2	R1	Equivalent MD-11s
F-100	69	25185	91500	0.6	21731	57000	15111	381	
A320	1	365	145505	0.6	34557	57000	219	66	
A340	2	730	542000	1	32181	57000	730	142	
737-200	46	16790	115500	0.6	27431	57000	10074	599	
737-300	15	5475	135000	0.6	32063	57000	3285	434	
737-400	2	730	150000	0.6	35625	57000	438	123	
737-500	5	1825	133500	0.6	31706	57000	1095	185	
757-200	112	40880	255000	1	30281	57000	40880	2,297	
767-200	7	2555	315000	1	37406	57000	2555	576	
767-300	12	4380	350000	1	41563	57000	4380	1,287	
727-200	122	44530	209500	0.6	49756	57000	26718	13,676	
747-F	1	365	700000	1	41563	57000	365	154	
*ATR	50	18250	40000	0.6	9500	57000	10950	45	
DC-10-10	11	4015	443000	1	42085	57000	4015	1,249	
DC-8-F	13	4745	350000	1	41563	57000	4745	1,378	
DC-9-50	4	1460	121000	0.6	28738	57000	876	123	
DC-9-30	21	7665	110000	0.6	26125	57000	4599	302	
DC-9-10	3	1095	90700	0.6	21541	57000	657	54	
*Embraer	101	36865	25000	0.6	5938	57000	22119	25	
*Jetstream J-31	10	3650	15212	0.5	7226	57000	1825	14	
L1011	8	2920	466000	1	55338	57000	2920	2,597	
L1011-500	2	730	500000	1	59375	57000	730	836	
MD-11	8	2920	600000	1	57000	57000	2920	2,920	
MD-80	268	97820	149500	0.6	35506	57000	58692	5,802	
*Shorts 330	151	55115	27000	0.6	6413	57000	33069	33	
*Swearingen Metro	17	6205	14000	0.6	3325	57000	3723	7	
*indicates commuter aircraft									
** source 1994 OAG data									
Total	1061	387265						35,304	

TABLE 3.3. MD-11 EQUIVALENTS WITH WIDEBODY ASSUMPTION ON W1 ONLY

Aircraft	**flights per day	Annual Dep.	MTOW	Gear Type	W2	W1	MD-11 Equivalents R2	MD-11 Equivalents R1
F-100	69	25185	91500	0.6	21731	35625	15111	1,837
A320	1	365	145505	0.6	34557	35625	219	202
A340	2	730	542000	1	32181	35625	730	527
737-200	46	16790	115500	0.6	27431	35625	10074	3,257
737-300	15	5475	135000	0.6	32063	35625	3285	2,168
737-400	2	730	150000	0.6	35625	35625	438	438
737-500	5	1825	133500	0.6	31706	35625	1095	737
757-200	112	40880	255000	1	30281	35625	40880	17,849
767-200	7	2555	315000	1	37406	35625	2555	3,101
767-300	12	4380	350000	1	41563	35625	4380	8,575
727-200	122	44530	209500	0.6	49756	35625	26718	170,461
747-F	1	365	700000	1	41563	35625	365	586
*ATR	50	18250	40000	0.6	9500	35625	10950	122
DC-10-10	11	4015	443000	1	42085	35625	4015	8,257
DC-8-F	13	4745	350000	1	41563	35625	4745	9,350
DC-9-50	4	1460	121000	0.6	28738	35625	876	439
DC-9-30	21	7665	110000	0.6	26125	35625	4599	1,369
DC-9-10	3	1095	90700	0.6	21541	35625	657	155
*Embraer	101	36865	25000	0.6	5938	35625	22119	59
*Jetstream J-31	10	3650	15212	0.5	7226	35625	1825	29
L1011	8	2920	466000	1	55338	35625	2920	20,845
L1011-500	2	730	500000	1	59375	35625	730	4,972
MD-11	8	2920	600000	1	57000	35625	2920	24,177
MD-80	268	97820	149500	0.6	35506	35625	58692	57,627
*Shorts 330	151	55115	27000	0.6	6413	35625	33069	83
*Swearingen Metro	17	6205	14000	0.6	3325	35625	3723	12
* indicates commuter aircraft		** source OAG 1994 data						
Total	1061	387265						337,234

TABLE 3.4. MD-11 EQUIVALENT DEPARTURES WITH WIDEBODY ASSUMPTION ON W1 AND W2

Aircraft	**flights/day	Annual Dep.	MTOW	Gear Type	W2	W1	MD-11 Equivalents R2	MD-11 Equivalents R1
F-100	69	25185	91500	0.6	21731	35625	15111	1,837
A320	1	365	145505	0.6	34557	35625	219	202
A340	2	730	300000	1	35625	35625	730	730
737-200	46	16790	115500	0.6	27431	35625	10074	3,257
737-300	15	5475	135000	0.6	32063	35625	3285	2,168
737-400	2	730	150000	0.6	35625	35625	438	438
737-500	5	1825	133500	0.6	31706	35625	1095	737
757-200	112	40880	255000	1	30281	35625	40880	17,849
767-200	7	2555	315000	1	35625	35625	2555	2,555
767-300	12	4380	350000	1	35625	35625	4380	4,380
727-200	122	44530	209500	0.6	49756	35625	26718	170,461
747-F	1	365	300000	1	35625	35625	365	365
*ATR	50	18250	40000	0.6	9500	35625	10950	122
DC-10-10	11	4015	300000	1	35625	35625	4015	4,015
DC-8-F	13	4745	350000	1	41563	35625	4745	9,350
DC-9-50	4	1460	121000	0.6	28738	35625	876	439
DC-9-30	21	7665	110000	0.6	26125	35625	4599	1,369
DC-9-10	3	1095	90700	0.6	21541	35625	657	155
*Embraer	101	36865	25000	0.6	5938	35625	22119	59
*Jetstream J-31	10	3650	15212	0.5	7226	35625	1825	29
L1011	8	2920	300000	1	35625	35625	2920	2,920
L1011-500	2	730	300000	1	35625	35625	730	730
MD-11	8	2920	300000	1	35625	35625	2920	2,920
MD-80	268	97820	149500	0.6	35506	35625	58692	57,627
*Shorts 330	151	55115	27000	0.6	6413	35625	33069	83
*Swearingen Metro	17	6205	14000	0.6	3325	35625	3723	12
* indicates commuter aircraft		** source OAG 1994 data						
Total	1061	387265						284,810

TABLE 3.5. 727 EQUIVALENT DEPARTURES, WITH WIDEBODY ASSUMPTION

Aircraft	**flights/day	Annual Dep.	MTOW	Gear Type	W2	W1	R2	MD-11 Equivalents R1
F-100	69	25185	91500	1	21731	49756	25185	810
A320	1	365	145505	1	34557	49756	365	137
A340	2	730	300000	1.7	35625	49756	1241	415
737-200	46	16790	115500	1	27431	49756	16790	1,371
737-300	15	5475	135000	1	32063	49756	5475	1,002
737-400	2	730	150000	1	35625	49756	730	265
737-500	5	1825	133500	1	31706	49756	1825	401
757-200	112	40880	255000	1.7	30281	49756	69496	5,989
767-200	7	2555	315000	1.7	35265	49756	4343.5	1,155
767-300	12	4380	350000	1.7	35265	49756	7446	1,818
727-200	122	44530	209500	1	49756	49756	44530	44,530
747-F	1	365	300000	1.7	35625	49756	620.5	231
*ATR	50	18250	40000	1	9500	49756	18250	73
DC-10-10	11	4015	300000	1.7	35625	49756	6825.5	1,755
DC-8-F	13	4745	350000	1.7	41563	49756	8066.5	3,720
DC-9-50	4	1460	121000	1	28738	49756	1460	254
DC-9-30	21	7665	110000	1	26125	49756	7665	653
DC-9-10	3	1095	90700	1	21541	49756	1095	100
*Embraer	101	36865	25000	1	5938	49756	36865	38
*Jetstream J-31	10	3650	15212	0.8	7226	49756	2920	21
L1011	8	2920	300000	1.7	35625	49756	4964	1,341
L1011-500	2	730	300000	1.7	35625	49756	1241	415
MD-11	8	2920	300000	1.7	35625	49756	4964	1,341
MD-80	268	97820	149500	1	35506	49756	97820	16,431
*Shorts 330	151	55115	27000	1	6413	49756	55115	50
*Swearingen Metro	17	6205	14000	1	3325	49756	6205	10
* indicates commuter aircraft			**source 1994 OAG data					
Total	1061	387265						84,324

the midpoint of Runway 17R/35L. As a result, the lightest loads occur in the center, with only 184,877 equivalent 727 departures. Table 3.6 shows the equivalent departures per section of Runway 17R/35L and Taxiway L. Table 3.7 shows the forecast MD-11 equivalent departures for the runway. Table 3.8 shows the forecast 727 equivalent departures for the runway. After analyzing the traffic and developing a correlation between the number of departures and the amount of wear, a future amount of wear can be predicted. The remaining life in a runway can now be predicted based on cumulative aircraft operations.

TABLE 3.6. CUMULATIVE EQUIVALENT DEPARTURES BY SECTION

Runway 17R/35L	1990	1990	1995	1995
Section	MD-11	727	MD-11	727
1	2,386,578	568,750	3,059,237	730,492
2	2,386,578	568,750	3,059,237	730,492
3	2,386,578	568,750	3,059,237	730,492
4	607,239	143,985	779,695	184,877
5	746,974	177,066	959,115	227,420
6	746,974	177,066	959,115	227,420
7	746,974	177,066	959,115	227,420
8	746,974	177,066	959,115	227,420
Taxiway L	MD-11	727	MD-11	727
1	20,400	4862	26,150	6244
2	1,606,090	3,82,750	2,058,768	491,598
3	1,359,376	323,956	1,742,517	416,082
4	1,823,157	432,296	2,340,934	555,069
5	1,914,031	453,710	2,457,617	582,736
6	600,415	142,325	770,933	182,799
7	600,415	142,325	770,933	182,799
8	746,974	177,066	959,115	227,420
9	746,974	177,066	959,115	227,420

TABLE 3.7. CUMULATIVE MD11 EQUIVALENT DEPARTURES FOR RUNWAY 17R/35L

Aircraft	<1990	1991	1992	1993	1994	1995	2000	2005	2010
B727		22066	19469	16104	13673	9429	7199	5201	2722
B737		8987	9297	10135	8560	11315	13882	16644	17968
B747		69	19	41	40	38	40	42	44
B757		6789	7423	9348	10677	11315	13882	14564	15245
B767		2742	2364	2380	2422	2263	2181	2081	2178
DC-8		175	59	866	1158	943	992	1040	1089
DC-9		6203	4218	3003	3214	2829	1487	0	0
DC-10/MD11		5282	5298	3736	2036	1886	1983	2081	2178
MD80		37058	42227	43530	41922	43372	45612	47852	50092
L1011		1021	987	1238	1118	943	0	0	0
F100		0	2	1958	8492	9957	11899	14564	17423
Total 17R		90393	91363	92339	93312	94288	99157	104069	108940
MD-11 Equiv.		170525	162347	137280	109271	93236	83609	81232	77843
Cumulative MD11s	2,386,578	2,557,103	2,719,450	2,856,730	2,966,001	3,059,237	3,501,350	3,931,453	4,329,141

TABLE 3.8. CUMULATIVE EQUIVALENT 727 DEPARTURES FOR RUNWAY 17R/35L

Aircraft	<1990	1991	1992	1993	1994	1995	2000	2005	2010
B727		22066	19469	16104	13673	9429	7199	5201	2722
B737		8987	9297	10135	8560	11315	13882	16644	17968
B747		69	19	41	40	38	40	42	44
B757		6789	7423	9348	10677	11315	13882	14564	15245
B767		2742	2364	2380	2422	2263	2181	2081	2178
DC-8		175	59	866	1158	943	992	1040	1089
DC-9		6203	4218	3003	3214	2829	1487	0	0
DC-10/MD11		5282	5298	3736	2036	1886	1983	2081	2178
MD80		37058	42227	43530	41922	43372	45612	47852	50092
L1011		1021	987	1238	1118	943	0	0	0
F100		0	2	1958	8492	9957	11899	14564	17423
Total 17R		90393	91363	92339	93312	94288	99157	104069	108940
727 Equiv.		37121	35236	33020	30022	26343	24965	24065	22475
Cumulative 727s	568,750	605,871	641,107	674,127	704,149	730,492	836,061	938,762	1,033,722

CHAPTER 4. DEVELOPMENT OF TESTING PROGRAM

A testing program was developed specifically for the concrete pavements that comprise Runway 17R/35L and Taxiway L. This testing plan was formed with the assistance of Drs. B. Frank McCullough, Thomas W. Kennedy, and Kenneth Stokoe of the Center for Transportation Research at The University of Texas at Austin. Several different types of tests were utilized during the course of the investigation. Each type of test allows CTR researchers to evaluate the condition of the concrete pavements from different aspects. The current level of distress pertaining to each specific type of test will be reported in subsequent chapters of this report.

The tests and measurements that were deemed necessary to be performed on the pavements included in this study are listed below:

- Pavement Condition Index
- Measure Longitudinal Roughness Profile
- Coring and Associated Tests
- Cross-hole Seismic Testing
- Rolling Dynamic Deflectometer
- Heavy Weight Deflectometer

The format and structure of each of these items will be discussed in this chapter. A discussion of the actual tests and results of those tests will follow in later chapters.

PAVEMENT CONDITION INDEX

The pavement management division at the DFW Airport maintains a system of videotapes and a corresponding database that controls the video system. PaveTech, Inc., developed the database and videotaping system with the intent to measure the Pavement Condition Index (PCI) of the pavements at the airport. This video system is somewhat useful as it allowed CTR researchers to perform two tasks. The first is that it allowed researchers to view the longitudinal joint 50 ft. east of centerline on Runway 17R which has a specific pattern of corner spalling distress. The second advantage of the video system to this project was that distresses recorded in the PCI evaluation performed by PaveTech could be identified and verified on site. However, the low quality of the video and the difficulty in viewing an entire slab because the video only sweeps a 12-ft. highway lane width, seriously hinders productivity in reviewing distresses at specific locations.

Using the original field notes from the Harding Lawson study, the pattern of distress was mapped for Runway 17R and Taxiway L and entered into a MicroStation CAD

drawing for visual analysis. This pattern of distress is coded using the MicroPAVER number codes and is shown in Appendix A of Volume III of this report.

Harding Lawson Report

The reports on pavement condition performed by Harding Lawson in 1991 and PaveTech in 1994 provided information that was vital to performing the required tasks for this report. Information such as cumulative aircraft traffic, future predictions of aircraft traffic, pavement condition, estimates of material strength, and many other items were found in the Harding Lawson report and proved very useful to the researchers at CTR throughout the duration of the project.

Inclusion of Fatigue Cracking

A type of distress that was not included in the PCI performed by Harding Lawson or PaveTech was the amount of fatigue cracking in the concrete pavements. This type of cracking is difficult to notice, and is also difficult to quantify and compile into a condition index. The fatigue cracking was in many cases equal to the width of a human hair and does not photograph well or show up in video. This type of cracking is, however, an important and fundamental occurrence signifying the onset of concrete fatigue. Dr. Michael McNerney, in consultation with Dr. B. Frank McCullough devised a method of quantifying the level of fatigue cracking in the pavement. The staff of CTR assigned to this project spent time on the runway and taxiway to implement this method and to obtain a correlation between fatigue cracking and the level of cumulative equivalent aircraft traffic on the pavement. This method will be discussed later in this report.

LONGITUDINAL RUNWAY ROUGHNESS PROFILE

The profiles of Runway 17R/35L and of Taxiway L are important data to obtain in order to perform an analysis of the ride quality index and the present serviceability of the concrete pavements. The profile is one aspect that can influence the effective life of the pavement. If a runway profile is *rough* — a subjective measure which will be defined later in this section — aircraft impacts on the pavement will be of greater force during landing and takeoff operations than on a smoother runway. In addition to damage to the runway, excessive fatigue to structural components of the aircraft and discomfort to pilots and to passengers are general effects of rough runways.

APR Consultants of Medway, Ohio, performed the profile measurements for Runway 17R/35L and for Taxiway L. A summary of their report of the profile analysis and further investigation is presented in Chapter 5. The full report obtained from APR

Consultants is given in Appendix E. An example of the profile data obtained is presented in Figure 4.1.

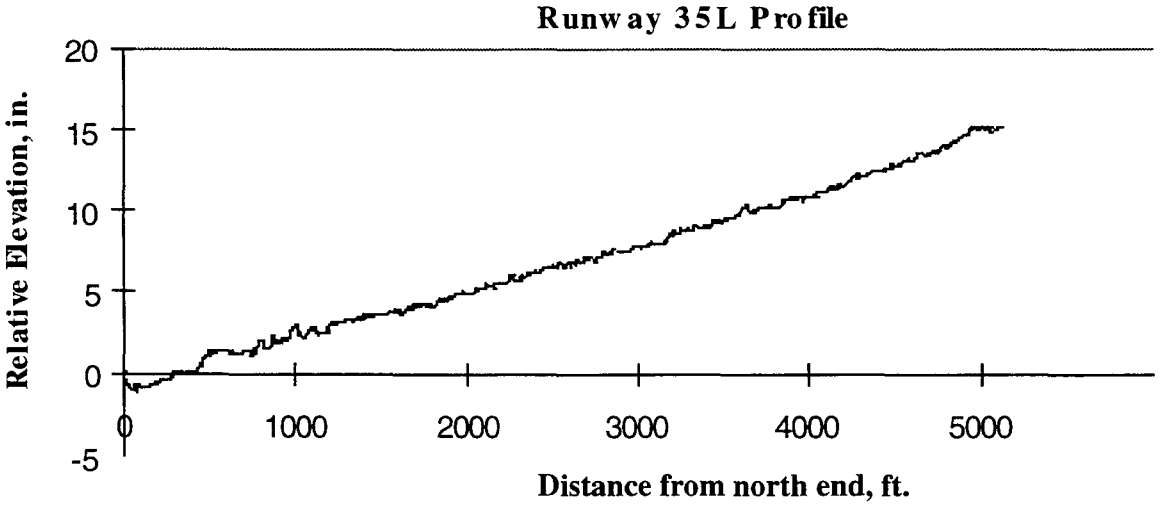

Figure 4.1. Example of Runway 35L profile data.

Since aircraft have very long wheelbases, i.e., distance between the main gear and the nose gear, and because aircraft travel at high speeds across the pavement, only long wavelengths in the profile will affect the pavement performance. For the same reasons, since localized roughness will not affect aircraft operations, the profile was taken only along the centerlines of the runway and taxiway.

CORING AND ASSOCIATED TESTS

Core samples were taken from the section of Taxiway K which was later reconstructed, Runway 17R, and Taxiway L. Many of the core samples include the Portland Cement Concrete (PCC), Cement Treated Base (CTB), and the underlying subbase and subgrade. In several sections, cross-hole testing was performed between two adjacent holes left by the coring operation. Cross-hole testing allows the in situ properties of the layers underlying the PCC to be evaluated. In addition, the properties of the PCC layer can be found and compared to the results of other tests which were performed.

The other tests that were performed on the concrete cores include both nondestructive and destructive testing. The nondestructive tests were performed first, for obvious reasons. These tests include different types of sonic testing, or the evaluation of material properties by measuring the velocity of stress waves through a material. The free-free resonance test measures the velocity of stress waves through an unrestrained core sample, and the P-wave test measures the velocity of waves reflected from one end of a

core sample to the other. These tests allow measurements of elastic modulus, shear modulus, and Poisson's ratio to be made and compared among different core samples.

Destructive testing performed for this study includes indirect (splitting) tensile, resilient modulus, and fatigue tests. The indirect tensile test results allow the strength of the concrete to be known, and to be used in other analyses such as computer simulations of stress levels and estimations of remaining life. Resilient modulus is the ratio of a repeated stress applied to a material to the recoverable deformation, or axial strain, of the material. Fatigue testing produces a fatigue curve which can be used to estimate the remaining life of the PCC structure. This type of remaining life prediction can be correlated and calibrated so that the actual level of fatigue can be properly modeled, and the true remaining life predicted. After the model is calibrated, it can then be applied to predict future performance based on forecast traffic volumes and loads on the runway and taxiway.

Core Samples

Several different coring programs were implemented in the testing plan submitted to the DFW technical advisors for review. First, a coring and testing program was developed for Taxiway K before its reconstruction. The intent was to identify the properties of the concrete at the end of its service life. Another coring and cross-hole seismic testing program was implemented for Runway 17R/35L, as well as for Taxiway L. The coring was done by Maxim Engineers located at the DFW airport. The purpose of the coring was to obtain concrete samples to test in the laboratory, and to provide holes deep enough to perform the cross-hole seismic testing,

Since the aircraft wheel path is approximately at the middle of the first slab adjacent to the centerline of the runway and the taxiway, it was desirable to obtain core samples from this location to test the properties of the concrete from a loaded portion of concrete. This means that the concrete from the wheel path section has been loaded by numerous aircraft over its service life. Approximately half of the concrete cores were taken from the wheel path area of the pavements. The other half of the cores were taken from a portion of the pavement which has seen very little aircraft loads, near the edge of the pavement. The furthermost slab from the centerline sees little, if any, traffic loading over the years. The concrete taken from this location represents concrete that is new, with the exception of environmental loads.

This difference in the historic loading patterns of the two locations provides a basis for analysis. A comparison can be made between the properties of the concrete cores taken from the wheel path and of those of the cores taken from the non-trafficked area. In

addition to the in and out of traffic concrete, a distinction can be made between concrete taken from the north of the runway or taxiway and concrete taken from the south end.

CROSS-HOLE SEISMIC TESTING

Cross-Hole Seismic Testing

Cross-hole seismic testing was performed at four general locations on Runway 17R/35L and at eight general locations on Taxiway L. At each of these locations, a pattern with 3 to 9 core holes was drilled into the pavement system to depths ranging from 3 to 9 ft.. A typical pattern with three core holes is shown in Figure 4.2. Generally, horizontal spacing between core holes ranged from 3.5 to 7 ft..

Testing was performed by initiating stress waves in one core hole and monitoring their arrivals in the adjacent core holes. The purpose of these test was to evaluate the stiffness of each component of the pavement system independently and in-place. The results of this investigation will be discussed in Chapter 5.

DESCRIPTION OF THE ROLLING DYNAMIC DEFLECTOMETER

The Rolling Dynamic Deflectometer (RDD) is a truck mounted device that measures continuous deflection profiles of pavements. A drawing of the RDD is shown in Figure 4.3. The device consists of a large truck with a gross weight of about 195 kN (44,000 lb.) on which a servo-hydraulic vibrator is mounted. The vibrator has a 33-kN (7,500-lb.) reaction mass which is used to generate vertical dynamic forces as large as 310 kN peak-to-peak (70,000 lb. peak-to-peak) over a frequency range of about 10 to 100 Hz. Simultaneously, the hydraulic system generates a constant hold-down force ranging from 65 to 180 kN (15,000 to 40,000 lb.). The static and superimposed dynamic forces are transferred to the pavement through two loading rollers as shown in Figure 4.4.

As the RDD slowly rolls over a pavement, it applies a cyclic load to the pavement surface through the loading rollers. Dynamic displacements are measured with four rolling sensors. By measuring the applied forces and the resulting deflections, a continuous deflection profile for the pavement is determined, with soft regions of the pavement exhibiting large deflections and stiff regions lower deflections.

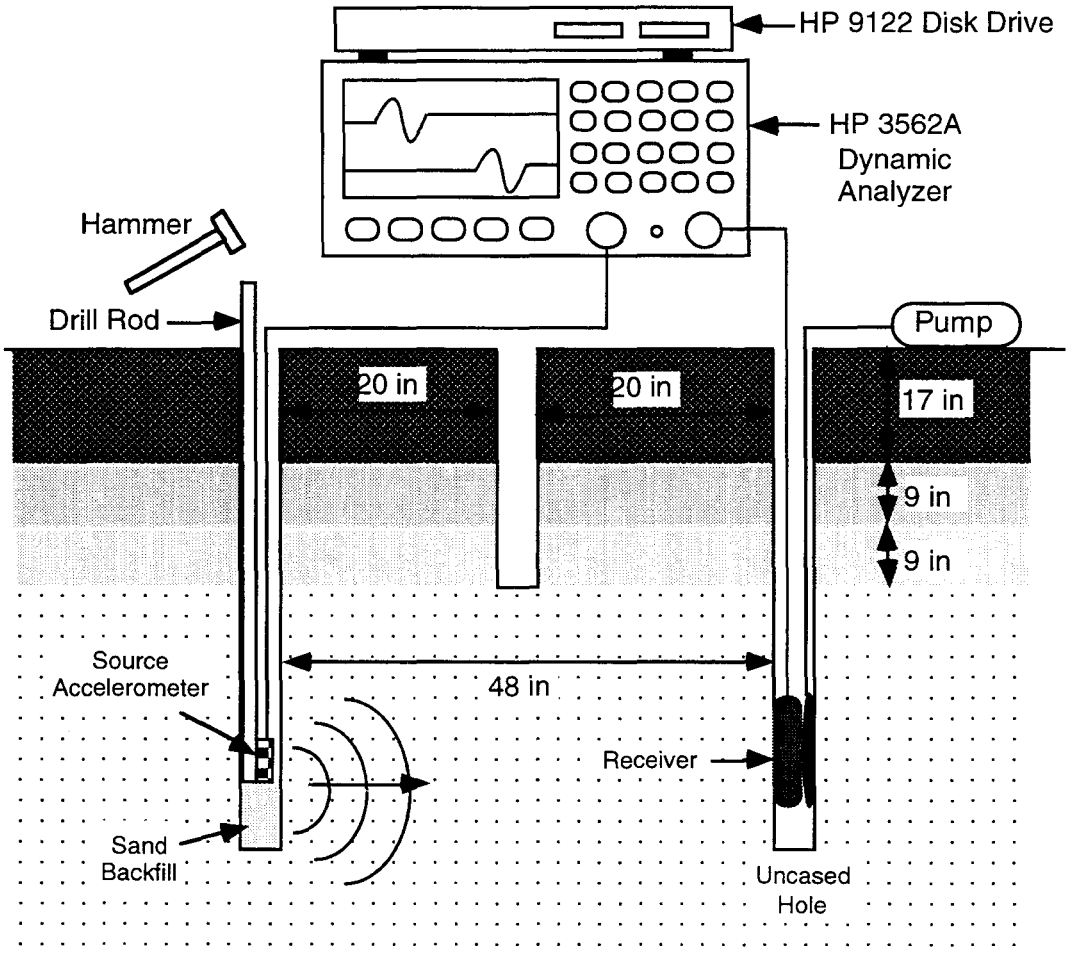

Figure 4.2. Example Cross-hole Seismic Test

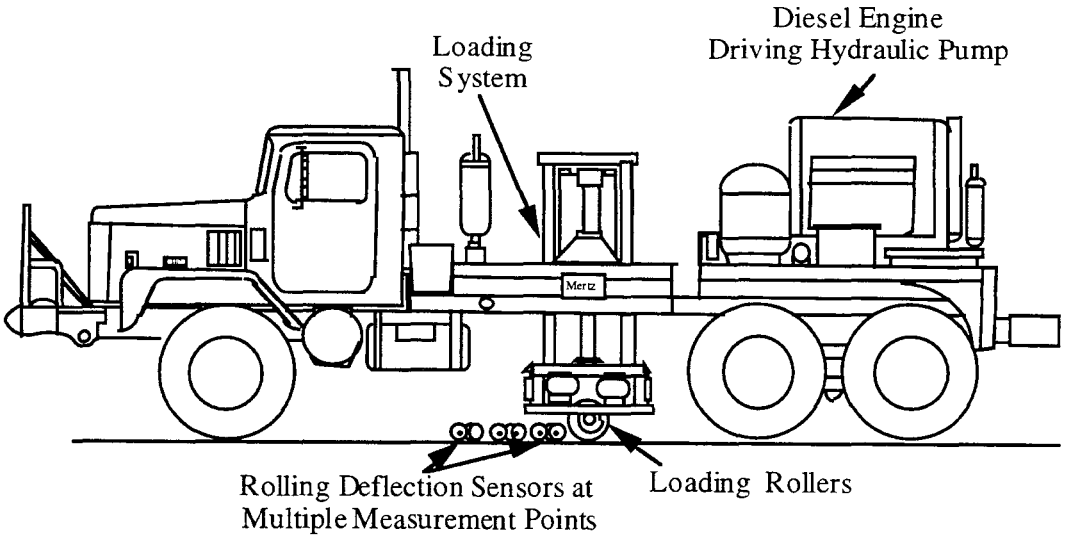

Figure 4.3. General Configuration of the Rolling Dynamic Deflectometer (RDD)

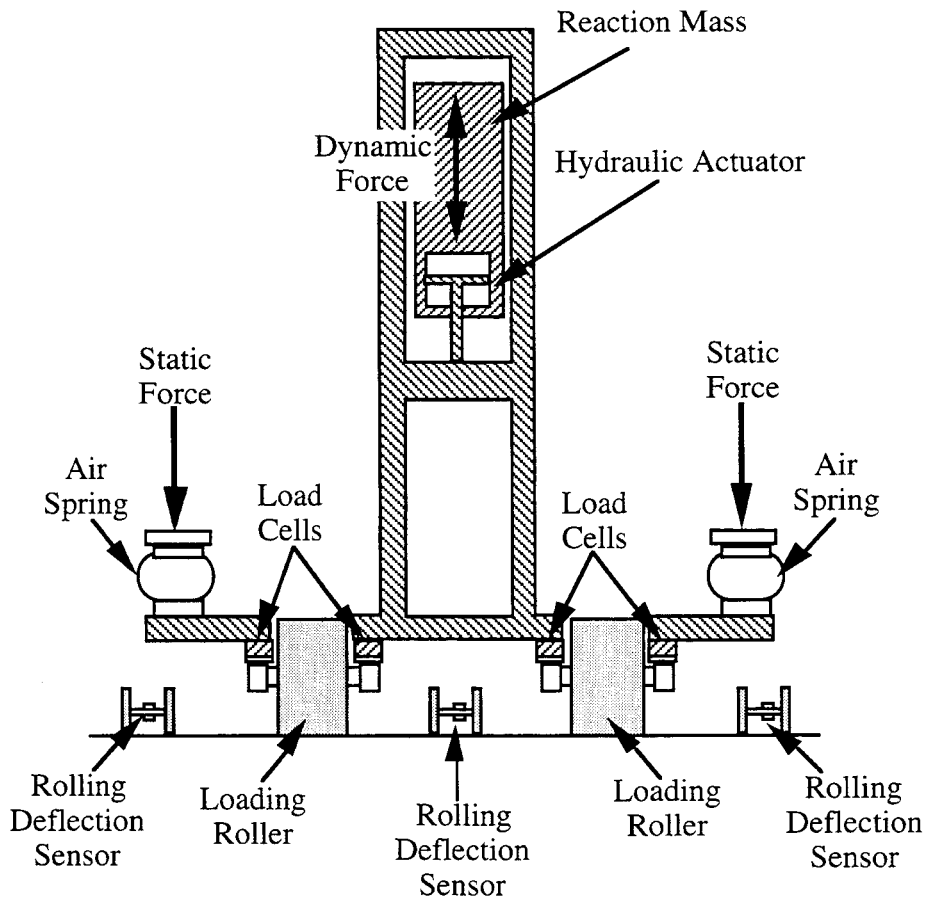

Figure 4.4. Front Cross-Sectional View of the RDD Loading and Measurement Systems

RDD TESTING AT THE DFW AIRPORT

On July 28-29, 1996 and August 30-September 2, 1996 RDD testing was performed at DFW airport. Deflection profiles were measured along the entire length of Runway 17R near the runway center line. Three additional longitudinal profiles were measured on two 2000 ft. intervals: between the centerline and the first saw joint; along the first saw joint; and, along the undowelled construction joint. Transverse profiling was also performed on eight alignments next to transverse joints. The same battery of tests were performed on Taxiway L, the entire taxiway length was profiled near the centerline and the three additional longitudinal profiles were measured on a single 2000 ft. section. Transverse profiling was conducted at two locations on the taxiway near transverse joints.

Additional profiling was performed on the newly constructed Runway 17L/35R. These profiles provide a valuable comparison to the results from Runway 17R/35L, showing the effects of traffic on pavement degradation. The same battery of tests were performed on the new runway as on Runway 17R. Profiling was conducted on about 5000

ft. on this runway near the centerline. At one 1000 ft. section additional longitudinal profiles were measured between the centerline and the first longitudinal saw joint, at the saw joint and at the longitudinal construction joint. Two transverse profiles were measured next to transverse joints.

ROLLING DYNAMIC DEFLECTOMETER OUTPUT

The RDD produces the similar deflection type of data that the FWD or HWD produces, but it is a continuous record of the *flexibility* of the pavement. The flexibility of the pavement is a measure of the deflection under a known load. The RDD produces a cyclic load from 5,000 to 65,000 pounds of force with a frequency of about 40 cycles per second. The cyclic loading of the RDD produces a significant improvement over the impact loading of the Falling Weight Deflectometer. A data acquisition system records the force, deflection, time, and distance along the pavement. A sample of the output from the RDD is shown in Figure 4.5. Note that every 25 ft., where a transverse joint is encountered, the deflection of the pavement increases due to the decrease in load transfer at the joint. Also note that every other deflection is higher than the intermediate ones. This may be attributed to the difference in joint types. The higher values are associated with the doweled contraction joints, whereas the lower peaks are the warping joints, i.e., controlled cracks with steel across them.

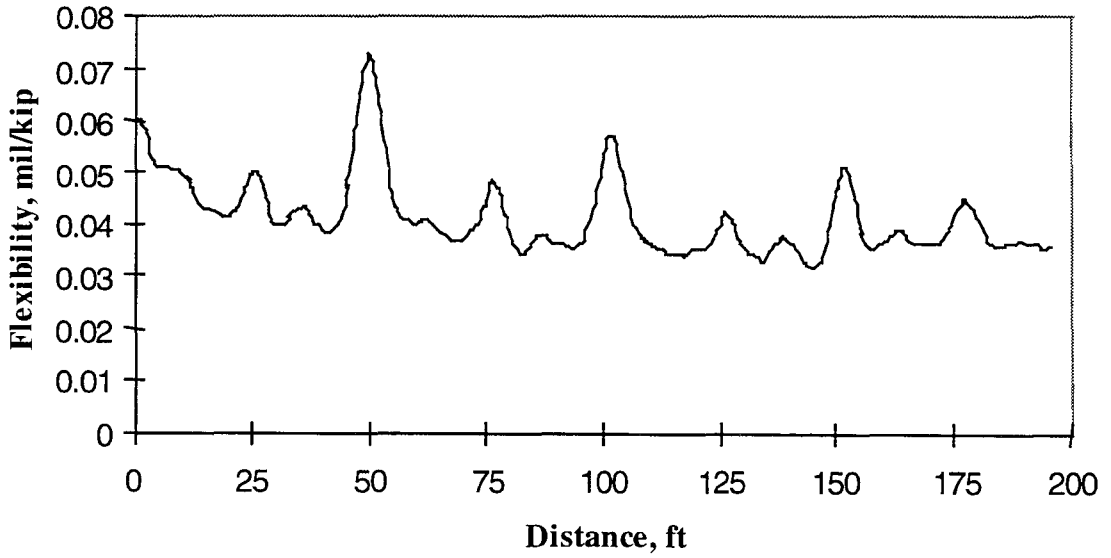

Figure 4.5. Sample of data output from the RDD showing transverse joints at 25' intervals.

Other uses of the RDD were determined as the project progressed. CTR staff members found that the RDD could provide a measure of load transfer efficiency (LTE) along longitudinal joints which can help identify locations of weakened subgrade or other distresses along the joint. This became an important type of information in light of the fact that the second joint from the centerline of Runway 17R displayed distress in the form of corner spalls and occasional spalls along the longitudinal joint. The LTE of this joint is shown for two 1000' sections in Figures 4.6 and 4.7. The load transfer efficiency of this joint in the first section is much better, overall, than that of the second section, measured over 6000' away. The points in these two figures are taken from measurements taken at 6 inch intervals, averaged over 10 ft.. The effects of the low LTE in the second section will be discussed in a later section of this report, such as the spalled longitudinal joints on both the runway and the taxiway.

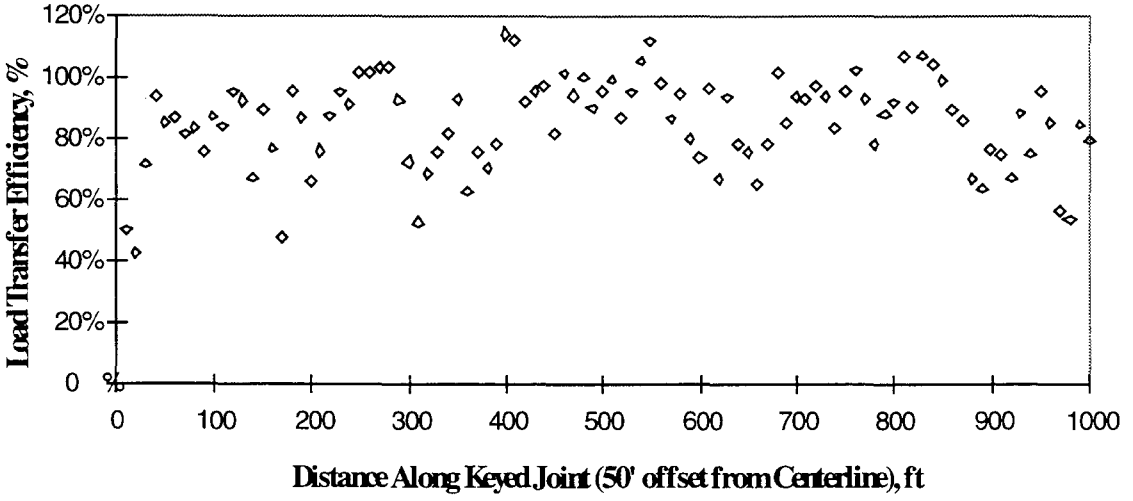

Figure 4.6. Load Transfer Efficiency of Keyed Joint (South End).

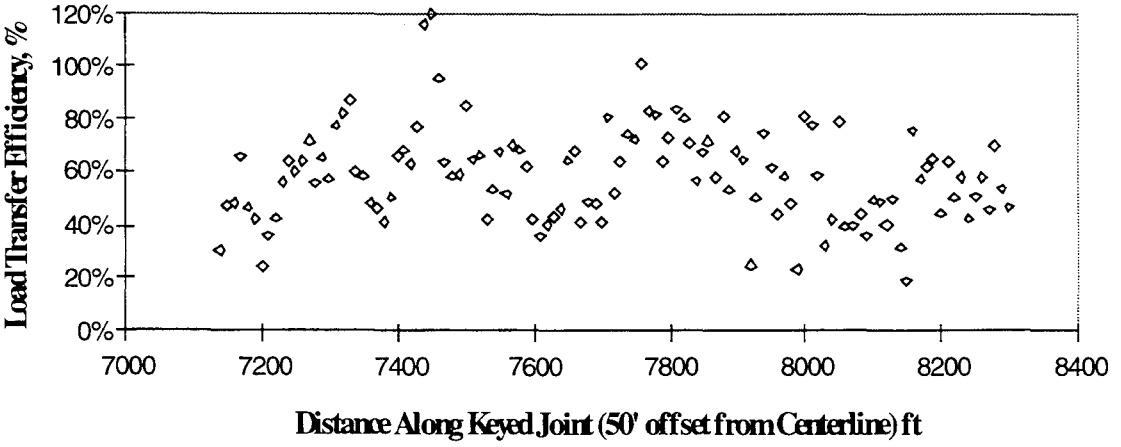

Figure 4.7. Load Transfer Efficiency of Keyed Joint (North End).

A method of determining the effectiveness of joints on the runway as well as the taxiway was devised at CTR after analyzing preliminary results from the RDD. This method allows DFW Airport management to more effectively set policy decisions regarding the rehabilitation of longitudinal joints depending on funding, budgeting, or any other criteria. The method will provide management with sound engineering analysis of the joints with which to make these decisions. A detailed report of the analysis performed on RDD output is provided in Chapter 5.

HEAVY WEIGHT DEFLECTOMETER

The heavyweight deflectometer (HWD) is similar to the falling weight deflectometer in that it uses a weight dropped from a certain height that produces a deflection in the pavement structure. The deflection curve, or deflection basin, is made up of seven sensors that measure the deflection in the pavement structure starting at the load and for one ft. intervals for six ft.. The basin shape is related to stiffness of the layers, thus it is possible to backcalculate properties of the pavement structure such as modulus of elasticity and Poisson's ratio.

The HWD was used at the DFW Airport in part to compare the results of the rolling dynamic deflectometer as well as to provide additional information regarding the elastic properties of the PCC pavement and the underlying layers on Runway 17R and Taxiway L. In addition to measuring the concrete properties of the runway and taxiway, the load transfer efficiency at several locations along the runway and taxiway was also measured.

CHAPTER 5. FIELD TESTING—ANALYSIS AND RESULTS

This chapter presents the methods, analysis, results and conclusions for field testing items in the test plan. The field testing plan was comprised of four major components. These included:

I. Profile measurement
II. Sampling and Testing
    A. Coring Program
    B. Cross-hole Testing
III. Visual inspection of cracking
IV. Deflection
    A. Rolling Dynamic Deflectometer
    B. Heavy Weight deflectometer testing

In Chapter 4, the general methods of each test plan item were discussed. This chapter will present those methods in more detail and will also discuss the analysis and results for each type of test. Although the results of the testing are presented in this chapter, these results will be used to predict the remaining life of the pavement structure using various analyses in Chapter 6 which will focus on the remaining life of the pavement.

PROFILE MEASUREMENT

As mentioned in Chapter 4, Airport Pavement Roughness Consultants (APR) of Medway, Ohio performed the measurement of the profile of Runway 17R/35L and of Taxiway Lima during the nights of October 31 and November 1, 1995. The profile of an airport pavement is important to obtain during a large scale analysis such as this. As aircraft travel down runways during takeoff or landing operations, or along taxiways during taxi operations, the roughness of the pavement has several effects on the aircraft, the pilots, and the passengers, depending on the magnitude of the roughness. Figure 5.1 is the profile of Runway 17R that was measured by APR, and Figure 5.2 is the profile of Taxiway L.

Runway Roughness

When an airport pavement becomes too rough, the aircraft reacts adversely, as do the pilot and the passengers. The aircraft experiences more relative damage during an operation on a rough pavement than on a more smooth pavement. Likewise, passengers begin to feel uncomfortable during a landing or takeoff in which the pavement causes the aircraft to bounce and to shake. Damage to aircraft occurs when vertical accelerations are developed in the aircraft due to surface roughness of the pavement.

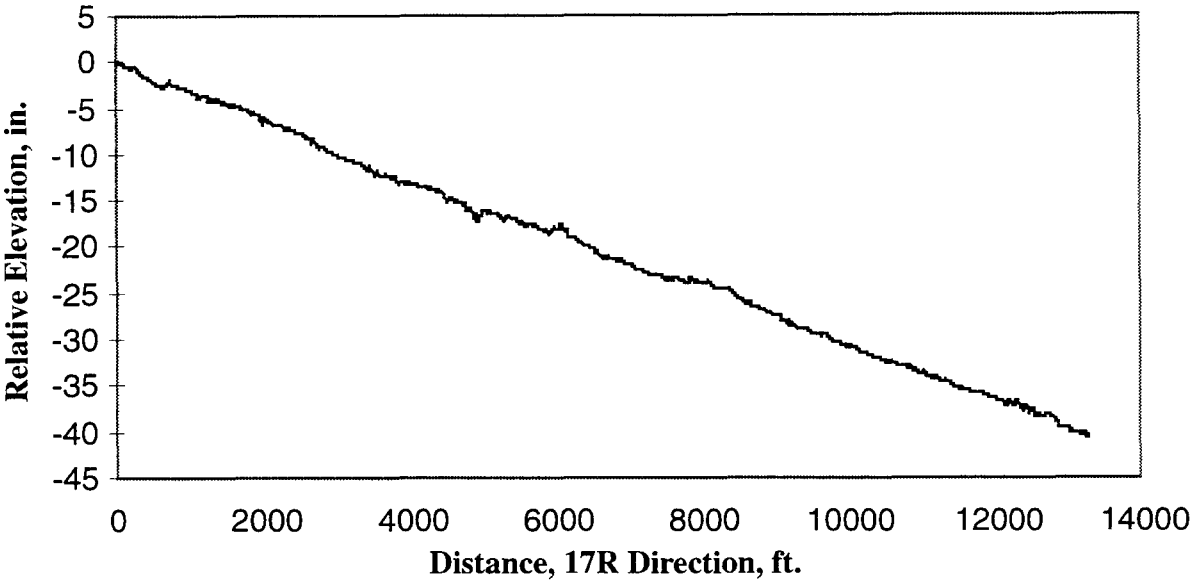

Figure 5.1. Profile of Runway 17R/35L, moving South on RW17.

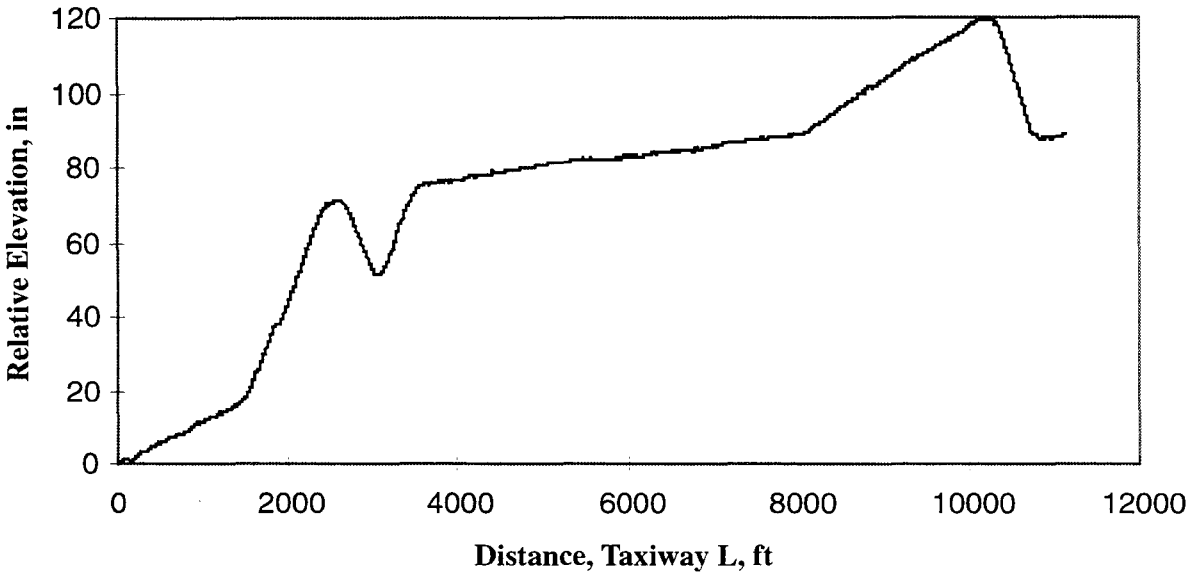

Figure 5.2. Profile of Taxiway L, moving north.

The Boeing Corporation has performed detailed studies that produced a correlation between vertical accelerations and relative fatigue damage to aircraft (Ref. 1). Figure 5.3 presents a curve that indicates how vertical accelerations affect the fatigue life of an aircraft. The graph shows relative damage, based on a 0.35g (or 0.35 times the acceleration of gravity) vertical acceleration. For example, a vertical acceleration of 0.45g would cause over 30 times as much damage relative to a 0.35g acceleration, i.e. a 30% increase in acceleration increases damage 3000%. An acceleration of 0.55g would cause 1000 times

more damage as a 0.35g acceleration. Another way to look at this effect is to say that runway roughness that causes a 0.45g vertical acceleration during a takeoff or landing operation would cause as much damage to the aircraft as 30 operations on a smooth runway which produces an acceleration of only 0.35g. At a vertical acceleration level of 0.4g, or 0.4 times greater than the acceleration of gravity, the effects on aircraft can become detrimental. In addition, vertical accelerations of this magnitude begin to have adverse effects on pilots and passengers.

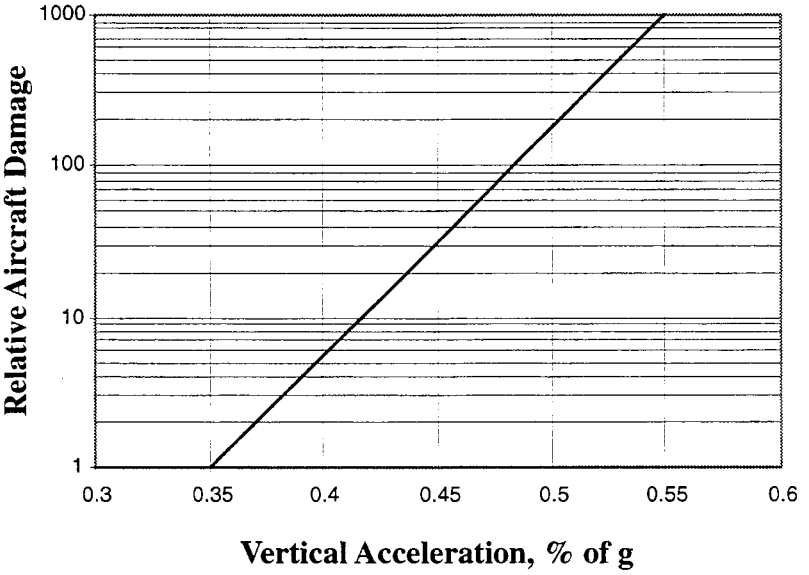

Figure 5.3. Relative Aircraft Damage Due to Vertical Accelerations (Ref. 1).

Vertical acceleration values that Runway 17R and Taxiway L exhibited will be presented in the section of this chapter relating to the computer programs TAKEOFF and LANDING, which were produced by Mr. Gerardi and APR Consultants. These computer programs calculate the vertical accelerations at the pilot station and at the aircraft's center of gravity as well as the related loads on the pavement due to the vertical accelerations at the nose gear and the main landing gear.

Riding Quality Evaluation

The Ride Quality Index (RQI) is an arbitrarily computed scale developed by Mr. Tony Gerardi based upon the accelerations observed in the simulation of several subject aircraft. A runway with an RQI value below 3.00 is considered to be in good condition, from a roughness, or ride quality standpoint.

TABLE 5.1. RQI Values, Runway 35L.

	Location, ft.			Straightedge
Section No.	From	To	RQI	Deviation, in.
1	0	500	1.96	
2	500	1000	2.09	
2	500	1000	2.09	
3	1000	1500	1.77	
3	1000	1500	1.77	
4	1500	2000	1.23	
4	1500	2000	1.23	
5	2000	2500	1.46	
5	2000	2500	1.46	
6	2500	3000	1.22	
6	2500	3000	1.22	
7	3000	3500	1.28	
7	3000	3500	1.28	
8	3500	4000	1.53	
8	3500	4000	1.53	
9	4000	4500	1.20	
9	4000	4500	1.20	
10	4500	5000	1.42	
10	4500	5000	1.42	
11	5000	5500	1.18	
11	5000	5500	1.18	
12	5500	6000	1.39	
12	5500	6000	1.39	
13	6000	6500	1.60	
13	6000	6500	1.60	
14	6500	7000	1.18	
14	6500	7000	1.18	

TABLE 5.1. RQI Values, Runway 35L (continued).

	Location, ft.			Straightedge
Section No.	From	To	RQI	Deviation, in.
15	7000	7500	2.17	
15	7000	7500	2.17	
16	7500	8000	1.56	
16	7500	8000	1.56	
17	8000	8500	2.56	
17	8000	8500	2.56	
18	8500	9000	1.81	
18	8500	9000	1.81	
19	9000	9500	1.14	
19	9000	9500	1.14	
20	9500	10000	1.95	
20	9500	10000	1.95	
21	10000	10500	1.06	
21	10000	10500	1.06	
22	10500	11000	1.98	
22	10500	11000	1.98	
23	11000	11500	2.19	
23	11000	11500	2.19	
24	11500	12000	1.23	
24	11500	12000	1.23	
25	12000	12500	1.55	
25	12000	12500	1.55	
26	12500	13000	1.98	
26	12500	13000	1.98	
27	13000	13334	1.46	
	Average: 160			

Table 5.1 shows the RQI values for Runway 35L, calculated for each 500 ft. analysis section. The RQI values vary from a minimum of 1.06 to a maximum of 2.56 with an average of 1.60. The maximum value occurred in section 17 of Runway 35L (8000 - 8500 ft.), and the minimum value of 1.06 was at 10,000 to 10,500. As stated previously, a pavement section with an RQI value below 3.00 is considered to be in good condition. This table is modified from the APR Consultants' report of November 18, 1995.

Another analysis performed by Mr. Gerardi on each section of Runway 17R and Taxiway L is a straightedge simulation passing along the profile of the runway or taxiway. The 70 ft. straightedge measures the maximum vertical deviation of the pavement in inches from the straightedge. The length of the straightedge was chosen to be 70 ft. because this is approximately the distance between the main landing gear and nose gear on several types of commercial aircraft. Mr. Gerardi indicates that, based on experience, although the straightedge is not as consistent as the RQI value for the same pavement, a runway or taxiway with deviations of 1.5 inches or greater will cause pilot complaints. The straight edge deviations averaged 0.52 inch over the entire runway, and the maximum value was 0.91 inch. This measure of deviation is far below the 1.50 inch level described by Mr. Gerardi as the point where pilots will complain of roughness.

Since all the values, even the maximum value for the entire runway, are below 3.00, it can be inferred that Runway 17R/35L is in good condition, and is not presenting problems for pilots, passengers, for the aircraft or the pavement systems.

Taxiway L was also profiled in order to assess aircraft response to roughness at taxiway speeds. The RQI values are calculated at speeds between 9 and 39 knots only, whereas runways are analyzed at speeds up to rotation speed. The average RQI value for the taxiway is 1.95, while the maximum is 3.92 on Section 7 (3000 - 3500 ft). Since this section showed much a higher RQI value, further investigation was performed. The straight edge deviation average was 0.33 inch and the maximum was 1.46 inch. This maximum was observed in Section 7 as well.

The analysis of Section 7 consisted of two taxi simulations at constant speeds. One was at 27 knots and the other at 30 knots. While these speeds are relatively high for taxi operations, the analysis was performed at speeds that would produce responses that approach the limiting criteria for passenger and pilot comfort and for aircraft response.

The analysis previously described is based on the RQI values calculated by the roughness measurement method described above, and so the conclusions drawn in this section are only applicable to this measure of roughness. The next sections will investigate the vertical accelerations caused by roughness of the pavement on several types of commercial aircraft.

It is possible that the other types of analysis that will be performed in this chapter could show some deficiencies in the surface of the pavement. The TAKEOFF and LANDING programs will be used to analyze the same data to provide insight into the effect that the pavement roughness has on vertical accelerations in aircraft.

TAKEOFF and LANDING

The TAKEOFF and LANDING computer programs were developed by APR Consultants, Inc. These programs were used to calculate the vertical accelerations and pavement loads that occur when an aircraft takeoffs, lands or taxis. A discussion of vertical accelerations and their effects can be found in this report.

Introduction. In addition to the vertical accelerations experienced by the aircraft during takeoff, landing, or taxi operations, the programs calculate the loads on the pavement by the landing gear due to the vertical accelerations. This information is valuable because it can be used in calculations that will be used later to determine the stresses in the pavement due to the increased pavement loads. When the laboratory analysis and results are discussed in the next chapter, the increased pavement loads will be used in the fatigue calculations and in the remaining life predictions. Table 5.2 gives a list of aircraft that can be simulated by these programs, and the aircraft weight that is used for each.

TABLE 5.2. AIRCRAFT SIMULATED BY TAKEOFF AND LANDING COMPUTER PROGRAMS

Aircraft	Weight (lb.)
Cessna Citation 500	13,000
DC-9-40	114,000
737-200	117,000
727-200	160,000
707-320	306,000
L-1011	391,500
DC-10-10	440,000

Figures 5.4 and 5.5 show a sample of the output of the two programs, simulating a Boeing 737-200 aircraft. Figure 5.4 shows the vertical accelerations induced in the aircraft due to the roughness of the runway. The runway profile has been superimposed in the chart to show how the vertical accelerations and pavement loads are related to the profile of the facility.

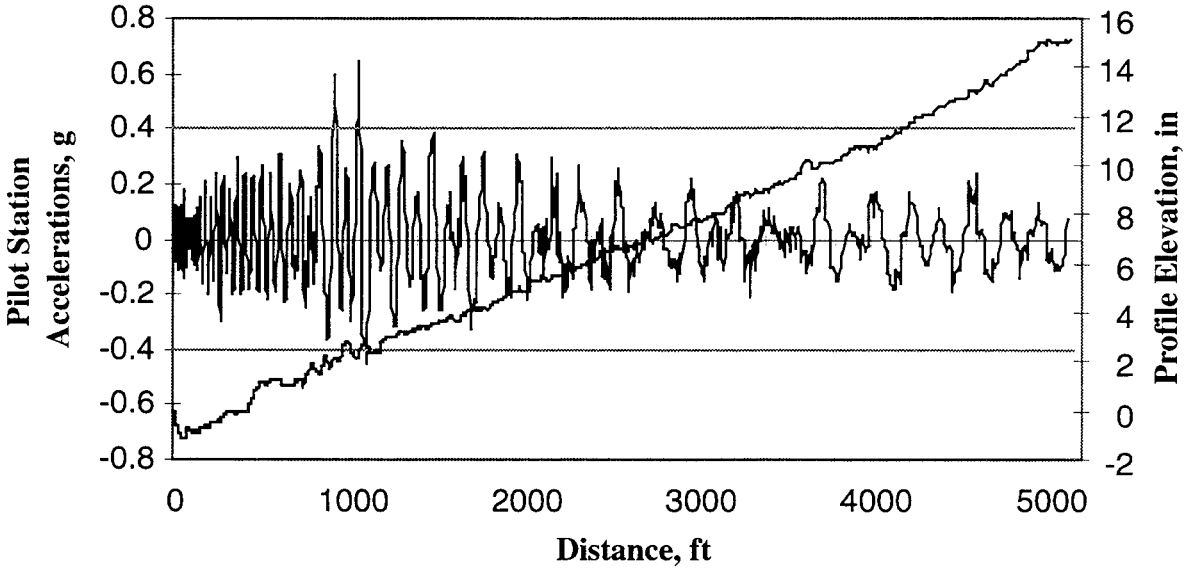

Figure 5.4. Vertical Accelerations at Pilot Station, Calculated by TAKEOFF, APR Consultants.

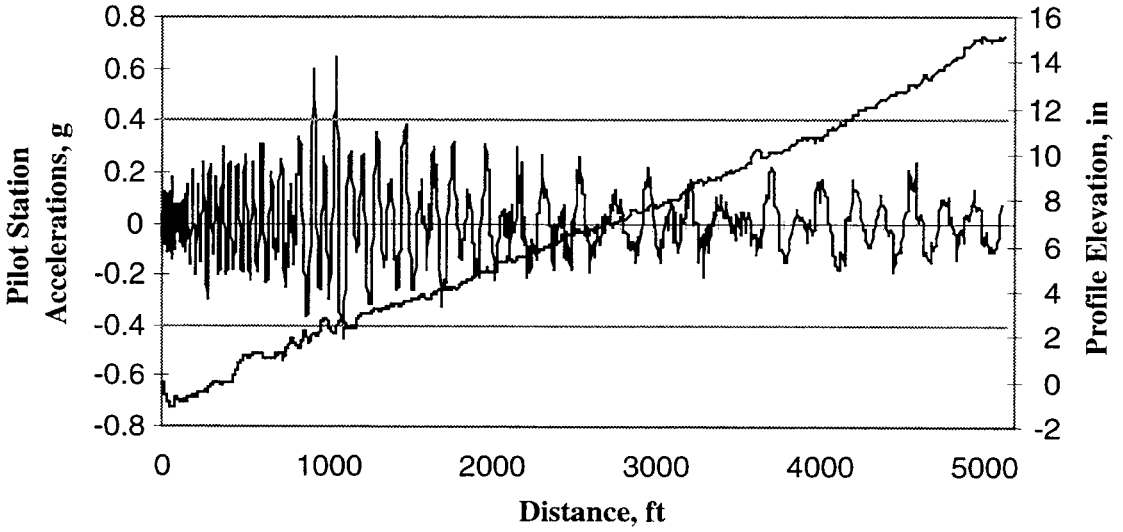

Figure 5.5. Pavement Loads at Main Gear During Takeoff Operation, RW35L.

It can be seen in these two figures that the vertical accelerations and the pavement loads at the main gear fluctuate more during and just after the aircraft has passed over a rough spot on the runway. The evaluation of the runway and taxiway pertaining to vertical accelerations will be made primarily on the magnitude of those accelerations, positive or negative. If an aircraft experiences, during an operation, one acceleration that is above the 0.4g limit discussed earlier, the entire operation is said to produce unacceptable accelerations.

TAKEOFF. The program TAKEOFF was used to evaluate Runway 17R/35L and Taxiway L regarding the roughness of the respective facilities. Table 5.3 gives the maximum vertical accelerations predicted for takeoff operations on Runway 17R and Runway 35L. The values in bold type are those that exceed the 0.4g criteria for limiting relative damage to aircraft and for pilot and passenger comfort. In this table, each type of aircraft was simulated in a takeoff operation at the runway threshold and at 2000 ft. from the threshold, or at the beginning of the original portion of Runway 17R. In each of the simulations, the accelerations at the pilot station (PS) are much greater than those at the center of gravity (CG). There does not seem to be a noticeable difference in the accelerations reported for takeoff operations at 0 or 2000 ft. from the threshold.

TABLE 5.3. VERTICAL ACCELERATIONS DURING TAKEOFF OPERATIONS

TAKEOFF					
		R17R		R35L	
Aircraft	Distance from Threshold	PS	CG	PS	CG
737-200	0	0.45	0.31	0.66	0.41
737-200	2000	0.44	0.29		
L-1011	0	0.31	0.15	0.23	0.14
L-1011	2000	0.29	0.16		
DC-9-40	0	0.33	0.24	0.35	0.30
DC-9-40	2000	0.32	0.18		

LANDING. Table 5.4 shows the maximum vertical accelerations produced during a landing operation. Again, the values in bold type are those that exceed the 0.4g criteria for limiting relative damage and for passenger comfort. It seems that runway 17R causes high accelerations at the pilot station (PS) for many of the simulations performed. The accelerations at the center of gravity (CG) approach the limiting criteria, but only one exceeds it. At the other end of the runway, landing in the 35L direction, the accelerations are much lower.

TABLE 5.4. VERTICAL ACCELERATIONS DURING LANDING OPERATIONS

		LANDING			
		R17R		R35L	
Aircraft	Distance from Threshold, ft.	PS	CG	PS	CG
737-200	500	**0.41**	0.28	0.32	0.25
737-200	1500	0.38	0.28		
737-200	2500	**0.61**	0.36		
737-200	3500	**0.47**	0.35		
L-1011	500	0.37	0.35	0.28	0.35
L-1011	2500	0.35	**0.43**		
DC-9-40	500	0.39	0.24	0.33	0.22
DC-9-40	2500	0.40	0.25		

Runway 17R was recently extended 2000 ft., and therefore the simulations were performed for several distances from the threshold. In Table 5.4, it can be seen that there is no difference between the landing operations that begin at 500 ft. from the threshold and those that begin 2500 ft. beyond the threshold. For two of the aircraft types the acceleration rises slightly, and in the other the PS acceleration decreases.

Taxiway L. On Taxiway Lima, two different types of simulations were performed. First, TAKEOFF was used to simulate a 20 knot taxiing operation. Then, in order to evaluate the effect of a takeoff operation on the taxiway, in cases of emergency, both the TAKEOFF and LANDING programs were used to simulate these aircraft in takeoff and landing operations. For the taxiing operation, it can be seen in Table 5.5 that the accelerations at the pilot station exceed the limit for all three aircraft types that were simulated. The taxi simulations performed on taxiway Lima were done at a constant 20 knot speed over the entire taxiway. As would be expected, however, the taxiway is much rougher than the runways. The reported vertical accelerations for takeoff and landing operations are much greater than those for the runways. In fact, most of the reported accelerations are in excess of the 0.4g limit, and many are far greater than the range of values reported in Figure 5.3.

Implementation of Results. The results which have been presented in the previous sub-sections of this chapter can be implemented fairly easily. The TAKEOFF and LANDING programs identify, by nature, rough sections of airport pavements. Using the

TABLE 5.5. VERTICAL ACCELERATIONS ON TAXIWAY LIMA.

TAXIWAY LIMA									
Aircraft	Distance from Threshold	20 Knot Taxi PS	20 Knot Taxi CG	Takeoff (north) PS	Takeoff (north) CG	Takeoff (south) PS	Takeoff (south) CG	Landing (north) PS	Landing (north) CG
737-200	0	**0.68**	**0.47**	**0.86**	**0.64**	**0.73**	**0.48**	**0.62**	**0.46**
737-200	2000			**0.63**	**0.59**				
L-1011	0	**0.42**	0.18	**0.62**	0.36	0.33	0.18	**0.61**	0.40
L-1011	2000								
DC-9-40	0	**0.41**	0.35	**0.70**	**0.53**	**0.62**	**0.46**	**0.78**	**0.54**
DC-9-40	2000			**0.66**	**0.63**				
Cessna Citation 500	0			0.36	0.25	**1.00**	0.30	**1.06**	**0.41**
Cessna Citation 500	2000			**1.76**	**0.50**				

report and the results in Appendix F of this report, Airport Management can make decisions on which sections of the airport pavements are in greatest need of repair to minimize damage to aircraft and discomfort to passengers and pilots.

In addition to identifying rough sections of the airport pavement, the programs described herein also have the ability to preview the effect of maintenance. Rough sections of a runway can have simulated maintenance and the analysis can be performed once again to view the results of a repair in a particular section. In this manner, several maintenance alternatives can be viewed and the one that provides the most improvement for the least cost can be identified.

Root Mean Squared Vertical Acceleration

The root mean squared vertical acceleration (RMSVA) is a method for reducing road profiles to a set of quantities which are easy to handle and best characterize the profile of the road. It was initially developed to study highway profiles and to more easily quantify the present serviceability index of highways. The procedure that follows is taken from CTR Report 354-1F (Ref. 2). The measurement is the *root mean square difference between adjacent profile slopes, where each slope is the ratio of elevation change to distance over a fixed distance increment.* The basic equation to calculate the second derivative, an initial step in finding the RMSVA, is as follows:

$$[S_b]_i = \frac{(Y_{i+k} - 2Y_i + Y_{i-k})}{(k \cdot s)^2} \tag{5.1}$$

where:

s = the sampling interval,

k • s = b = the horizontal distance, or the base length corresponding to Va_b, and

Y_i = the elevation at point i along the profile.

The root mean squared vertical acceleration equation is shown below.

$$VA_b = C\left[\sum_{i=k+1}^{N-k} \frac{(s_b)_i}{(N-2k)}\right]^{1/2} \tag{5.2}$$

where:

N = number of profile data points, and

C = a constant required for unit conversion.

Using the above equations, the CTR staff has written a simple computer program to analyze the profiles taken by Mr. Gerardi at the DFW Airport. Because the wavelengths of airport pavements affect aircraft at different levels than those used for highway applications, the computer program computes the RMSVA at longer wavelengths as well as shorter ones. The following table shows the results of the RMSVA analysis on Runways 17R, 35L, and Taxiway Lima. As can be seen in Table 5.6, the results for 17R and 35L are the same. Since they are the same runway, measured from opposing directions, their RMSVA values are the same.

TABLE 5.6. RMSVA VALUES FOR RUNWAY 17R/35L AND TAXIWAY LIMA.

RMSVA wavelength, ft	17R / 35L	Lima
1	9.779	15.226
2	3.067	4.758
4	1.041	1.583
8	0.369	0.558
16	0.140	0.204
32	0.041	0.085
64	0.013	0.055
128	0.004	0.043
256	0.001	0.024
512	0.000	0.009

For highway applications, CTR Report 354-1F produced several regression equations to estimate the present serviceability index of a specific section of highway. In order to provide some quantification of the roughness of the runway and taxiway, the following regression equation was used (Equation 6.10 from CTR Report 654-1F):

$$PSI = 4.34 - 0.092 \cdot VA_4 - 0.47 \cdot VA_8 \qquad (5.3)$$

For Runway 17R/35L, the PSI value would be 4.07, and for Taxiway Lima, 3.93. As stated earlier, for aircraft applications the vertical accelerations at longer wavelengths would have more of an effect on the performance of the airport pavement. Further research should be performed to estimate the PSI of airport pavements, or to provide an application for RQI values, which were discussed previously. It should be noted, however, that Mr. Gerardi has established a procedure and equations for correlating the profile with RQI values. These values are reported using the TAKEOFF and LANDING programs, as discussed earlier.

CORING PROGRAM

Several different coring programs were included in the testing plan submitted to the DFW technical advisors for review. First, a coring and testing program was developed for Taxiway K before its reconstruction. The intent was to identify the properties of the concrete at the end of its service life. Another coring and cross-hole testing program was implemented for Runway 17R/35L, as well as for Taxiway L.

From the core holes, material from several layers was removed. The Portland cement concrete layer and the cement treated base were removed on all the runway and Taxiway L locations. Material from the lime treated subbase was also removed from many of the core holes for the cross-hole testing that was performed.

Concrete Coring Locations

The coring that was performed on the pavements at the airport was done by Maxim Engineers located at the DFW airport. The purpose of the coring was to obtain concrete samples to test in the laboratory, and to provide holes deep enough to perform the cross-hole testing, which will be discussed in the next section.

Since the aircraft wheel path is approximately located at the middle of the first slab adjacent to the centerline of the runway and the taxiways, it was desirable to obtain core samples from this location so as to test the properties of the concrete from a loaded portion of concrete. This means that the concrete from the wheelpath section has been loaded by numerous aircraft over its service life and approximately half of the concrete cores were taken from the wheelpath area of the pavement. The other half of the cores were taken from a portion of the pavement which has seen very little aircraft loads, near the edge of the pavement. The furthermost slab from the centerline sees little, if any traffic loading over the years. The concrete taken from this location represents concrete that is new, with the exception of environmental loads.

This difference in the historic loading patterns of the two locations provides a basis for analysis. A comparison can be made between the properties of the concrete taken from the wheel path and of those of the concrete taken from the non-trafficked area. In addition to observable differences of the trafficked and untrafficked concrete cores, differences were also observed in the testing data from concrete cores taken from the north end of the runway and cores taken from the south end.

The figures in Appendix B show the location of all cores that were taken from the pavements on Runway 17R/35L, Taxiway L, and Taxiway K, for this project. Table 5.7 shows the core numbers assigned to the cores as they were extracted from the pavement. The core numbers correlate with the database of test results presented in the next chapter.

TABLE 5.7. EXTRACTED CORES: LOCATION AND CORE REFERENCE NUMBER

Core Number	Branch	In / out of traffic lane
RA1	R17R	in
RA2	R17R	in
RA3	R17R	in
RA4	R17R	out
RA5	R17R	out
RA6	R17R	out
RA7	R17R	out
RA8	R17R	out
RA9	R17R	in
RA10	R17R	out
RA11	R17R	in
RA12	R17R	in
RB1	R17R	in
RB2	R17R	in
RB3	R17R	in
RB4	R17R	out
RB5	R17R	out
RB6	R17R	out
RB7	R17R	out
RB8	R17R	out
RB9	R17R	in
RB10	R17R	out
TL1A	TW L	in
TL1B	TW L	in
TL1C	TW L	in
TL2D	TW L	out
TL2E	TW L	out
TL2F	TW L	out
TL3D	TW L	out
TL3E	TW L	out
TL3F	TW L	out
TL4A	TW L	in
TL4B	TW L	in

TABLE 5.7. EXTRACTED CORES: LOCATION AND CORE REFERENCE NUMBER (continued)

Core Number	Branch	In / out of traffic lane
TL4C	TW L	in
TL5A	TW L	in
TL5B	TW L	in
TL5C	TW L	in
TL6D	TW L	out
TL6E	TW L	out
TL6F	TW L	out
TL7A	TW L	in
TL7B	TW L	in
TL7C	TW L	in
TL7E	TW L	out
TL8D	TW L	out
TL8F	TW L	out
TK29F	TW K	
TKP59A	TW K	
TKP55B	TW K	
TK67A	TW K	
TKP55E	TW K	
TK63F	TW K	
TK63G	TW K	
TKP55G	TW K	
TKP59E	TW K	
TKP55A	TW K	
TKP59G	TW K	
TKP60-6	TW K	
TKP63C	TW K	
TK67F	TW K	
TK67E	TW K	
TK56B	TW K	
TK63A	TW K	
TK56-3	TW K	
TK29E	TW K	

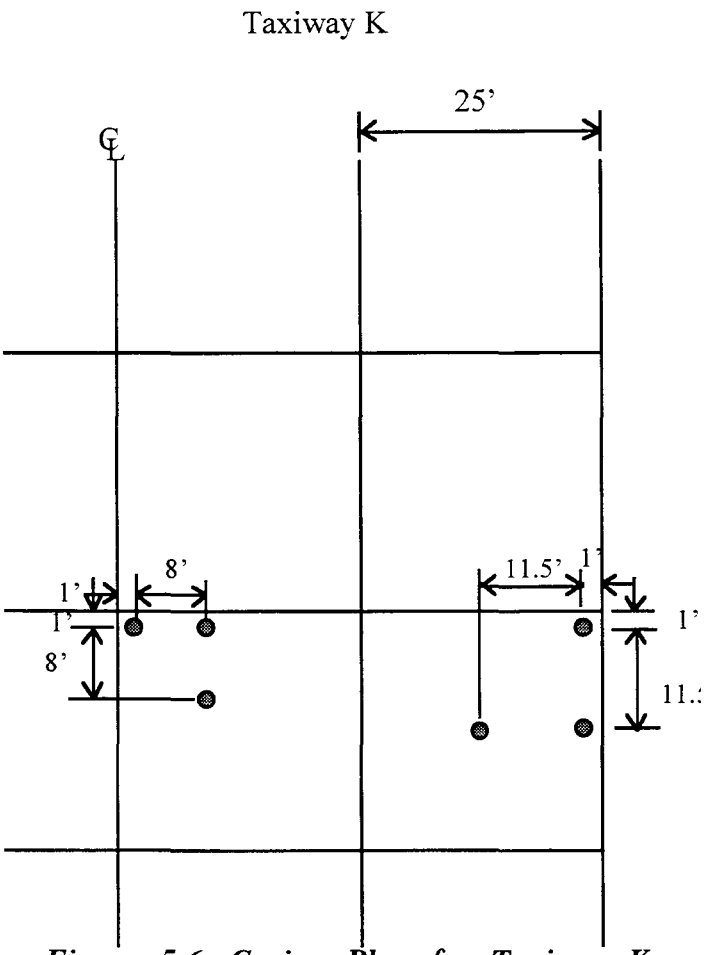

Figure 5.6. Coring Plan for Taxiway K.

The diagram in Figure 5.6 shows the coring plan for Taxiway K, which was reconstructed shortly after the cores were taken from the concrete. Two coring plans were made for the other sets of cores that were taken from the airport, one for Runway 17R/35L, and one for Taxiway L. These coring plans, and a more detailed plan for Taxiway K, are found in Appendix B of this report.

Shelby Tube Samples

Shelby tube samples of the lime stabilized subgrade and natural subgrade were obtained from beneath Taxiway L and Runway 17R/35L using the core holes. However, the Taxiway samples were extruded from the tubes by, Maxim Technologies, the DFW contractor taking the samples rendering them useless for testing. The runway samples were delivered as requested still in the tubes, however the ends were only partially sealed with

wax. However, the samples were unable to be tested due to disturbance caused by the lack of good sealing.

CROSS-HOLE TESTING

The stiffness determined from the cross-hole tests were expressed in terms of Young's modulus of each material: concrete surface layer, cement-treated base, lime-stabilized subgrade (also called the subbase) and natural subgrade. The results show that, on Runway 17L/35R, the trafficked areas have cumulative damage compared to the untrafficked areas. This damage is shown in Table 5.8 by the decrease in Young's modulus of each material. Similar results were also determined at Taxiway L as shown in Table 5.8.

TABLE 5.8. Damage from Cumulative Traffic to Pavement Layers Expressed as a Change in Young'S Modulus of each Layer.

	Runway 17L/35R	Taxiway L
Material	$E_{trafficked}/E_{untrafficked}$	$E_{trafficked}/E_{untrafficked}$
Concrete Surface Layer	0.87	0.95
Cement-treated Base	0.54	0.68
Lime-treated Subbase	0.75	0.77
Natural Subgrade	0.83	0.88

The results shown in Table 5.9 were determined from measurements performed in midslab areas. Cross-hole seismic tests were also performed in the base, subbase and subgrade materials beneath transverse joints and longitudinal saw cuts. In each case, the moduli of the materials ranged from 35 to 95% of the corresponding moduli measured in the midslab areas. These results clearly show that additional damage has occurred to the supporting materials beneath the joints in the trafficked areas. The effect of this reduction in Young's Modulus is that the life of the pavement is significantly reduced. This effect is discussed in more detail in Chapter 6.

ROLLING DYNAMIC DEFLECTOMETER

The Rolling Dynamic Deflectometer (RDD) was described in short detail in Chapter 4. This chapter will present a fully detailed description of the device and of the analysis that was performed on the RDD results. The RDD is a new device, and as such, the full scope of what can be determined through data analysis is not known. Several conclusions can be made, however, about the pavements at the airport, which will be discussed in this section.

TABLE 5.9. DFW CROSS-HOLE TEST RESULTS

Layer	North Runway E(ksi)	South Runway E(ksi)	EK E(ksi)	K7 E(ksi)	EM E(ksi)
Trafficked					
Concrete	5413	4588	5859	5284	4929
CTB	340	422	242	225	196
LTB	259	138	166	129	94
Subgrade	11	26	20	30	14
RDD Deflection	3.98	3.78	3.16	3.03	3.54
Untrafficked					
Concrete	5472	6085	6087	5745	5002
CTB	727	679	342	395	233
LTB	262	275	281	112	110
Subgrade	15	18	N/A	33	15

Analysis of RDD Deflection Profiles

Figure 5.7 is the longitudinal deflection profile of Runway 17R/35L normalized to a 20-kip load. Notice that the 2000-ft. extension of the runway which was only two years old has significantly higher deflection. Although, analysis of the runway extension was specifically excluded from our research, it appears that a significantly reduced pavement life should be expected.

For comparison purposes, a selected portion of Runway 17L/35R RDD deflection profile is shown in Figure 5.8. Notice that the deflection profile of Runway 17L which had not been opened to traffic has significantly lower deflection with less variation between the joints and midslabs.

Figure 5.9 shows the transverse profile of Runway 17R/35L at 8187. The large deflection peaks occur at the centerline joint (100 ft.) and the keyed but undowelled joints (50 and 150 ft.). Smaller peak values are noticeable between each construction joint where the longitudinally sawed reinforced joints are located. The poor performance of the doweled joints are evident on all the profiles. All the longitudinal RDD profiles are provided in the data appendices and are depicted in reference to the slabs on the delivered MicroStation design file.

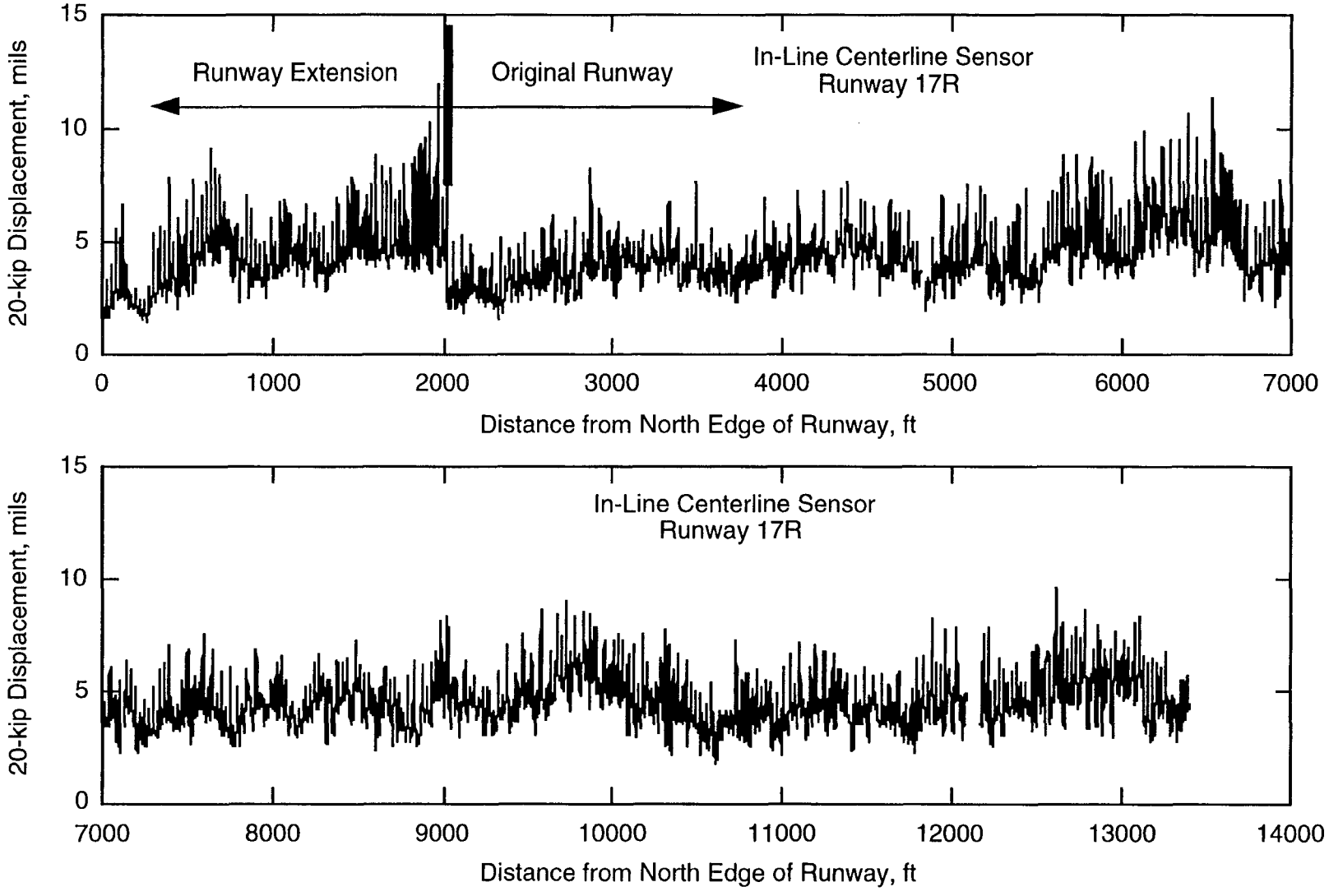

Figure 5.7. RDD Deflection Profile of Runway 17R.

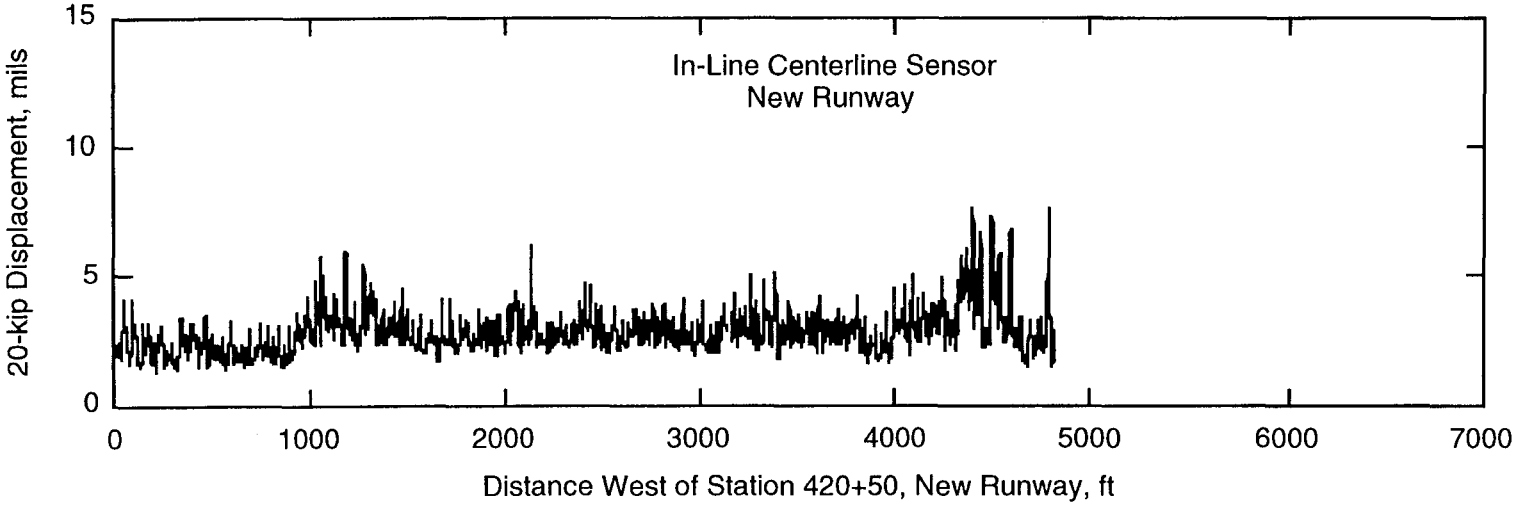

Figure 5.8. Partial RDD Deflection Profile of Runway 17L.

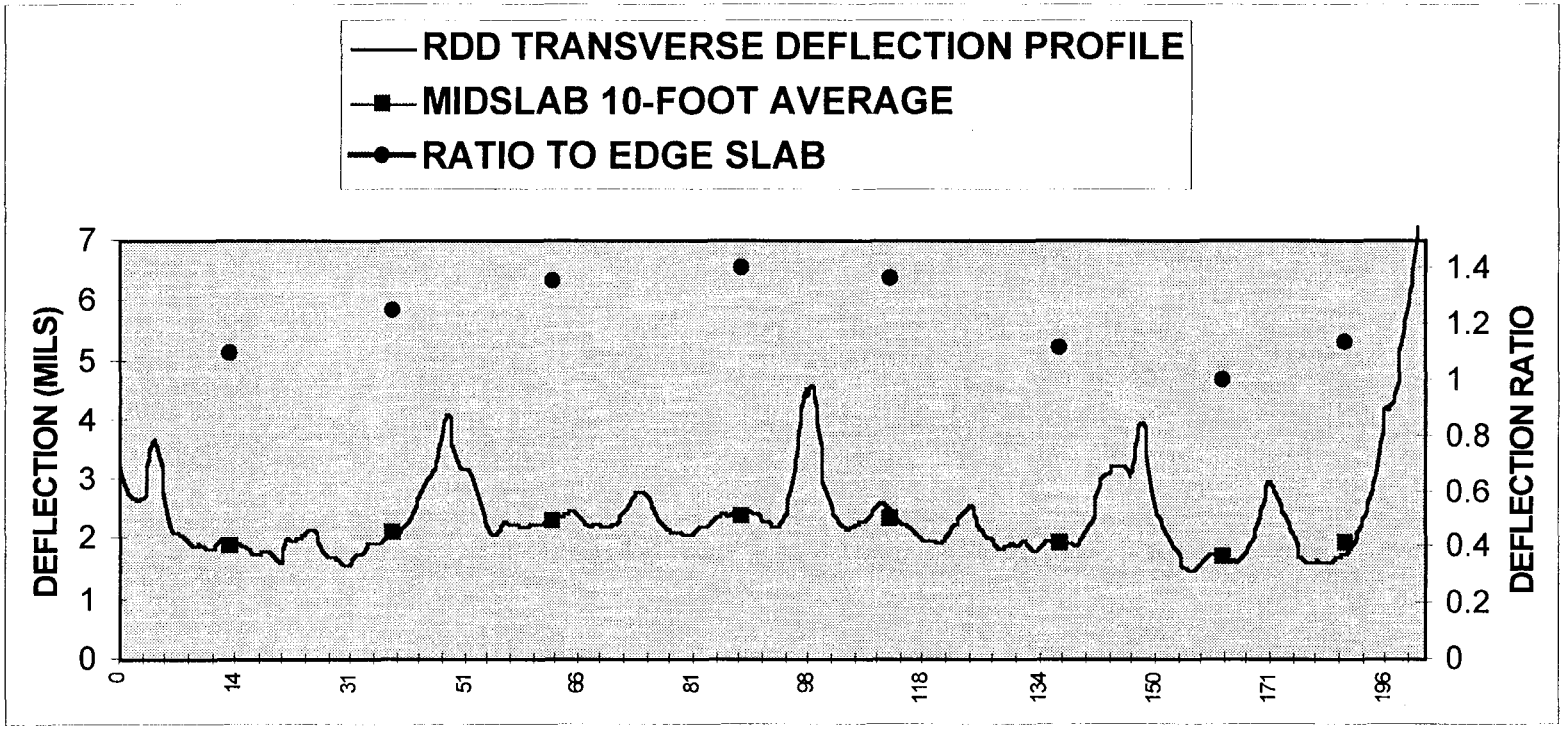

Figure 5.9. Runway 17R/35L Transverse Deflection Profile.

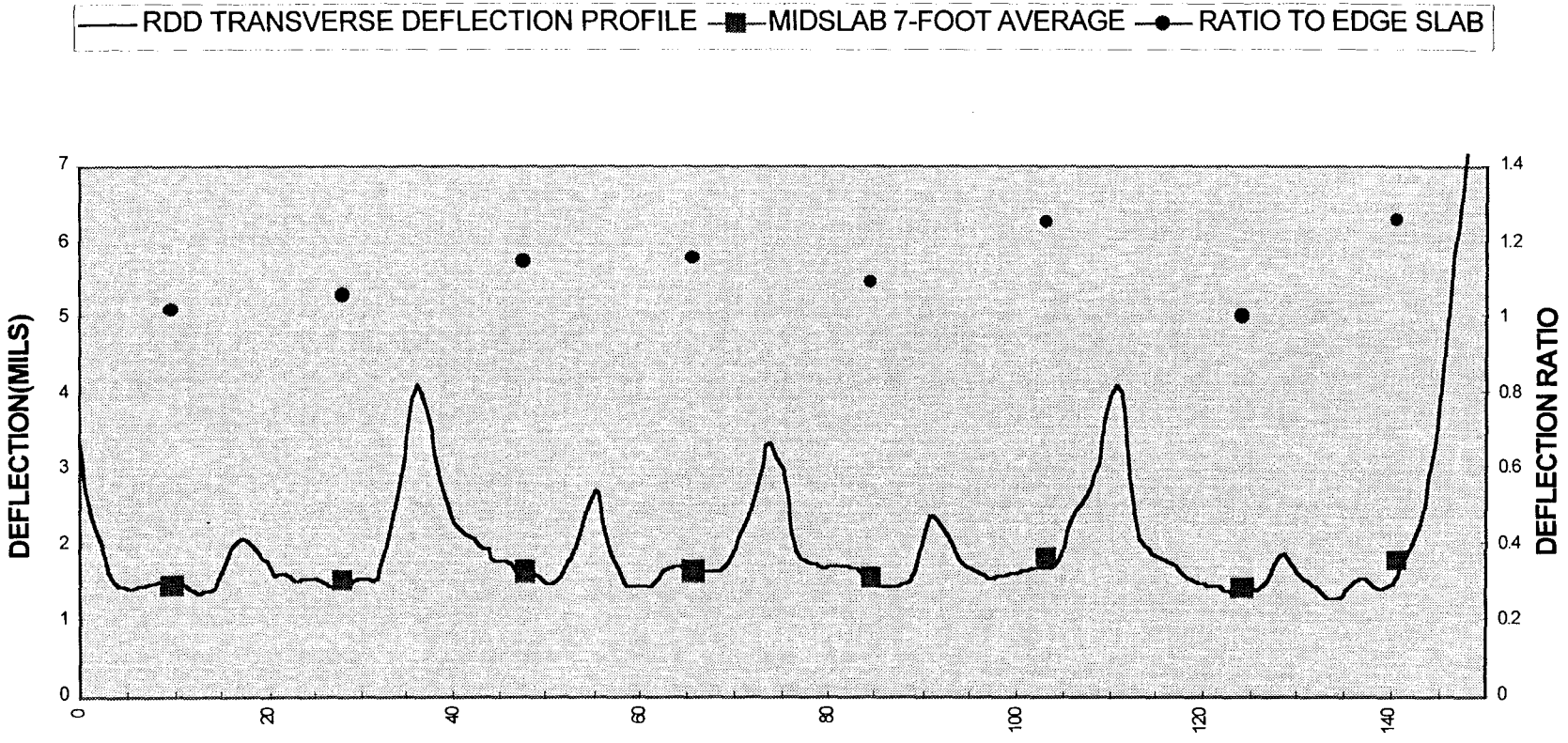

Figure 5.10. Runway 17L/35R Transverse Deflection Profile.

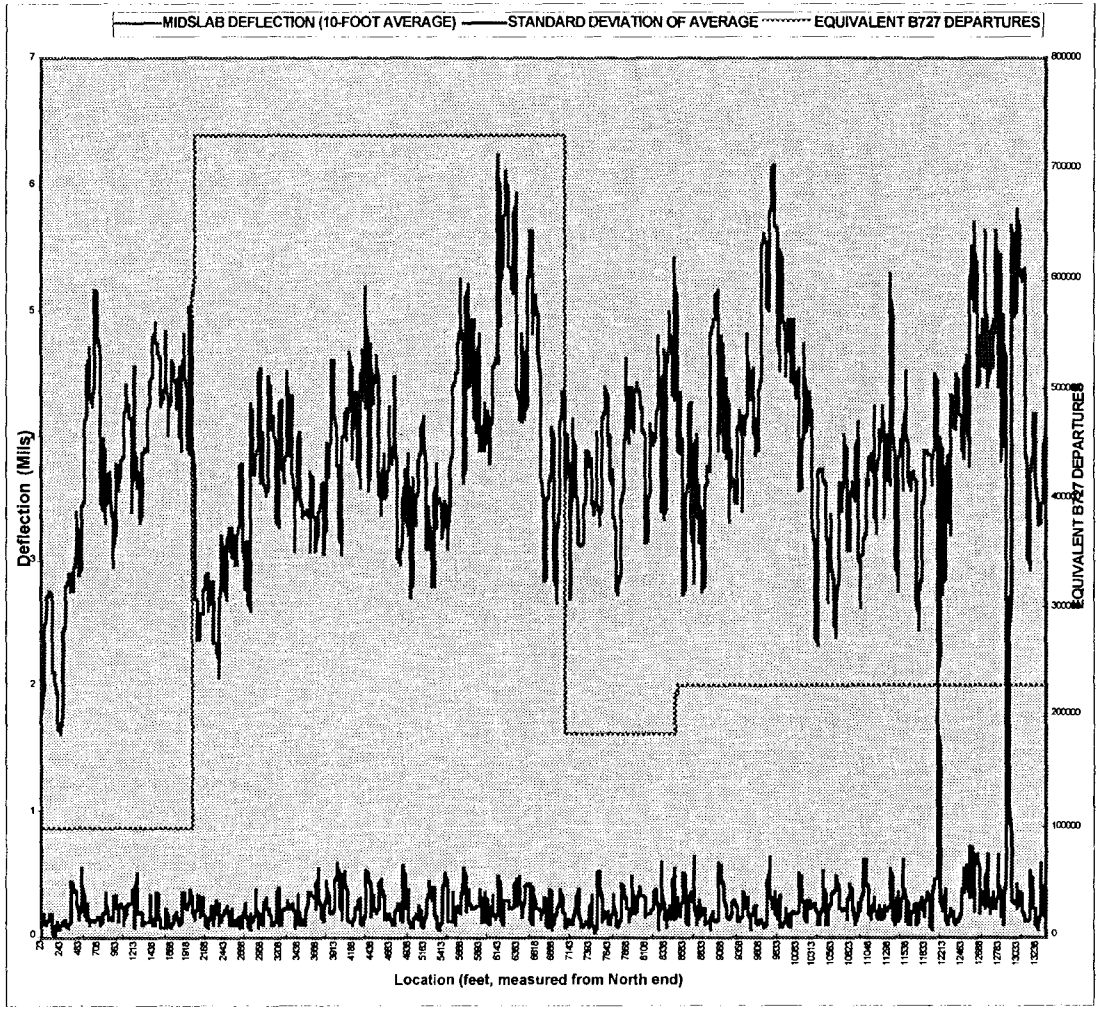

Figure 5.11. Runway 17R/35L Midslab RDD Deflections.

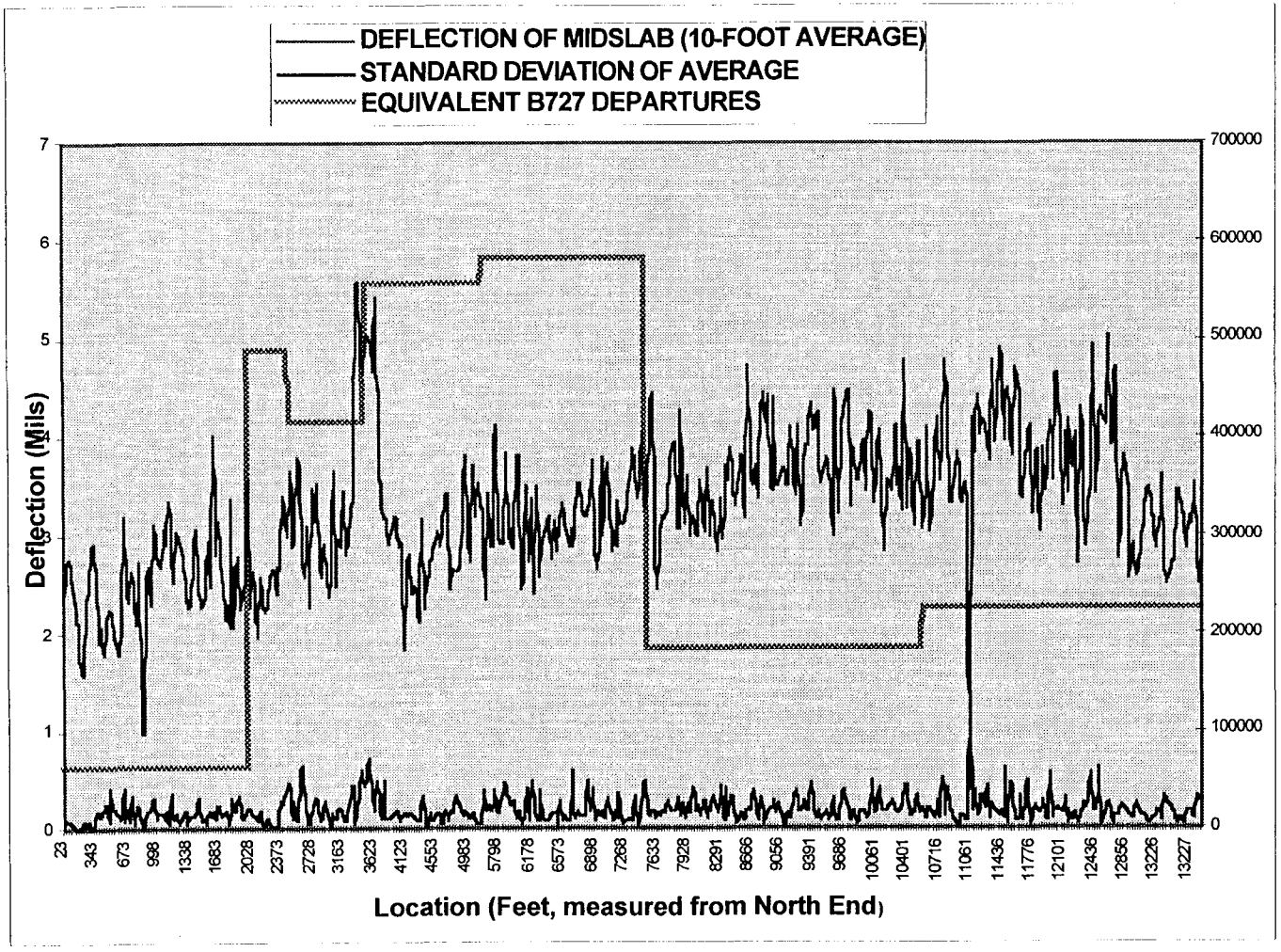

Figure 5.12. Taxiway L Midslab RDD Deflections.

Additional analyses were performed on the transverse and longitudinal data files using a computer program to locate the joints and then calculate on average midslab deflection and standard deviation. In Figure 5.9 notice the average midslab values across the runway profile. The figure shows that even the midslab deflection at the slab closest to the shoulder is influenced by the free end conditions. Also in Figure 5.9, the ratio of the midslab 10-ft. Average deflection to a reference deflection near the edge of an untrafficked slab and are plotted as dots using the scale on the right. From Figure 5.9 it can be seen that the two midslab points in the keel section (87.5 and 112.5 ft.) have 30 to 40 percent greater deflections than the midslab average at 162.5 ft. This greater deflection is due to aircraft trafficking, even though the transverse profile shown is in the area of lightest accumulated traffic. Unfortunately, identifying evidence of trafficking was not part of our testing plan. Therefore, we have an insufficient number of transverse profiles to substantiate this since the transverse profiles were not picked in the best location to demonstrate deterioration due to trafficking. In Figure 5.9, you can also note that higher than normal ratio are observed at distances of 37.5 ft. and 62.5 ft. from the left edge. However, upon close examination those slabs are receiving traffic because of the high speed exit taxiway adjacent to those slabs which cause aircraft to move closer to the west edge.

In Figure 5.10, compare the transverse profiles of runway 17L/35R which was tested before it was opened to traffic with the profile in Figure 5.9. Notice that the new runway does not exhibit a keel section with increased deflection. The effect of this deflection in the keel section of Runway 17R, will be discussed in the following section.

Figure 5.11 shows the longitudinal plot of the midslab deflection averaged over 10 ft. with its standard deviation for the entire length of Runway 17R/35L. The areas of highest deflection are the areas of greatest concern for future performance under traffic. Those areas which receive heavy traffic and have high deflections are most likely to show load related distress sooner.

In Figure 5.11, the midspan average plot is shown for Taxiway L. The taxiway generally has less average midspan deflections under a 20 kip load than the runway. Notice in Figure 5.11 that there appears to be an abnormally high (5 mils) around the 3600-ft. location. When this taxiway was tested, preparation for slab replacements were started and those slabs had already been saw cut into smaller free slabs. This higher deflection would indicate a worst case limit for pavement performance.

Evaluation of Different Joint Types

This section presents the analysis procedures and the results of the analysis of the data that was collected by the Rolling Dynamic Deflectometer (RDD) on Runway 17R/35L, Taxiway L, and

Runway 17L/35R. The data was collected during the week of August 26, 1996. In addition to this information, data collected by the RDD on Taxiway L in February, 1995, will be included in the analysis for comparison. The analysis contained in this section will provide the staff of the Dallas / Fort Worth International Airport with a tool to evaluate the load-carrying condition of the concrete pavements at the airport and to schedule maintenance and other rehabilitation.

Introduction. As a concrete pavement is subjected to constant repetitive loads over time by heavy aircraft, the concrete loses stiffness, and provides less resistance to deflection induced by loads as it begins to fatigue. This concept is presented in Figure 5.13 which shows that as more equivalent loads are applied to a concrete pavement, the deflections will increase after a certain point, when the concrete becomes fatigued. Eventually, failure results in the pavement.

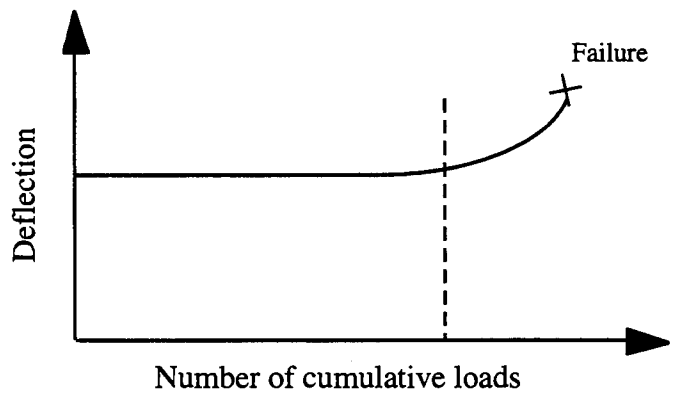

Figure 5.13. Increase in deflection as number of cumulative loads reaches maximum.

It is possible to measure this phenomenon in the pavements at the DFW airport using the Rolling Dynamic Deflectometer. The vertical dashed line in Figure 5.13 represents a limit whose location on the load / deflection curve can be set by airport management and engineers depending on rehabilitation strategy, funding, or other policy, and after understanding the effects of fatigue on a pavement.

As Figure 5.13 indicates, toward the end of a concrete pavement's service life, the deflections produced by loads become quite large. This increase in deflection can indicate that fatigue cracking is imminent, or that it is becoming worse. Comparing the deflections on a new pavement to those on an older pavement under the same loads, an idea can be inferred as to the remaining life of the pavements. As already mentioned, the RDD vehicle has the capability of applying loads to the pavement and measuring the deflections induced by those loads. Upon

analysis, this information can provide critical information relating to the condition of the pavement structure. These topics will be discussed in this section.

Notation and RDD Test Configuration. Figure 5.14 shows a plan view and a cross section of Runway 17R/35L from the centerline to the edge of the pavement. There are essentially four slabs between the centerline and the edge. The joints between slabs are denoted A through D, beginning at the centerline joint. Examining the cross section, the centerline joint (A) and joint C are construction joints. The former has dowels and the latter does not have dowels, but has a keyed section. Joints B and D are sawed longitudinal contraction joints, and joint E is the edge where the asphalt shoulder abuts the runway. The "X" patterns in Figure 5.14 represent the deflection measurement instruments mounted on the RDD to receive deflections in the pavement. In the figure, there are two sets of the pattern to indicate how the RDD deflection receivers can be placed as it is rolling along the pavement. The configuration of the X patterns in Figure 5.14 is presented in more detail in Figure 5.15.

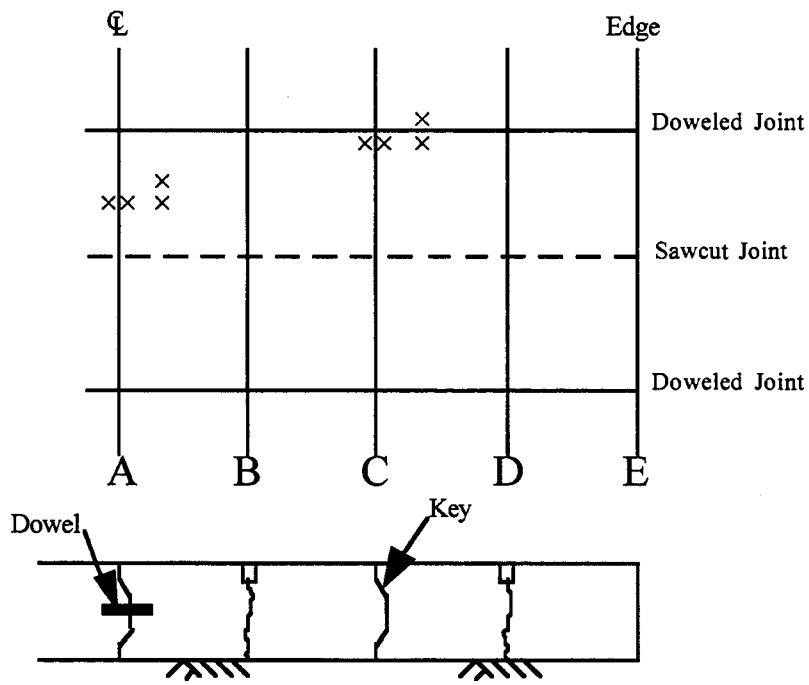

Figure 5.14. Slab Layout and RDD Test Configuration on Runway 17R/35L.

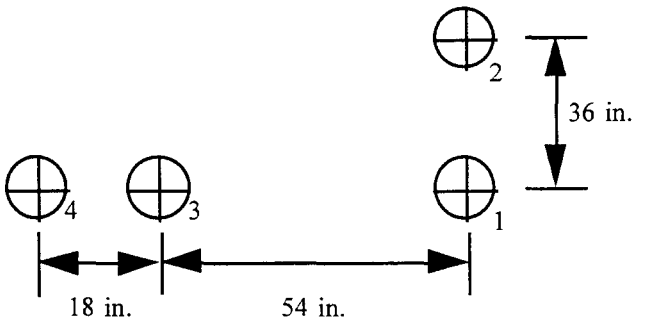

Figure 5.15. Configuration of RDD sensors.

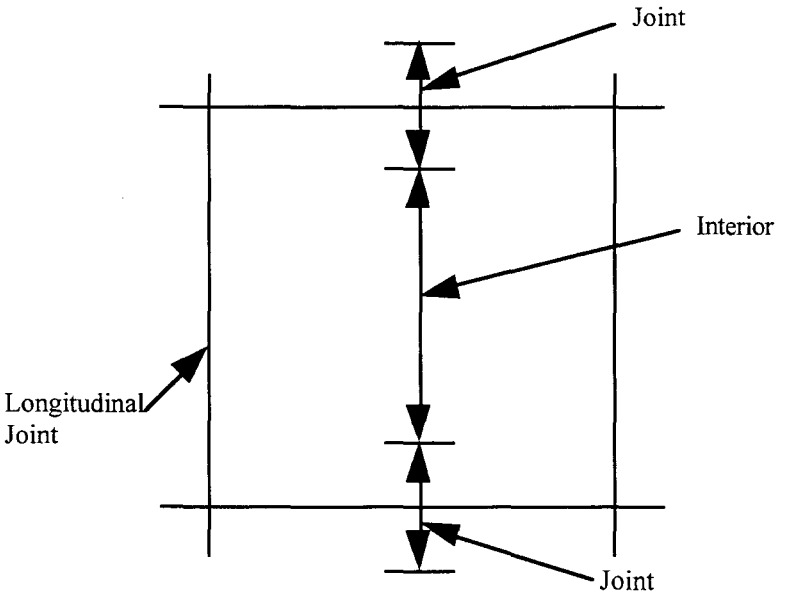

Figure 5.16. Definition of Interior and Joint Locations on Slabs.

The definition of interior or joint on a slab will depend on its deflection characteristics. Since slabs have greater deflection at the joint than at the interior of the slab, which is not due to fatigue, but to support and to load transfer at the joint, the point at which the deflection begins to increase near a joint is called the zone of influence. The zone of influence of the joint may be larger in some slabs that have lost subbase support near the joint, or that have lost load transfer efficiency. A more direct definition of the zone of influence is given in Figure 5.17.

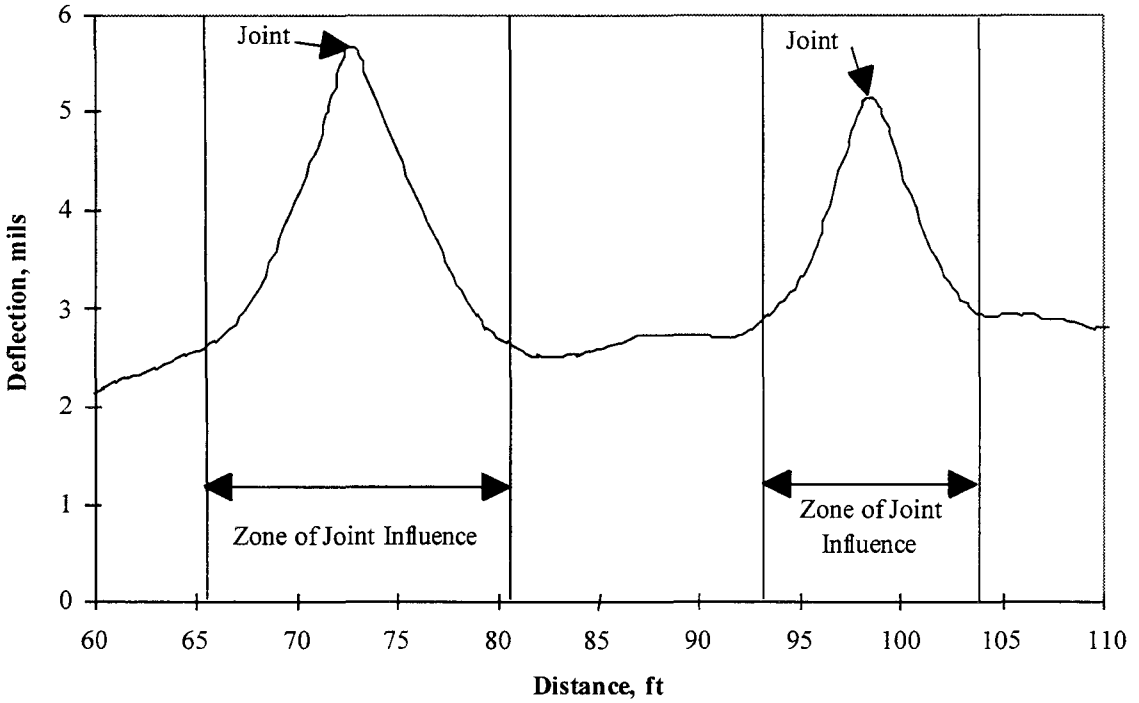

Figure 5.17. Joint Zone of Influence Based on Deflection Measured by RDD.

The notation for deflection measurements throughout the remainder of this section will reference the slab letter, the sensor number, and if the measurement is taken at the interior of a slab, or at a joint. For example, in the notation $w_{j\text{-}1A}$, the w stands for deflection, the j notes that the measurement is taken at a joint (an i would indicate that the measurement was taken at the interior of a slab), 1 means sensor one in the configuration in Figure 5.15, and A means that the slab tested is in lane A in Figure 5.14.

Comparison of Interior Deflections. Using the above notation, the following comparisons were made to determine if the slab adjacent to centerline, A, shows more fatigue than the third slab from centerline, C. Two comparisons can be made on measurements taken at or near the interior of the slab.

$$\frac{W_{i-1A}}{W_{i-1C}} > 1.0 \qquad (5.4)$$

$$\frac{W_{i-3A}}{W_{i-3C}} > 1.0 \qquad (5.5)$$

If any of the above cases exist, it is an indication that the center slabs along the centerline of the runway are experiencing more fatigue damage than the slabs between joints C and D, in the interior loading case. Ideally, the deflections in the two lanes would be equal, or similar. If this were the case, the ratios described above would be equal to one. Sections where the ratios described in Equations 5.4 and 5.5 are greater than 1.0 indicate locations that have experienced some level of fatigue, as indicated by the center two slabs showing greater deflections under load than the slabs in Lane C.

Another method of viewing the results of this analysis is to compare Figures 5.9 and 5.10 in this chapter. The deflections in Figure 5.9, from Runway 17R/35L, show that the pavement has been more fatigued on the center slabs than on the outside slabs. In addition, Figure 5.10, which shows identical measurements to those shown in Figure 5.9, but on Runway 17L/35R, the deflections are much more uniform over the width of the runway. This is due to the fact that Runway 17L/35R is new and had not had any aircraft traffic at the time the deflections were measured. The ratios as described above for the new runway are very close to 1.0, and the ratios for Runway 17R/35L are much higher, as high as 1.4.

Comparison of Longitudinal Joint Types. There are three methods with which to compare longitudinal joint types and their performance of on Runway 17R/35L and Taxiway L at the DFW airport, and for any other jointed concrete pavement at the airport. The first is to directly compare the deflections at the centerline joint, whose adjacent slabs have experienced the great majority of loads have been applied, to those at the joint just 50 ft. to either side of centerline. This comparison is similar to the comparison of interior deflections noted in Equation 5.5 above.

$$\frac{W_{cj-3A}}{W_{cj-3C}} = 1.0 \qquad (5.6)$$

In Equation 5.6, the joints are said to be performing well if the deflections at both joints are equal. If this is the case, the ratio of the deflections will be equal to or near 1.0. This statement assumes that the joint at 50 ft. from centerline, which is being used as a basis, is in good condition, and that its performance is not affected by other circumstances. If the deflections noted in Equation 5.6 are not equal, the most likely case is that the deflections at Joint A will be greater, causing the ratio to be greater than 1.0, and indicating that the joint may be approaching the limit indicated in Figure 5.9. Using the RDD to provide a continuous measure of deflection, airport maintenance staff can prioritize and schedule maintenance activities to focus attention on those locations which are exhibiting the most fatigue damage or are closest to failure. The data described in this section are presented in Figures 5.18 and 5.19.

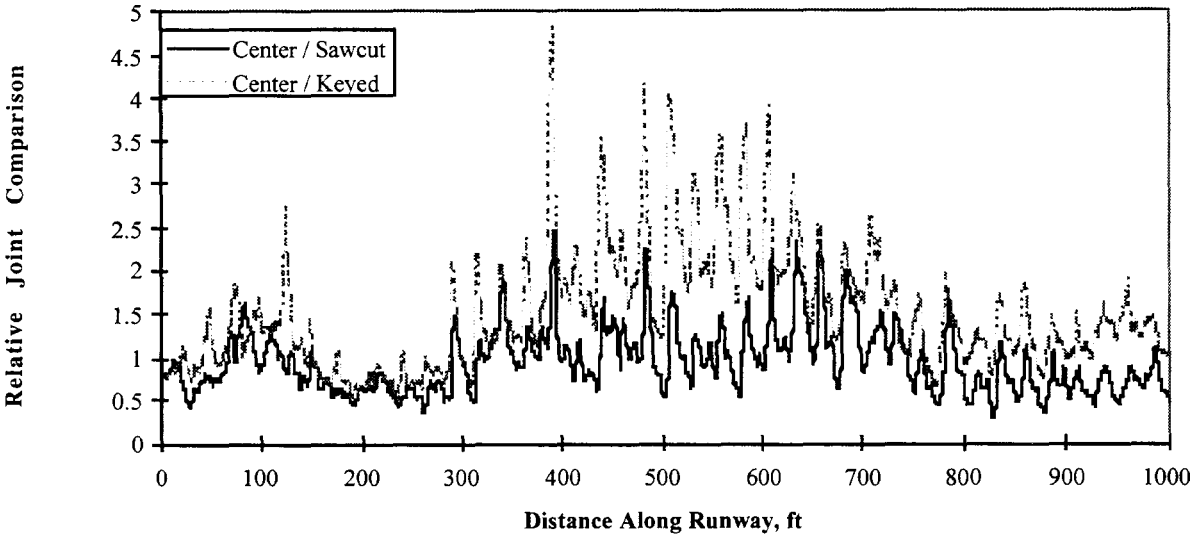

Figure 5.18. Relative Longitudinal Joint Deflection, Runway 17R/35L.

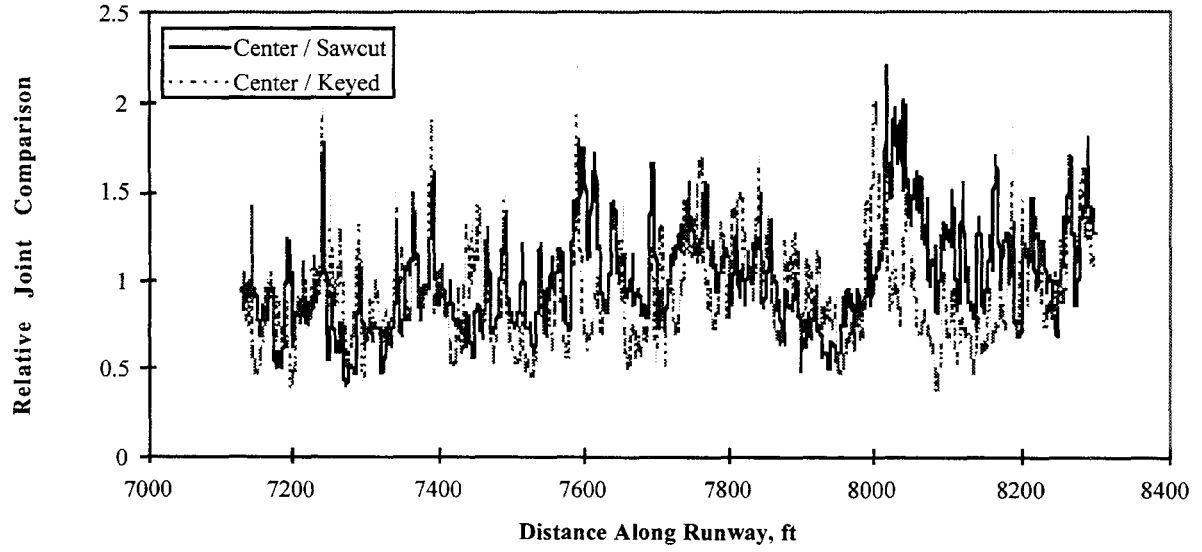

Figure 5.19. Relative Longitudinal Joint Deflection, Runway 17R/35L.

As can be seen in the previous two figures, the relative joint comparison shows where the deflections of two joints offset from centerline are greater or smaller than those at the same longitudinal location on the centerline joint. Where the values in the figures are greater than one, the centerline joint is deflecting more than the other joints. In the Figure 5.18, the relative differences are generally between 0.5 and 2.5, as there also are in Figure 5.19 from section 7100

ft. to 8100 ft. However, as shown in Figure 5.19, between section 400 ft. and 600 ft. the relative deflections are as high as 5.0. This may indicate a section where the centerline joint is beginning to become fatigued, and further investigation should be performed to identify the cause of the higher deflections.

The next type of comparison of longitudinal joints involves estimating the stresses induced in the concrete slabs by aircraft loading. A relative comparison can be made by again taking a ratio of deflections at any two joints for comparison. The ratio of the deflection at sensors 3 and 4 (from Figure 5.15) is found, by taking measurements across the joint. This configuration is shown in Figure 5.20. The purpose of this configuration is to determine how much a slab deflects when a load is placed on an adjacent slab. In an ideal situation, the joint would transfer half of the load to the adjacent slab, and both would deflect the same amount, thus the load transfer ratio should equal 1.0, or a Load Transfer Efficiency of 100 percent. Figure 5.21 shows the load transfer ratio for the entire distance of the centerline joint of Runway 17R.

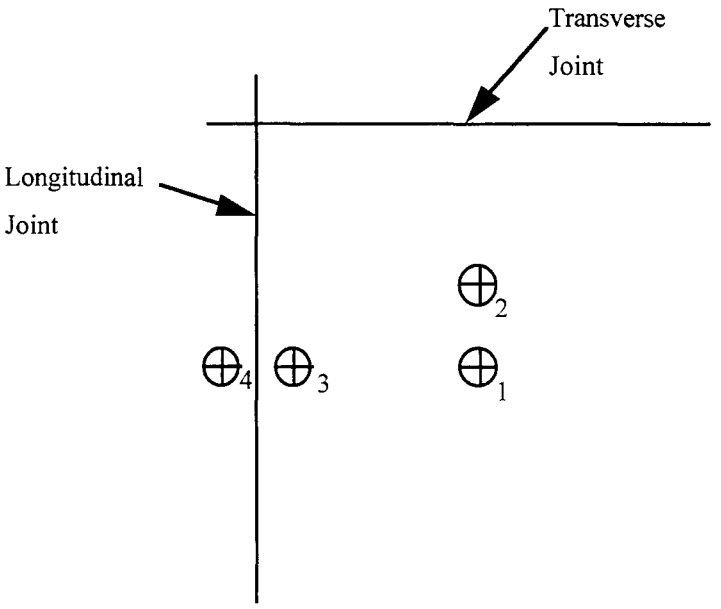

Figure 5.20. RDD sensor configuration for joint comparison and analysis.

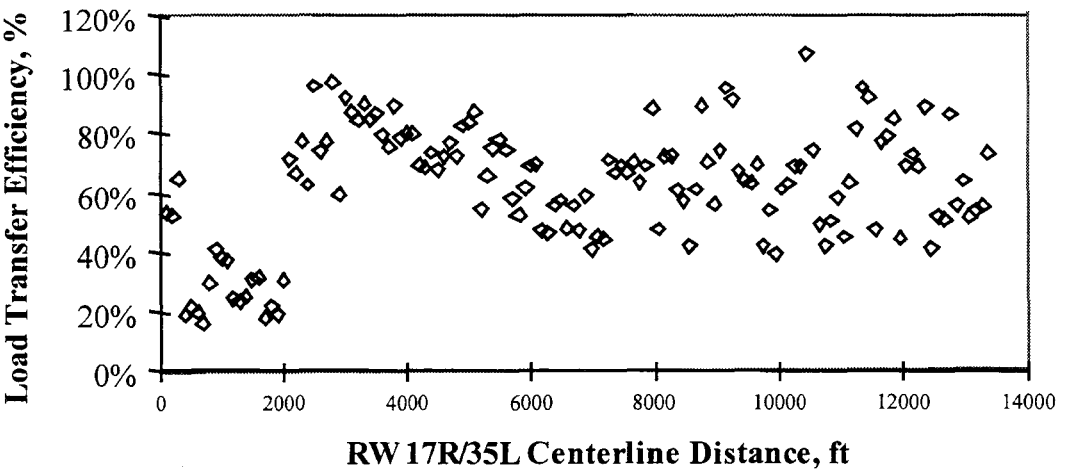

Figure 5.21. Load Transfer Efficiency of Centerline Joint, Runway 17R/35L.

The results of the centerline LTE analysis, shown in Figure 5.21, shows a characteristic similar to the deflection results in Appendix A. The LTE for the first 2000 ft. of the runway, the extension section which was constructed in 1995, has much lower LTE values than the rest of the runway which was constructed in 1974. In the RDD deflection data, which is given in Appendix A, the deflections of the 2000 ft. extension are much greater, overall, than are the deflections of the remaining 11,400 ft. of the runway. The results of this comparison are reasonable, since with greater deflections, the load transfer of the joint would be expected to be much less.

As will be presented in Chapter 6, the results of the RDD testing can be used in conjunction with computer programs to predict the modulus of subgrade reaction in the subbase below the concrete slab. When a problem location is identified using the RDD analysis, further investigation can be performed to identify the nature of the problem which will allow the cause to be more easily determined.

Comparison of Transverse Joint Types. For this part of the analysis, comparisons were made between the deflections at sensor 1 and 2. In this manner, the load transfer could be estimated across transverse joints and comparisons can be made between the two types of transverse joints. Again, the estimate of the relative concrete stress was made by the ratio in Equation 5.10, which is similar to that in Equation 5.7, with different deflection locations.

$$\frac{w_{j-2}}{w_{j-1}} \propto \sigma_{concrete} \tag{5.10}$$

The comparison for transverse joints is made between the two types of joints. The same measurements were made (the same sensor locations on each slab) and can be compared in the following manner. The deflection ratios, as calculated by Equation 5.10, are computed for each type of joint, and the values are then compared to determine which has a higher relative load transfer. This is illustrated in Equation 5.11.

$$\left(\frac{Wcj-2A,C}{Wcj-1A,C}\right)_{Doweled} \text{ vs } \left(\frac{Wcj-2A,C}{Wcj-1A,C}\right)_{Cracked} \tag{5.11}$$

As can be seen in Equation 5.11, the deflection measurements were taken at the same location on the respective slabs, and the data was partitioned into doweled and cracked or undowelled transverse joints. Deflection measurements can be taken at both A and C slabs, but the same location must be used in each analysis. This data can then be compared and inferences made concerning the performance of the two types of joints.

Another comparison available is the difference in deflection ratios for the same joint type, or the same individual joint, but comparing the joints at the A and C slabs. In this manner, the fatigue effects of aircraft loading on the pavement can be compared for the same joints. This can be done since Joint A has experienced many more load repetitions than Joint C. Figures 5.22 through 5.25 show the results of the analysis described above.

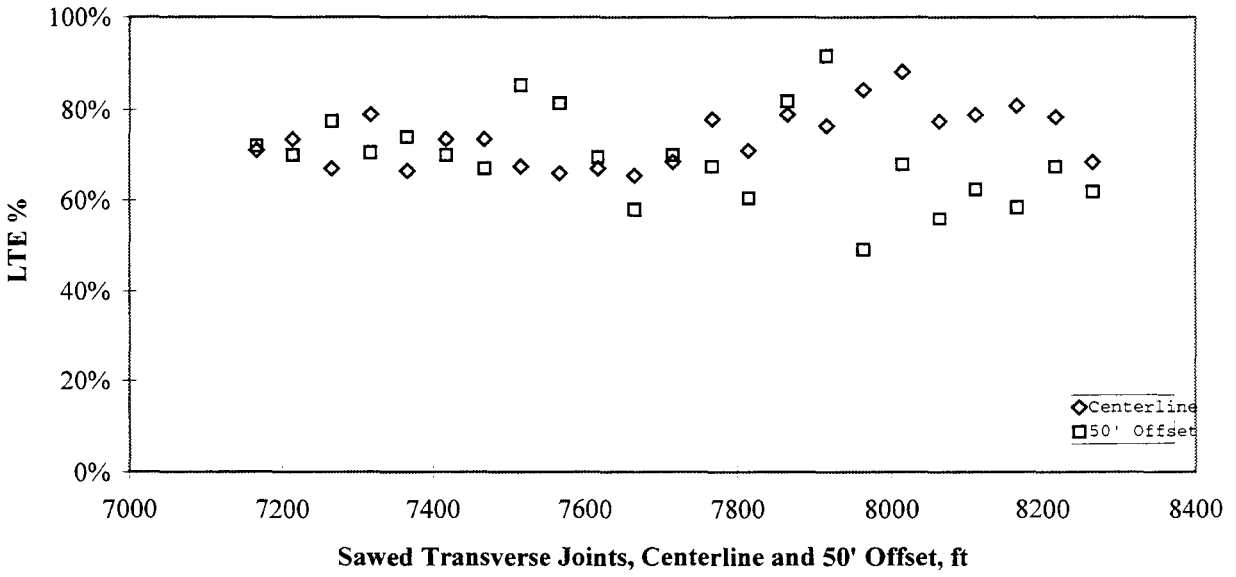

Figure 5.22. LTE of Sawed Transverse Joints at Centerline and at 50 ft. Offset.

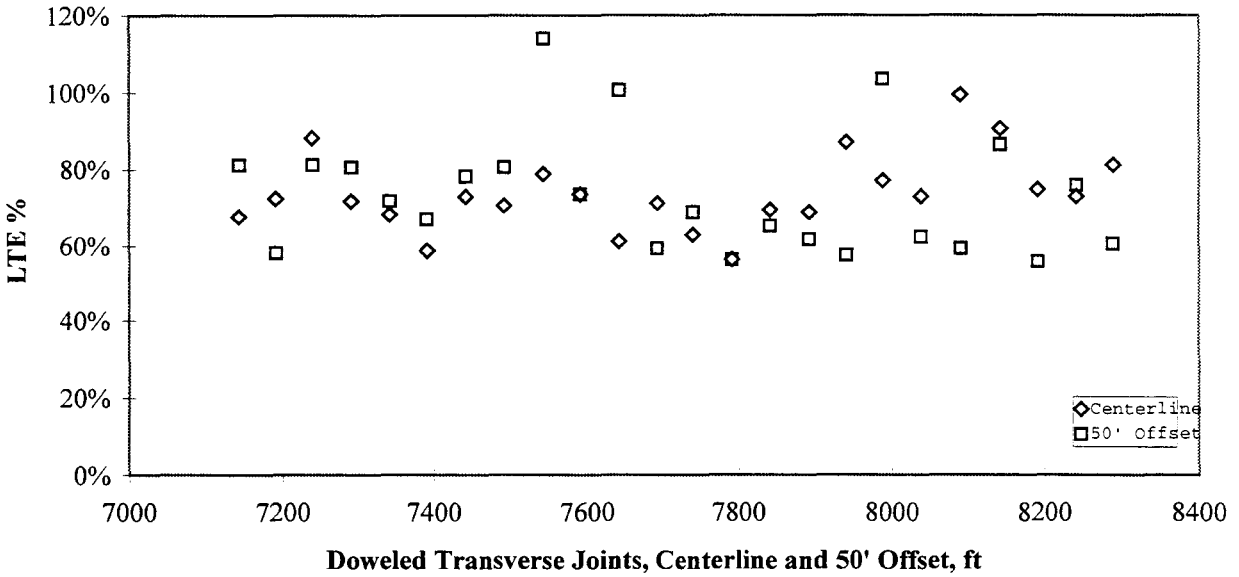

Figure 5.23. LTE of Doweled Transverse Joints, Centerline and 50 ft. Offset.

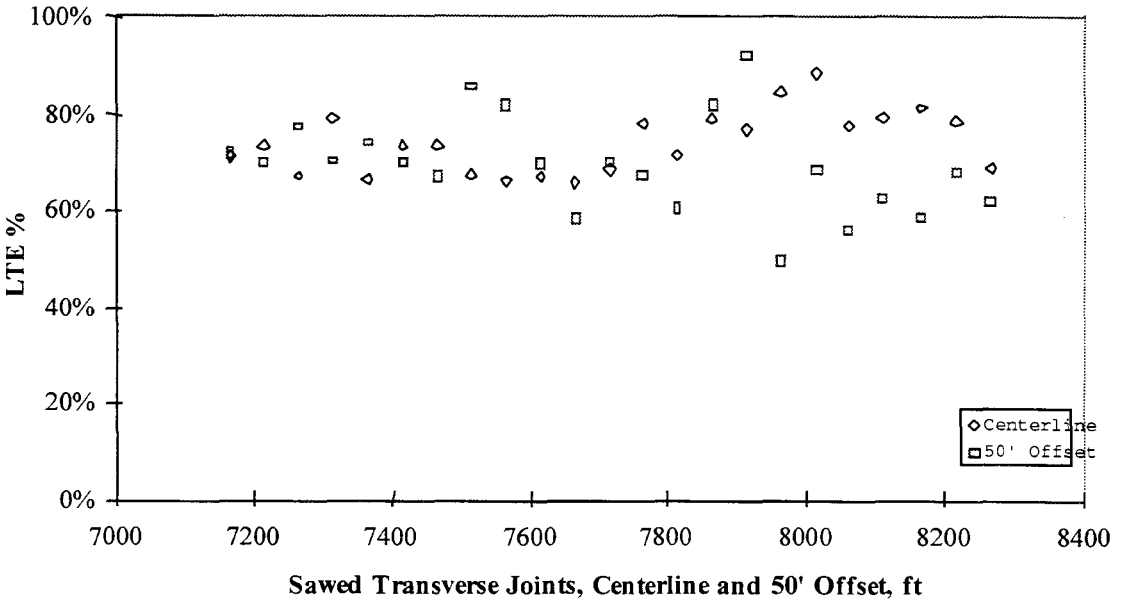

Figure 5.24. LTE of Sawed Transverse Joints, Centerline and 50 ft. Offset.

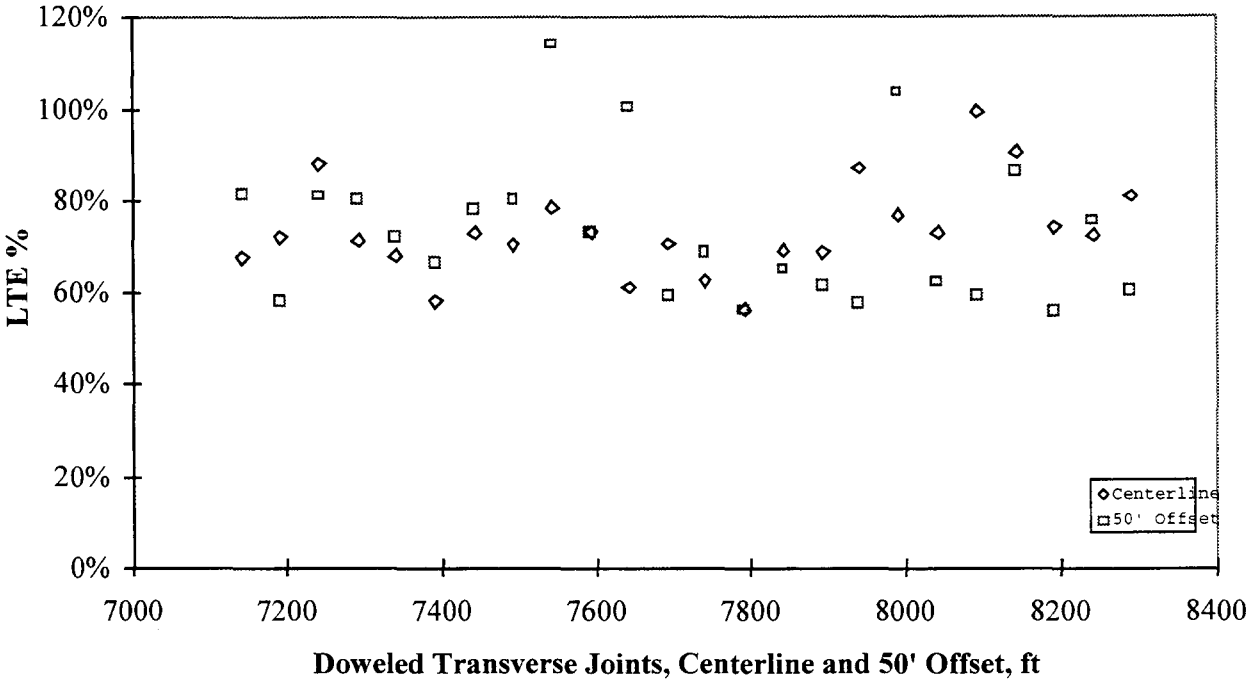

Figure 5.25. LTE of Doweled Transverse Joints, Centerline and 50 ft. Offset.

Figures 5.22 through 5.25 show a relative comparison of the load transfer efficiency between the sawed transverse joints at the centerline and at the construction joint at 50 ft. from centerline. They also show the LTE of the transverse joints of the doweled transverse joints at the same locations. It can be easily seen that the load transfer efficiency of the same joints at the centerline is much lower than at the joint 50 ft. from centerline. The major reason for this decrease in LTE is the hundreds of thousands of aircraft load applications that the centerline joint has experienced.

Effect of Soil Support on Stress and Fatigue. At the time that the DFW International Airport was constructed, a layer of lime treated soil was placed beneath the cement treated base (CTB) and the Portland cement concrete (PCC) layers. The thickness of the lime treated soil varies from approximately 3 to 25 ft.. This difference in thickness of the lime treated subgrade and the constant thickness of the CTB and PCC layers may lead to some differences in soil support beneath the pavement. The deflection measurements that were taken by the RDD can be used as an indicator of the quality of soil support and may lead to a measure of fatigue in the subgrade layer.

The following relationship exists within the pavement - soil structure:

$$\sigma_{concrete} \propto \frac{1}{Soil\ \ Support} \propto w \tag{5.12}$$

where w is the deflection induced in the pavement under load and $\sigma_{concrete}$ is the stress in the concrete due to the same load. Since the deflections in the interior of the slab have fewer other variables that interfere with the analysis, these deflections will be used.

Figure 5.26 represents the interior deflections at sensor 1 along Joint A plotted against distance. As can be seen, the deflections increase, generally, from the north to the south end of the runway. Something to note, however, is the 2000 ft. extension which was constructed in 1995. The deflections on the extension are much greater overall than the deflections on the older section of the runway. This indicates, with the analysis performed and reported in the previous sections of this chapter, that the extension was constructed with a less stiff subbase, and lower load transfer at the joints.

The calculated induced stresses at the bottom of the concrete slab are greater in sections of the runway with greater deflections. This will be discussed in more detail in the section titled *Stress Analysis of Concrete Slabs* in Chapter 6. The increased stress in the concrete has the direct effect of decreasing the life of the pavement, as discussed in the Fatigue testing section of Chapter 6. It is estimated that the runway extension will have a much shorter life than the original life of the runway. This can be seen by the visual inspection of fatigue cracking, as discussed in the next section of this chapter. A more detailed discussion of the remaining life of the concrete pavement will be presented in Chapter 7 of this report.

Conclusions. This section of the report presented a method of analyzing the deflection data which was obtained from the Rolling Dynamic Deflectometer at the Dallas / Fort Worth International Airport during the week of August 26, 1996. This data was used to compare the performance of both longitudinal and transverse joints. In addition, the issue of soil support was investigated as it pertains to fatigue of the pavement structure. A limit was found which can be modified by the staff of the DFW airport to meet maintenance and rehabilitation strategies in order to prioritize the locations on the airfield pavements that require maintenance attention. This limit was determined in conjunction with the results of the cross-hole testing that was described in an earlier section of this report.

VISUAL INSPECTION OF CRACKING

Fatigue cracking of the concrete pavement was discovered during one of the site visits by CTR researchers. During a visit to the airport by Dr. McCullough, the existence of fatigue cracking was verified. A plan was subsequently devised to quantify and to characterize the fatigue cracking on the runway and taxiway. The normal PCI condition survey that is performed on pavements does not account for fatigue cracking. All cracks less than 1/8 in. wide are characterized as *Low Severity Cracking*. In the case of fatigue cracking, however, cracks much smaller than 1/8 in. in width can indicate a severe fatigue problem.

To obtain the desired measurements after the characterization procedure was developed, a team of CTR staff traveled to the airport and drove on the runway and the taxiway for several nights. The following sections detail the development of the characterization criteria, the methodology for obtaining the cracking information, and the analysis of the collected data. The analysis includes a correlation to the amount of aircraft traffic to which the pavement has been exposed.

Development of Fatigue Cracking Classification Criteria

Under the guidance of Drs. Frank McCullough and Michael McNerney, a procedure for characterizing the observed fatigue cracking was devised. Important characteristics of fatigue cracking and its effects on concrete pavement were considered. A three tiered characterization was outlined to quantify the amount of fatigue cracking on the runway and taxiway. The three measurements are as follows:

1. Number of fatigue cracks within a three ft. span
2. Number of fatigue cracks longer than three ft.
3. Number of fatigue cracks throughout the entire length of the slab

The first measurement is perhaps the most important. The number of fatigue cracks that can be encompassed in a three ft. span gives an indication of the density of fatigue cracking. To obtain this measurement, CTR staff members measured with a yardstick the largest number of fatigue cracks over which the yardstick could be placed. The upper limit for the measurement is five cracks within a three ft. span. This measurement provides the "crack density" of fatigue cracking, which can be correlated with the historical aircraft traffic pattern along with the other two measurements that were taken.

The second and third characteristics of the fatigue cracking pattern is the number of cracks that are longer than three ft. and the number of cracks that extend the length of the slab. These

measurements are indicative of the severity of the cracking. Fatigue cracks extend with higher levels of traffic loads and eventually grow to the entire length of the slab. The next sections detail the data that was collected and the results of the analysis that was performed.

Data Collection

The data was collected during two site visits to the runway and taxiway. Several locations were selected in order to obtain representative samples of pavements from each level of traffic loading. The north end south end, and midpoints of the runway and taxiway were sampled because of the highly varying levels of aircraft traffic loading that each section had experienced in the past 24 years. The number of slabs that were sampled varied from 10 to 30 slabs in each section. Only the slabs adjacent to the centerline of the facility were sampled as part of the cracking classification program. Random sampling of slabs nonadjacent to the centerline revealed that fatigue cracking was nonexistent.

Table 5.8 below shows a summary of the fatigue cracking data collection. The values shown in the table are averages of the sections that were measured by CTR Staff members. As mentioned above, the three criteria for evaluating the fatigue cracking were combined to form an index value. The table below combines several sections in each portion of the runway and taxiway. Figures 5.26 and 5.27 show graphically the relationship between the cumulative traffic and the fatigue index level.

TABLE 5.8. SUMMARY OF FATIGUE CRACKING DATA COLLECTION

Section	17R	TWL
South	37.3	12.6
Middle	28.3	36.1
North	128.7	99.7

Analysis Results

This section details the results of the data analysis of the fatigue cracking on Runway 17R/35L and Taxiway L. The data were correlated with the levels of traffic that each section had experienced in the past. From the analysis presented here, conclusions can be made about the remaining life of the pavement. A curve has been developed based on the fatigue cracking data and the historical traffic loading. Inferences can be made concerning the trends that are evident in the graph in the following two figures. The most obvious conclusion is that when the other sections of the runway or the taxiway have had as many applied loads as the north end, which displays the

most advanced fatigue distress, they should display fatigue cracking patterns similar to those currently observed at the north end.

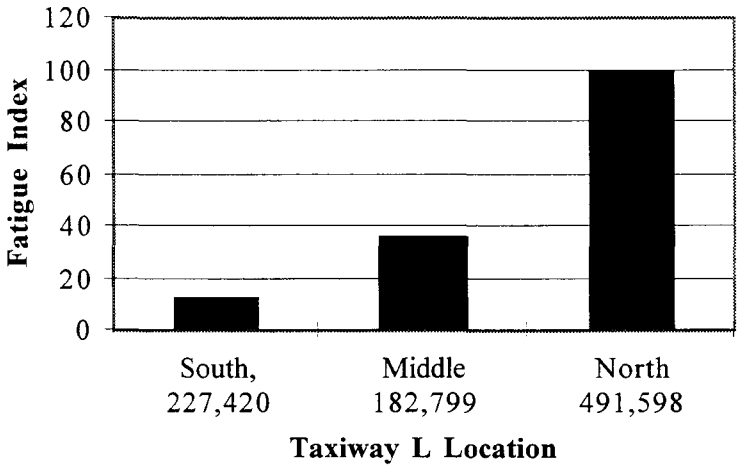

Figure 5.26. Correlation of Traffic Loading to Fatigue Cracking, Runway 17R.

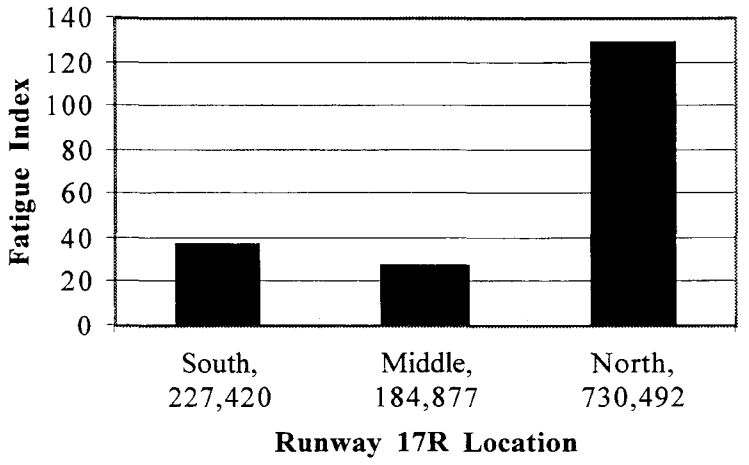

Figure 5.27. Correlation of Traffic Loading to Fatigue Cracking, Taxiway L.

The inferences that can be made based on these figures is that assuming consistent environmental conditions, the south and middle sections of the runway and the taxiway will show fatigue cracking at the same level as the north end when they have been exposed to the same

number of applications. It may be conceivable that they will arrive at the level of fatigue sooner than the north end has, since they will be exposed to more cycles of environmental conditions before arriving at the same amount of aircraft applications. Although the effect of the environment has not been included in this discussion on fatigue cracking, environmental conditions have the general effect of weakening the layers of the pavement, which can then provide less resistance to fatigue damage.

Discussion of Results

The results of this analysis provide several types of information. As discussed in an earlier chapter, the normal PCI analysis that has been conducted at least once in the recent past seems not to include some of the most important distresses, such as fatigue cracking. The level of fatigue cracking can indicate more accurately the remaining life of the pavement. The figures presented in this section show that there is a definite correlation between the level of fatigue cracking and the previously applied traffic loads.

The north end of the runway, which has experienced by far the most load applications, has more extensive fatigue cracking at much higher severity. The middle and southern end of the runway do not have fatigue cracking to the extent that the north end does. A similar condition exists on the taxiway, where the north end shows much more fatigue cracking than the middle or south end

With this information, a trend line can be constructed for the runway and taxiway and the remaining life of the middle and south end can be estimated based on the past performance of the north end. It is assumed that the environmental conditions will remain the same in the future as they were in the past, and that aircraft weights will not change considerably in the near future. The ultimate number of applications of the design load carried by the concrete at the north end can be used as the design life of the rest of the runway or taxiway as well. This estimated design life, minus the historical load applications provide the remaining life estimate for the runway or taxiway with respect to fatigue cracking.

CHAPTER 6. LABORATORY TESTING—ANALYSIS AND RESULTS

Both short term and long term laboratory testing were conducted for this project. Short term laboratory testing included tests such as the indirect tensile strength test, the indirect tensile resilient modulus, and sonic testing. Fatigue testing is termed long-term testing because tests can take as long as two weeks or more to perform. These tests were mentioned in Chapter 4 and will be described in detail in this chapter.

In addition to the testing, a discussion of the stress analyses that were performed is presented in this chapter. An analysis was performed of the stresses in the pavements induced by different aircraft types using the Westergaard method. Another analysis to estimate the stiffness of the subbase was performed using a discrete element computer program called SLAB49. The third type of stress analysis performed uses elastic layer theory to estimate stresses in the pavement using the results of the cross-hole testing discussed in Chapter 5.

A discussion of the results and recommendations for using the information presented is provided at the end of this chapter. A table of test results is provided in summarize the large volume of testing information. In addition, a simplified database of test results is provided in the Data Appendices, Volume III of this report. This database was developed for managing the data while testing was being performed, and it may be useful in the future to compare strength tests of new pavement analyses to those performed for this project.

Several different tests were performed and subsamples taken from each core. Figure 6.1 shows the generally followed, pattern of test sections of each core for the various tests described in this chapter. Fatigue testing was only performed on the Runway 17R/35L and Taxiway L cores which are all 4 inches in diameter. Some cores were not fatigue tested, therefore the 3-inch tall tensile strength specimen was taken from the bottom of the core. The 6-inch diameter cores taken from Taxiway K were not partitioned in this manner.

SHORT TERM LABORATORY TESTING

Two short term tests as well as the long term fatigue testing was performed at The University of Texas at Austin on core samples that were obtained as described in Chapters 4 and 5. The indirect tensile test was performed on an 80,000 pound hydraulic press, and the indirect tensile resilient modulus test was performed at the beginning of the fatigue tests which will be discussed in a later section. The resilient modulus of the concrete samples as well as the fatigue testing was performed on an MTS Laboratories hydraulic repeated load machine.

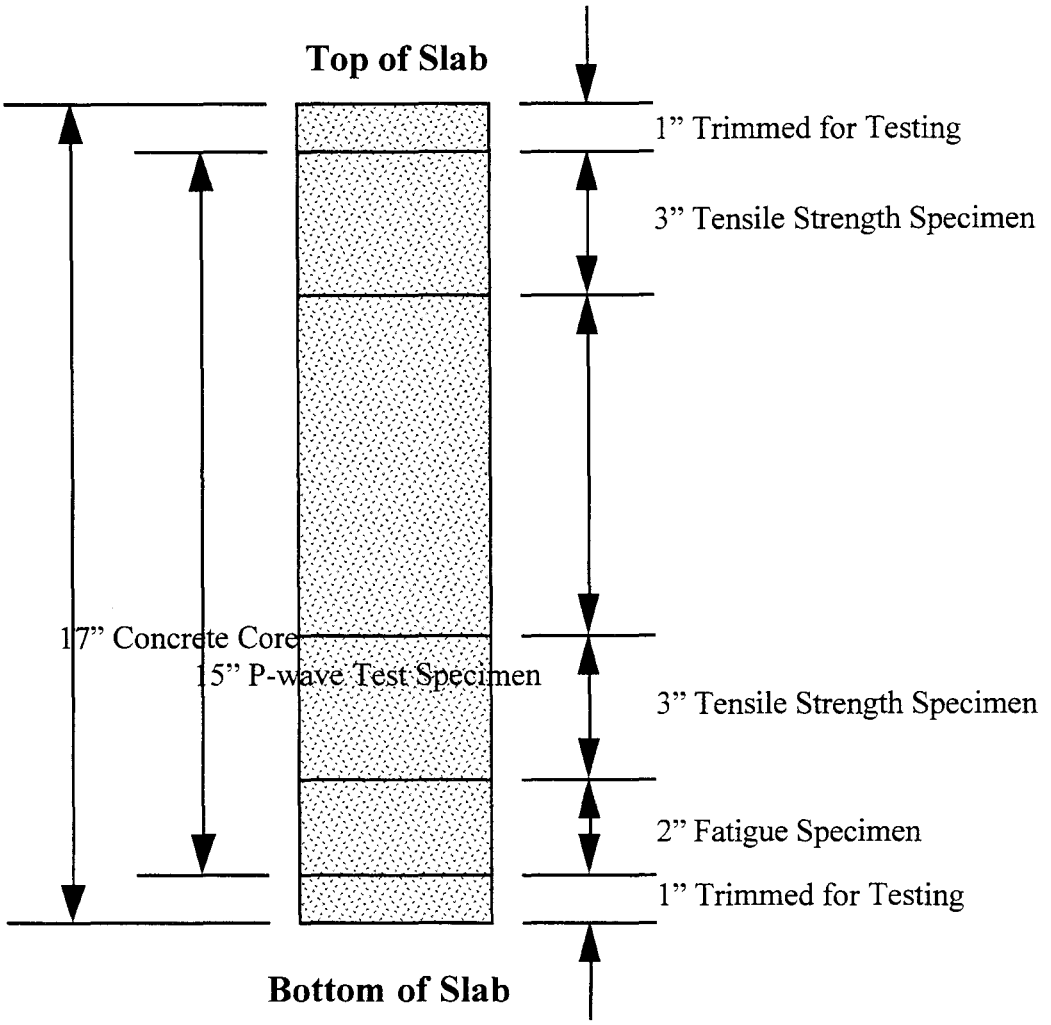

Figure 6.1. General Concrete Core Partitioning for Testing

Indirect Tensile Testing

The indirect tensile test was performed on useable test specimens from all the core samples. Core samples were taken from Taxiway K just prior to its reconstruction in 1995, Runway 17R/35L, and Taxiway L at the Dallas / Fort Worth International Airport. Test specimens from Taxiway K cores were six inches in diameter and approximately three inches long. Test specimens from the runway and Taxiway L were all approximately four inches in diameter and three inches long.

Test Method. The testing method, in accordance with ASTM C 496 and ASTM C 39, involved loading the specimens in compression with an 80,000 pound loading apparatus. The core

samples were loaded across the diameter to induce tension along the loaded axis. The following equation shows how the compressive load is converted to a tensile load in the transverse direction.

$$\sigma = \frac{2P}{\pi dh} \tag{6.1}$$

where:

σ = stress induced in specimen,

P = compressive load applied to failure,

π = pi,

d = diameter of specimen, and

h = height of specimen.

In measuring the strength of a concrete specimen, the maximum stress applied to fail the sample is taken as the strength.

The strength of the concrete ranged from 328 to 775 psi. The samples, as shown in the Tables 6.1, 6.2 and 6.3 for Taxiway K, Taxiway L and Runway 17R/35L, respectively, have differing levels of variability. The tables show the core, the branch from which it was taken, the dimensions of the core, and the indirect tensile strength, in psi. Table 6.4 gives the descriptive statistics of these samples: the maximum, minimum, average, standard deviation, and the number of samples.

Sonic Testing

Ultrasonic Pulse Velocity and Impact Resonance Frequency methods, as mentioned in Chapter 4, were performed on the 6-inch diameter concrete cores taken from Taxiway K before its reconstruction. Impact Resonance Frequency method of sonic testing was performed on the 4-inch diameter concrete cores from Taxiway L and Runway 17R/35L, and the cement treated base (CTB) cores from the runway. These tests were used to estimate the initial stiffness of the concrete cylinders.

TABLE 6.1 TAXIWAY K

Core Number	Branch	Original Thickness, in.	Diameter, in.	Indirect Tensile Strength
TK29F	TWK	17.0	6.0	505
TKP59A	TWK	17.5	6.0	517
TKP55B	TWK	17.3	6.0	481
TK67A	TWK	17.5	6.0	531
TKP55E	TWK	17.5	6.0	531
TK63F	TWK	17.0	6.0	527
TK63G	TWK	14.8	6.0	328
TKP55G	TWK	17.8	6.0	465
TKP59E	TWK	18.0	6.0	462
TKP55A	TWK	17.5	6.0	572
TKP59G	TWK	17.0	6.0	514
TKP60-6	TWK	18.5	6.0	515
TKP63C	TWK	17.9	6.0	481
TK67F	TWK	17.3	6.0	605
TK67E	TWK	17.4	6.0	390
TK63A	TWK	14.8	6.0	589
TK29E	TWK	17.3	6.0	586

TABLE 6.2 TAXIWAY L.

Core Number	Branch	In / out of traffic lane	Diameter, in.	Indirect Tensile Strength
TL1A	TW L	in	3.75	695
TL1B	TW L	in	3.75	617
TL1C	TW L	in	3.75	691
TL2D	TW L	out	3.75	570
TL2F	TW L	out	3.75	583
TL3D	TW L	out	3.75	734
TL3F	TW L	out	3.75	380
TL4A	TW L	in	3.75	466
TL4B	TW L	in	3.75	491
TL4C	TW L	in	3.75	602
TL5A	TW L	in	3.75	689
TL5B	TW L	in	3.75	611
TL5C	TW L	in	3.75	401
TL7A	TW L	in	3.75	775
TL7B	TW L	in	3.75	518
TL7C	TW L	in	3.75	659
TL8D	TW L	out	3.75	530

TABLE 6.3 RUNWAY 17R/35L.

Core Number	Branch	In / out of traffic lane	Original Thickness, in.	Diameter, in.	Indirect Tensile Strength
RA1	R17R	in	17.0	3.9	775
RA2	R17R	in	17.0	3.9	712
RA3	R17R	in	16.8	3.9	456
RA4	R17R	out	17.5	3.9	601
RA5	R17R	out	17.4	3.9	579
RA6	R17R	out	17.3	3.9	438
RA8	R17R	out	17.5	3.9	548
RA9	R17R	in	17.0	3.9	510
RA10	R17R	out	17.3	3.9	526
RB1	R17R	in	16.5	3.9	583
RB2	R17R	in	16.5	3.9	586
RB3	R17R	in	16.8	3.9	574
RB5	R17R	out	16.8	3.9	564
RB6	R17R	out	16.8	3.9	539
RB7	R17R	out	16.9	3.9	538
RB8	R17R	out	16.8	3.9	520
RB9	R17R	in	16.4	3.9	382

TABLE 6.4. INDIRECT TENSILE TEST RESULTS SUMMARY

(a) Indirect Tensile Test Results.

	Maximum	Minimum	Average	Std. Dev.	No. Samples
R17 A	775	438	572	111.54	9
R17 B	586	382	536	66.58	8
TW L	775	380	589	113.51	17
TW K	605	328	495	73.41	19

(b) Indirect Tensile Test Results, RW 17R, In and Out of Traffic Path.

	Maximum	Minimum	Average	Std. Dev.	No. Samples
R17A in	775	456	613	154.01	4
R17A out	601	438	538	63.01	5
R17B in	586	382	531	99.79	4
R17B out	564	520	540	18.24	4

(c) Indirect Tensile Test Results, TW L, In and Out of Traffic Path.

	Maximum	Minimum	Average	Std. Dev.	No. Samples
TWL in	775	401	601	111.12	12
TWL out	734	380	560	126.65	5

Sample Preparation

A total of 36 six-inch and 58 four-inch samples were transported from the Dallas Fort Worth International Airport to the University of Texas at Austin. A total of 78 concrete cores and 16 cement treated base samples were taken. The samples were measured and both ends were trimmed.

From the 36 six-inch samples obtained from Taxiway K, two samples were discarded because one was broken and the other did not have a true cylindrical shape. The ultrasonic pulse velocity test and the free-free resonance column test were conducted on the specimens. From the four inch samples from Runway 17R/35L and Taxiway L, only free-free resonance column tests were conducted.

Concrete Properties. The properties of the concrete measured with sonic testing methods are the modulus of elasticity, E_c, and Poisson's ratio, ν. These are calculated based on the velocity of sound through the concrete media. Two types of sonic tests were performed, the confined V-meter test, and the free resonance, or free-free P-wave test.

The ultrasonic pulse velocity test method utilizes a stress wave. The details of the method can be found in Richart et al. (Ref. 3). The method creates an ultrasonic pulse at a point on the concrete, and its travel time from that point to another is measured. Knowing the distance and the time of travel between these two points, the velocity of the pulse can be determined. The velocity of this wave, also known as the compression wave, for an infinite, homogenous, isotropic, elastic medium can be related to the constrained modulus as:

$$M = \frac{\gamma}{g} V_p^2 \tag{6.2}$$

where:

M = constrained modulus,

g = gravitation acceleration,

γ = bulk density, and

V_p = compression wave velocity.

The constrained modulus takes the average of constrained velocities measured at one inch increments down the sides of the concrete core. In the case of the core samples from Taxiway K, this amounted to about 15 measurements per core.

Using this test, Dr. James Lee was able to obtain velocities across the diameter of each of the 6-inch cores at intervals of one inch throughout the entire depth of the core. This type of test was only performed on the larger Taxiway K cores due to size restrictions. Smaller core samples do not have large enough distance between measurement points to provide accurate results.

The modulus of elasticity of a material can be related to the constrained modulus by the following formula:

$$E = M\frac{(1+\nu)(1-2\nu)}{(1-\nu)} \tag{6.3}$$

where:

E = Young's modulus, and

υ = Poisson ratio.

The shear modulus can then be expressed in terms of Young's modulus:

$$G = \frac{E}{2 \cdot (1 + \upsilon)} \tag{6.4}$$

where:

G = shear modulus.

The procedure used in this test is according to the ASTM C597-83 Standard. Tests were conducted on the side (across the diameter) and axially along the cylindrical specimen. The specimens are about 6 inches (152.4 mm) in diameter. The length of the specimens ranges from 12 inches (305 mm) to 17 inches (432 mm). Vacuum grease was used as couplant. Two transducers were used; one each for transmitting and receiving an ultrasonic pulse. When the test is conducted on the side, smaller transducers were used. At the beginning of each test, calibration correction is conducted according to ASTM C597-83. Tests were conducted at 1 inch intervals along the diameter of the cylinder.

Dividing the distance by the travel time between the source and receiver, the compression wave velocity (V_p) is calculated. The constrained modulus can then be obtained by using Equation 6.2. The bulk density of concrete is assumed to 150 pcf (2400 kg/m^3). By assuming Poisson's ratio to be 0.2, one can estimate Young's and shear modulus by using Equations 6.3 and 6.4, respectively.

Resonant Frequency Method

This method used is an alternative to the ASTM C215-85, titled *Standard Test Method for Fundamental Transverse, Longitudinal, and Torsional Frequencies of Concrete Specimens*. The method used in this test is also called impact resonance method. The concrete specimens are struck lightly with a small hammer or steel ball. The impact causes the specimen to vibrate at its natural frequencies. The amplitude and frequency of the resonant vibrations are obtained using a spectrum analyzer that determines the component frequencies via the Fast Fourier Transform. The power spectrum is the amplitude versus frequency plot. Once the resonant frequency of the specimen is

obtained, the rod velocity can be obtained by assuming a free-free resonant column system. The rod wave velocity is equal to:

$$V_c = \lambda \bullet f_n \tag{6.5}$$

where:

V_c = rod wave velocity,

λ = wavelength, and

f_n = resonant frequency.

In a free-free resonant column system, the wavelength is equal to 2 times the length of the specimen as described by Graff (Ref. 4). The rod wave velocity is then equal to:

$$V_C = 2 \bullet d \bullet f_n \tag{6.6}$$

where

d = length of the specimen.

Young's modulus can be calculated by using the following equation:

$$E = \frac{\gamma}{g} V_c^2 \tag{6.7}$$

where:

E = elastic modulus,

γ/g = mass density of the material, ($g = 32.2\ ft/s^{2)}$, and

V_c = rod velocity through the material.

Using resonant column testing, one can also obtain S-wave velocity. The main differences between the longitudinal and shear wave type are two folds. First, the source should be able to generate the shear wave type motion. Hence, the shear exciter is used to obtain S-wave velocity. Second, the receiver should be placed at the edge of the cylinder while the receiver was placed at

the center of the cylinder for longitudinal test. The reason is that the shear wave type particle motion at the edge of the specimen is the maximum. The shear wave velocity is equal to:

$$V_S = \lambda \bullet f_n \tag{6.8}$$

where:

V_s is shear wave velocity.

The values obtained in the core testing from the different taxiways and runway materials were separated into different groups. The first differentiation of the cores is between trafficked and non-trafficked cores. The assumption made is that the properties of the cores from trafficked areas will be weaker than those from the non-trafficked areas. This is due to the fatiguing of the concrete over many hundreds of thousands of aircraft loading applications. The second grouping was made between cores taken from the north end of the airfield and those from the south end. Since the predominant aircraft traffic movements are to the south from the north, the north end of the airfield has experienced many more aircraft loads than the south end. For the Taxiway K cores, the north - south differentiation was not performed, although results of such an analysis would be expected to be similar to those for the Runway or for Taxiway L.

Simple statistical analyses were performed to compare the means of these groups, to determine if the properties of the cores in different groups are statistically different. The results of these analyses are presented in the respective sections.

The statistical equations used in this analysis are as follows:

$$\mu_\Delta = \mu_{ABC} - \mu_{EFG} \tag{6.9}$$

$$\sigma_\Delta = \sqrt{\frac{\sigma^2_{ABC}}{N_{ABC}} + \frac{\sigma^2_{EFG}}{N_{EFG}}} \tag{6.10}$$

where:

μ_Δ = difference of mean of the two samples,

σ_Δ = difference of standard deviation of the two samples, and

N = number of samples in each population.

If the difference of the mean of the two samples, μ_{Δ}, is different with a sufficient level of confidence, the samples are said to be statistically different.

Taxiway K. A total of 34 cores were tested in this series. Those marked with an A, B, or C were taken from less trafficked or non-trafficked areas of the taxiway, while cores marked with an E, F, or G were taken from areas of the taxiway which had experienced approximately 22 years of aircraft loading. The calculated modulus values obtained for each core are given in Table 6.6. The average and standard deviation of the velocities for each core were computed from these values and are shown in Table 6.7. The standard deviation in the V-meter test results range from 223 to 964 ft/sec, which corresponds to a coefficient of variation ranging from 1 percent to 6 percent . It is assumed that the properties of the concrete from the trafficked and non-trafficked areas will be different. The hypothesis is that the cores from highly trafficked areas will have lower levels of elastic modulus than those cores which have not had significant aircraft traffic loads. All other forms of distress are ignored for this assumption. The following tables show the results of the analysis.

TABLE 6.5. SLAB LOCATIONS AND CORE LOCATIONS WITHIN EACH SLAB

	Core Location Within Slab					
Location (slab no.)	A	B	C	E	F	G
17				X	X	X
29				X	X	X
55	X	X	X	X	X	X
56		X	X			
59	X	X		X	X	X
60				X	X	X
63	X	X	X	X	X	X
67	X	X	X	X	X	X

TABLE 6.6. CORES AND ELASTIC MODULI MEASURED BY FREE-FREE RESONANCE TEST

Traffic		Non-Traffic	
ABC Series		EFG Series	
Number	E, ksi	Number	E, ksi
P55A	6681	17E	6458
P55B	6517	17F	6386
P55C	6480	17G	6430
P59A	6598	29E	6546
P59B	6660	29F	6280
P63A	6159	29G	5922
P63B	6686	P55E	6730
P63C	6071	P55F	6177
67A	6692	P55G	6409
67B	6760	P59E	6202
67C	6466	P59F	6187
		P59G	6080
		P63E	6493
		63F	6713
		63G	6303
		67E	6154
		67F	6274
		67G	6440
Average:	**6525**		**6344**
Std. Dev.:	**224**		**210**

TABLE 6.7. SUMMARY OF MEAN, STANDARD DEVIATION, AND NUMBER OF SAMPLES FOR FREE-FREE TESTS

Samples	Mean, ksi	St. Dev., ksi	No. of samples
ABC	6525	224	11
EFG	6344	210	18

Applying the values in Table 6.7 to Equations 6.9 and 6.10, and with a 98 percent confidence level, the means of the elastic modulus in the two sets of samples can be said not to be equal, the trafficked samples having lower values of elastic modulus.

The values in Table 6.8 give the results of the constrained modulus tests. As stated above, these results are not as reliable to use as an absolute elastic modulus value, but they are reliable for making a relative comparison between the modulus of cores using the same test. From the information in Table 6.8, and with a 98.8 percent level of confidence, the means of the two sets are not equal. Again, the cores taken from the traffic lane have a lower modulus of elasticity.

TABLE 6.8. SUMMARY OF MEAN, STANDARD DEVIATION, AND NUMBER OF SAMPLES FOR CONSTRAINED MODULUS TESTS

Samples	Mean, ksi	St. Dev., ksi	No. of samples
ABC	7741	260	10
EFG	7511	255	18

FATIGUE TESTING

The fatigue testing performed for this project consisted of selecting several concrete samples taken from the concrete pavements studied and preparing them for long term fatigue testing. The samples taken from the cores for fatigue testing were only two inches in diameter to accommodate the capacity of the MTS machine. Generally the core samples selected were from the bottom two inches of the core, since the greatest magnitude of destructive stresses are located there. Tensile stresses in the pavement induced by aircraft loads occur at the bottom of the slab. It is the tensile stresses that are the most damaging to the concrete, due to the relative strengths of concrete in tension and compression. Compressive strength of concrete is much greater than the tensile strength. Tensile strength is normally about 10 percent of the magnitude of compressive strength of the same concrete.

Fatigue Testing Procedure

This section will describe the procedure used to complete the fatigue testing program. The next section will present and discuss the results of the testing. The intent of fatigue testing is to build a fatigue curve from the test results. The curve produced from the testing for this project is presented in the next section.

The presentation of results of fatigue testing shows the relationship of the number of applications to failure with the cyclic stress level applied to the specimen. This represents the

number of aircraft applications on the runway which apply a certain amount of stress each. By changing the amount of cyclic stress applied to each specimen, and taking the ratio of the stress to the strength of the specimen, a fatigue curve can be produced. The number of cycles to failure, or the fatigue life of the concrete, decreases with increasing stress to strength ratio.

A problem in determining the stress to strength ratio is that before loading a test specimen to failure, the strength of that sample must be known. Given the variability of the concrete shown, the strength of the concrete could not accurately be estimated. To overcome this obstacle, the strength of the next higher three inches of each core tested in fatigue was obtained through further indirect tensile strength tests. The strength of the adjacent concrete on a particular core was assumed to be indicative of the strength of the actual fatigue sample.

Once the estimated ultimate tensile strength of the two-inch sample was determined, the physical dimensions of the sample were measured and a strength / stress ratio was assigned. From the strength, the stress to be used for the test was found. A thin layer of plaster was placed on opposite sides of the sample. The plaster served to smooth the surface of the concrete to avoid irregular loading of the sample.

The sample, once placed in the MTS machine, was loaded at the load determined from the calculated stress. The calculation of load from stress is the same as was presented in the section about indirect tensile strength testing. The cyclic load, at one cycle per second, was applied for 40 to 50 cycles at which point the resilient modulus was recorded from the sample, as discussed in the previous section.

After the resilient modulus of the concrete sample was measured, the load cycles were allowed to continue until the specimen failed. At that point, the total number of cycles to failure was recorded, and the sample was plotted on the fatigue curve.

Results of Fatigue Testing

The fatigue testing of the concrete at the DFW Airport produced a fatigue curve, as described in the previous section. This curve is presented in Figure 6.2 and shows how the fatigue life of the concrete decreases when the applied stress increases. In Figure 6.2, the cycles to failure is the number of load applications that each test specimen accumulated before failing in tension. The stress/strength ratio is the relationship between the tensile strength of the concrete and the tensile stress applied. The vertical axis is shown in a logarithmic scale for clarity.

The slope of the fatigue curve in the Figure 6.2 is -10.89, which is comparable to the slope of -20.224 obtain by Yimprasert and McCullough in CTR Report 123-16 *Fatigue and Stress Analysis for Modifying the Rigid Pavement Design System* (Ref. 5). The curve represents the

number of allowable cycles that the pavement can withstand before failing. In most of the test specimens in Figure 6.2, the cycles to failure is measured on concrete that has already been exposed to many thousands of loads and this accounts for the slope of the fatigue curve in Figure 6.2 being only about half of that in Report 123-16, which is about -20.224. The concrete slabs from which the cores were taken have been exposed to between 185,000 and 730,500 equivalent 727 departures since construction. The results of the fatigue analysis will allow a prediction of remaining life, based on the previous number of equivalent 727 departures, the magnitude of the stress induced by those aircraft. The remaining life will be estimated by taking the difference between the previous and ultimate number of equivalent 727 departures at the corresponding stress to strength ratio. If a different stress level is desired, Miner's hypothesis must be applied, which in Equation 6.11 states:

$$\sum \frac{n_i}{N_i} = 1 \tag{6.11}$$

where:

n_i = number of applications of a specific load

N_i = Total allowable applications of a specific load

Miner's hypothesis allows the fatigue relationship to be applied to several different load levels.

STRESS ANALYSIS OF CONCRETE SLABS

This section of the report is intended to provide a comparison of predicted stresses at the bottom of the concrete slabs to the measured tensile strengths and the fatigue results presented in previous sections of this chapter. This section will present three methods of predicting the stresses at the bottom of the slabs, and will then give a comparison of those results to the strengths from previous sections.

Westergaard Stress Approximation

Aircraft exert different stresses on pavement due to differences in maximum takeoff weight and differences in landing gear configurations. In order to determine the severity of the load exerted by an aircraft, it was necessary to calculate the Westergaard pavement corner stresses for each aircraft type serving DFW. Westergaard stresses take into account the load exerted by the aircraft on the pavement by each tire, tire pressure, tire contact area, slab size and slab thickness.

The maximum tensile stress in a single pavement slab occurs when the load is applied at the corner. The Westergaard corner tensile stress is indicated by Equation 6.12:

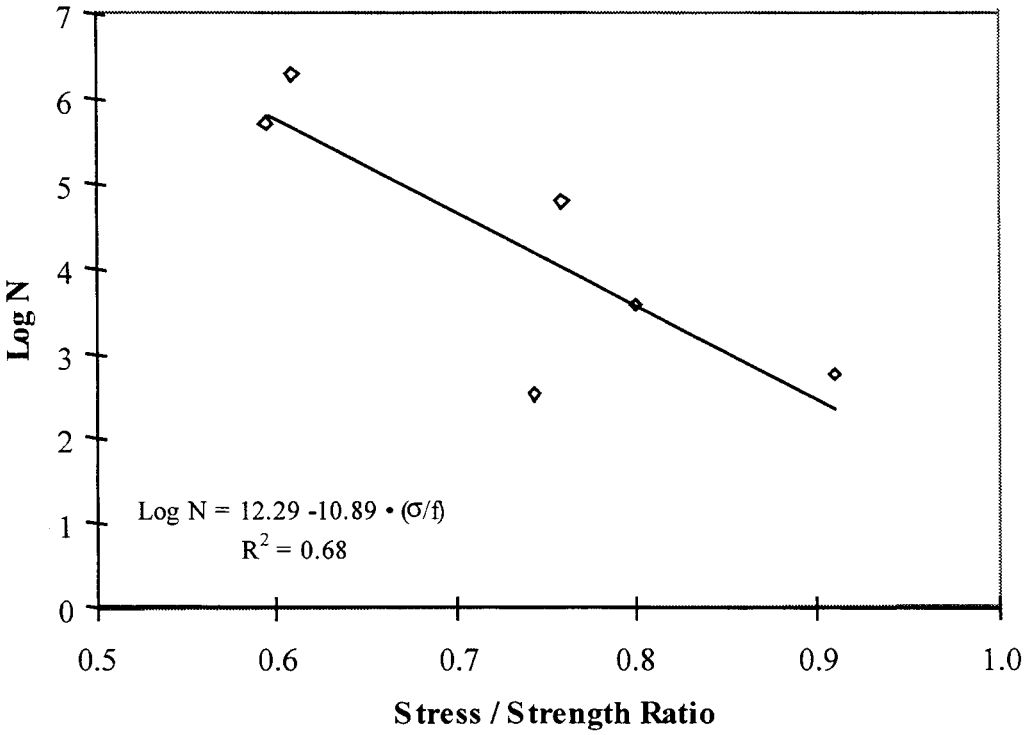

Figure 6.2. Fatigue Curve for RW17R/35L and TWL Concrete Cores.

$$\sigma_c = \frac{3P}{h^2}\left[1-\left(\frac{a_1}{l}\right)^{0.6}\right] \tag{6.12}$$

where:

P = load per tire (lb.)

h = pavement thickness (in)

a_1 = distance from tire centroid to pavement corner (in)

l = radius of relative stiffness (in) = $\sqrt[4]{\frac{Eh^3}{12(1-\mu^2)k}}$

where:

E = pavement modulus of elasticity (psi)
h = pavement thickness (in)
μ = Poisson's ratio
k = modulus of subgrade reaction (pci)

To calculate the stresses exerted on the pavement by each aircraft, the following values were used:

h = 17 in
a_1= f(tire contact area)
E = 4,000,000 psi
l = 50.88 in

Due to the many differences in configurations, a wide variety of stresses were found. The MD-11 was found to have the highest Westergaard corner stress. Its maximum takeoff weight is 600,000 pounds. Ninety-five percent of that weight (570,000) is assumed to be carried by the main gear. The MD-11 main gear consists of two dual tandem gears, each with four wheels, and a single dual gear in the middle. With ten wheels, the load per tire was found to be 57,000 pounds. With each tire having a contact area of nearly 300 square inches, the Westergaard pavement stress for the MD-11 was found to be 326 psi. As expected, commuter aircraft exhibit the lowest stress. The Shorts 330 has a Westergaard stress of only 50 psi. Table 6.9 shows Westergaard corner stresses for all aircraft serving DFW. Since the MD-11 creates the highest tensile stress in the pavement slab, it requires the greatest pavement thickness; thus it becomes the design aircraft.

SLAB49

The computer program SLAB49 was developed at The University of Texas in 1968 as a discrete element analysis program to analyze the stresses in a slab with a given applied load. The initial purpose of the SLAB49 analysis was to compare calculated deflections with those measured by the Rolling Dynamic Deflectometer. In addition to the RDD comparison, the stresses reported by SLAB49 can be compared to the results of the ELSYM-5 analysis, and can be used in the remaining life calculations in the next chapter. The SLAB49 program, however, is used primarily in this analysis to calculate the deflection near an applied load, while ELSYM-5 is used to calculate the stresses at different depths beneath the surface of the pavement.

TABLE 6.9 WESTERGAARD CORNER STRESS CALCULATIONS

Aircraft	Load/tire (lb.)	Tire pressure (psi)	Contact Area (in^2)	a (in)	al (in)	l (in)	stress (in)
F-100	21731	170	127.83	6.38	9.02	50.88	145.69
A320	34557	210	164.56	7.24	10.23	50.88	221.68
A340	32181	200	160.91	7.16	10.12	50.88	207.30
737-200	27431	200	137.16	6.61	9.34	50.88	181.75
737-300	32062	200	160.31	7.14	10.10	50.88	206.67
737-400	35625	190	187.50	7.73	10.92	50.88	222.89
737-500	31706	200	158.53	7.10	10.04	50.88	204.79
757-200	30281	140	216.29	8.30	11.73	50.88	183.99
767-200	37406	200	187.03	7.72	10.91	50.88	234.15
727-200	49756	195	255.16	9.01	12.74	50.88	291.43
747-F	41562	215	193.31	7.84	11.09	50.88	258.46
*ATR	9500	100	95.00	5.50	7.78	50.88	66.67
DC-10-10	42085	190	221.50	8.40	11.87	50.88	254.41
DC-8-F	41562	185	224.66	8.46	11.96	50.88	250.48
DC-9-50	28738	190	151.25	6.94	9.81	50.88	187.20
DC-9-30	26125	170	153.68	6.99	9.89	50.88	169.69
DC-9-10	21541	170	126.71	6.35	8.98	50.88	144.63
*Embraer 120	5938	100	59.38	4.35	6.15	50.88	44.30
*Jetstream J31	7226	150	48.17	3.92	5.54	50.88	55.19
L1011	55338	190	291.25	9.63	13.61	50.88	313.99
L1011-500	55338	180	307.43	9.89	13.99	50.88	309.73
MD-11	57000	202	282.18	9.48	13.40	50.88	325.96
MD80	35506	216	164.38	7.23	10.23	50.88	227.81
*Shorts 330	6412	150	42.75	3.69	5.22	50.88	49.59
*Swearingen Metro	3325	150	22.17	2.66	3.76	50.88	27.29

concrete thickness = 17"
K = 250
u = 0.15
E = 4,000,000 psi

* indicates commuter aircraft

Development of SLAB49 Analysis. The objective of this analysis involves the estimation of the modulus of subgrade support, or k-value, from deflection measurements taken from the RDD device, described in previous sections of this report. In order to accomplish this estimation, a range of k-values was selected, from 100 to 500 psi per inch (pci). These k-values were input, along with other properties of the concrete, into the SLAB49 program. In addition to the concrete properties, loading information was also used as input to the program. The load used

in the analysis was similar to that used on the RDD device, in order to simulate the deflections experienced by the RDD. For each k-value used, a deflection was calculated at every node on the discrete element mesh, and the one corresponding to the inline-centerline sensor was noted. Below is a chart showing the relationship of k-value to deflection. The deflection was measured at 20" from the source of the load.

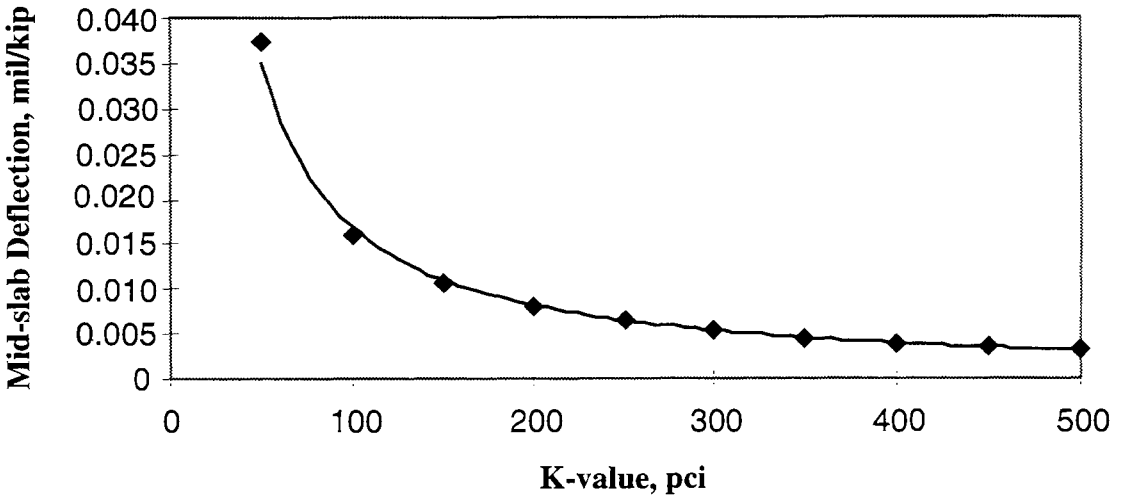

Figure 6.3. Relationship of Soil K-value to Deflection.

Analysis Results. From this chart, the measured deflection can be used to estimate the k-value of the subgrade at a particular location. The equation of the line in Figure 6.3 is:

$$\delta = 201.88 \bullet k^{-0.815} \tag{6.13}$$

where δ is the deflection at the inline-centerline sensor, and k is the modulus of subgrade reaction.

Although a plot of the k-value against distance along the runway will look similar to the deflection versus distance plot in the previous chapter, the general trend of the k-value over distance will be distinguishable. Ignoring the peaks in the plot, where edge conditions and joints have a much greater effect on the deflection, the estimated k-value at the midslab locations represent actual conditions more accurately. The plot shown in Figure 6.4 presents the estimated k-value along the centerline of Runway 17R/35L.

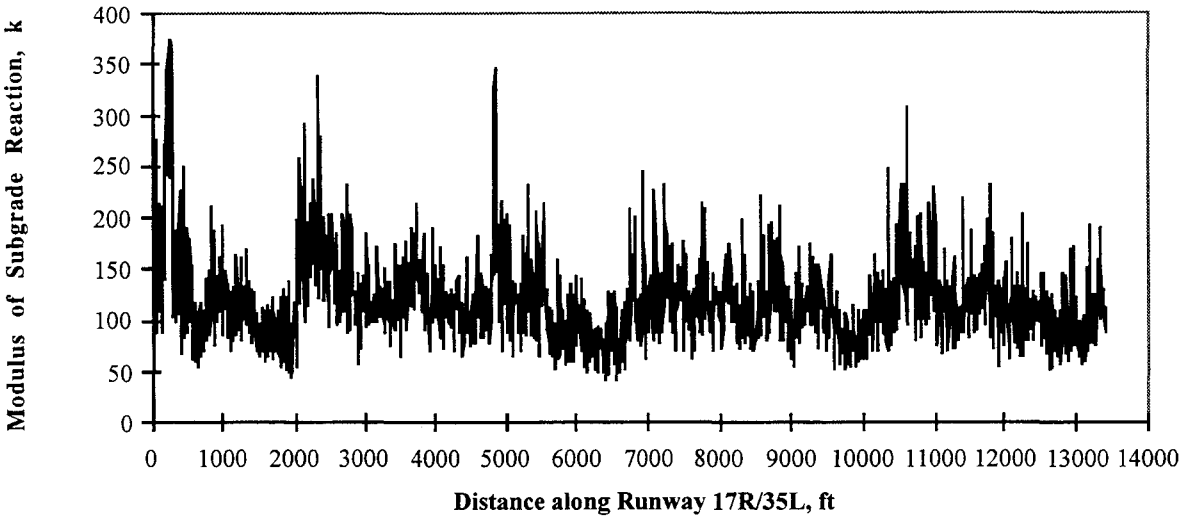

Figure 6.4. K-value along Runway 17R/35L.

As has been used several times in this report, the different levels of aircraft traffic on the different segments of the runway and taxiway give a range of distress levels from which to compare fatigue. In other words, a comparison of the north end of the runway with the south end, the north having experienced many more aircraft loads than the south, should give airport engineers an idea of how many loads the pavement system can take before the subsurface deteriorates to levels observed at the north end.

ELSYM-5

The computer program ELSYM-5 uses elastic theory to calculate the stresses and deformation in a layered system such as a concrete pavement. The analysis performed using this computer program utilized the layer properties obtained from crosshole testing. The deformation under a given load can be indicative of the relative remaining life of a pavement. For two pavement sections with identical layer thickness but different moduli of elasticity, the same load will cause different deflections. To obtain an idea of the relative damage done by loads that cause different deflections, the relative deflection is raised to the 4^{th} power. For example, twice the deflection will cause 16 times the damage. Or, if the deflection of one new pavement is twice that of the deflection of another new pavement of similar thickness, the expected life of the first will be 1/16 of the second.

Analysis Configuration. As mentioned, the layer thickness and properties were determined for two sections each of the runway and taxiway. These properties were input into the

ELSYM-5 program, and deflections at the bottom of the concrete slab were calculated. Figure 6.5 indicates the location of the calculated deformation in the pavement structure. The vertical deformation has been exaggerated to show detail. The horizontal stress that is induced in the slab bottom by the applied load was calculated by the program, and the results were analyzed in the manner described above.

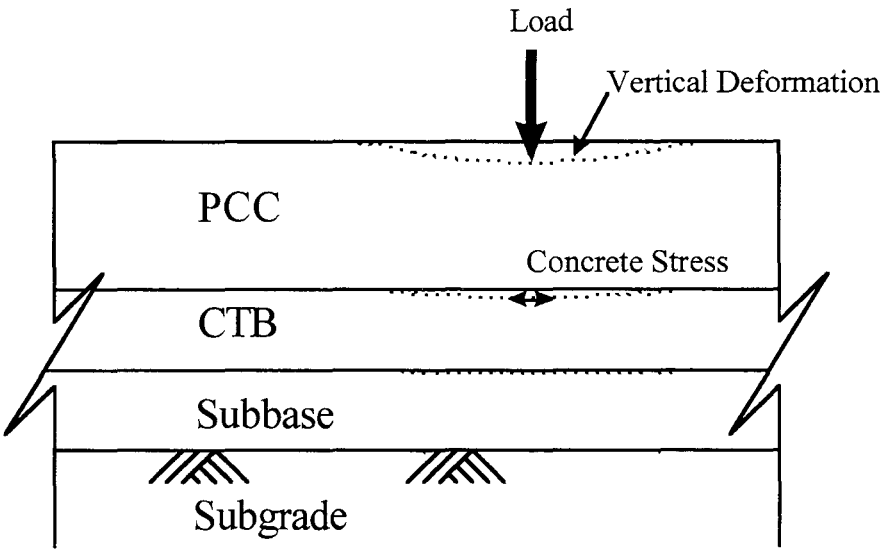

Figure 6.5. Applied Load, Calculated Vertical Deflection and Stress at Slab Bottom.

Using the properties of the soil and the other layers in the pavement system, a comparison was made between the pavement sections which had experienced many load applications with those that had not experienced as many. In this manner, an inference can be made as to the remaining life of the less damaged pavement when compared to the observed performance of the more damaged pavement.

Analysis Results. Using the results of the cross-hole testing performed on the runway, which are presented in Table 6.10, the results of the analysis provided some insight into the relative remaining life of the different pavement sections.

Using the fourth power rule, the stresses, or the strains, calculated from ELSYM-5 were used to estimate the remaining life of the pavement sections that have experienced years of aircraft traffic compared to those that have not. The non-trafficked areas are those to the side of the centerline of the runway, which experience very little, if any, aircraft traffic. The only loads applied to the non-trafficked areas are environmental, which are identical to the environmental

loads experienced by the trafficked areas, which provides a basis for comparison, since the only differences in the performance will be due to the difference in traffic loading.

TABLE 6.10. LAYER PROPERTIES OBTAINED FROM CROSS-HOLE TESTING

		Elastic Modulus, psi	
Depth, in	Material, Thickness, in	Trafficked	Non-trafficked
0 - 17	PCC, 17 in	4,812,000	6,224,000
17 - 26	Cement Treated Base, 9 in	1,055,000	1,305,000
26 - 35	Lime Treated Subbase, 9 in	205,000	286,000
> 35	Subgrade	43,000	65,000

If the remaining life of the untrafficked area of pavement can be assumed to be equal to the remaining life of the original design, the remaining life of the trafficked area can be estimated as a percentage of this original life. Using the result of the cross hole testing, as shown in Table 6.10 above, the trafficked area is determined to have a remaining life of 33 percent of the untrafficked area, or of the original life of the pavement. The manner in which this was determined will be discussed next.

Using an analysis similar to the fatigue 11 in this chapter, a damage equation was developed by researchers. The general form of the equation is as follows:

$$\left(\frac{\varepsilon_{non-traf}}{\varepsilon_{traf}}\right)^4 = \frac{N_{traf}}{N_{non-traf}} \tag{6.14}$$

Performing an analysis using the information in Table 6.10, the computer Program ELSYM5 provides the stresses, strains and deflections which are shown in Table 6.11.

TABLE 6.11. ELASTIC LAYER ANALYSIS USING RDD AND CROSS HOLE TEST RESULTS

	Trafficked	Untrafficked
Deflection, mil	3.42	2.43
Strain, in/in	10.41	7.90
Stress, psi	53.3	52.0

Using the ratio of these values, the untrafficked area has strains only about 76 percent of the strains of the trafficked area. The ratio taken to the fourth power, then, is about 33 percent when related to remaining life. This means that the trafficked area, or the keel section of the runway, has about 33 percent of the original life left.

CHAPTER 7. CONCLUSIONS ON REMAINING LIFE OF RUNWAY 17R/35L AND TAXIWAY L

CONCLUSIONS

1. The prediction of remaining life of Runway 17R/35L and Taxiway L are shown in Figure 7.1 for five different modes of failure. The most severe mode of potential failure is due to concrete fatigue. It is in the caution zone already as evidenced by the high degree of fatigue cracking on the north end of the runway and taxiway. It is predicted that concrete fatigue will become a dangerous problem in 2 to 3 years at the north end of both the runway and taxiway. As the fatigue continues, surface distress will become a problem as the longitudinal fatigue cracking observed becomes closer together and transverse cracking leads to block cracking and eventually punchouts. If the pavements were not steel reinforced, they would have reached failure already. The steel reinforcement is holding some of the crack widths small and preventing slabs breaking into pieces.

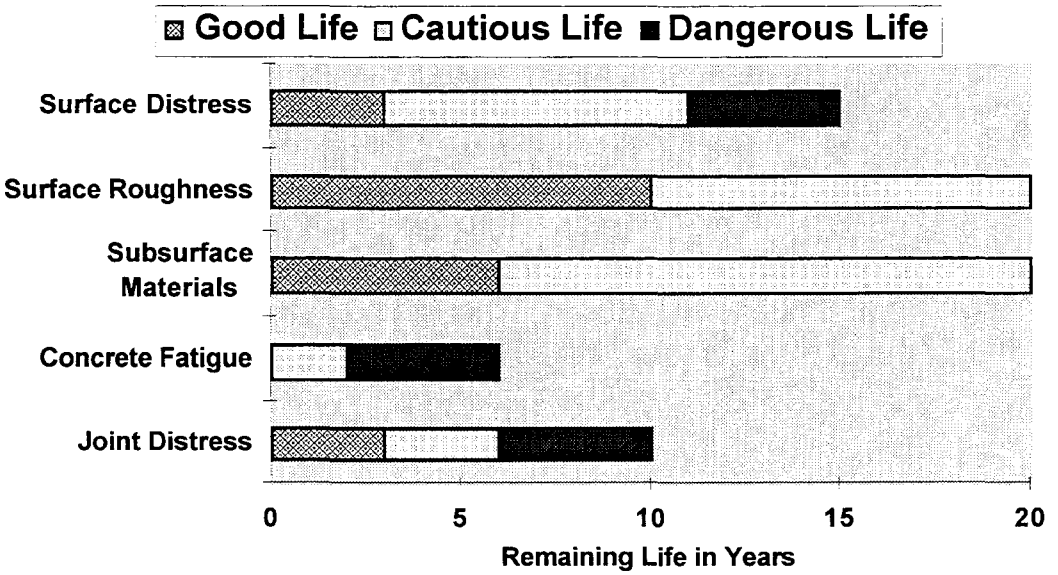

Figure 7.1. Remaining Life of Runway 17R/35L in years.

The middle section of the runway and the southern section of the runway and taxiway have shown a lesser degree of fatigue cracking and may have up to 8 years of life due to concrete fatigue. However, these pavement sections require careful inspection during this time. We

would recommend that specific control sections be maintained and inspected every 4-6 months for measurable signs of further deterioration.

2. Joint deterioration is not a problem now but the loss of load transfer efficiency observed from the RDD data and cross-hole testing indicates that most doweled joints are not performing well. The transverse sawed joints are performing much better than the doweled joints. However, the less than perfect load transfer from the sawed joints is an reaffirmation that the steel reinforcement was somewhat under-designed.

   Dr. B. Frank McCullough has determined from research performed much later than the initial construction, that the actual subgrade function is much higher than was estimated during the design. Therefore, either more steel is required or steps must be taken to reduce the subgrade friction in future designs.

3. The end result of the surface roughness analyses was that Runway 17R/35L and Taxiway L are within acceptable ride quality limits and produce no excessive vertical accelerations for the using aircraft. There is small hump at the south of end of Taxiway L which could be a factor if aircraft were taxiing in excess of 40 knots. Taxiway L should not be used for high speed taxiing or for emergency takeoffs or landing at the south end without a change in elevation profile.

4. We believe that the excellent runway profile of Runway 17R is a result of the attention paid to stabilizing the subgrade moisture before construction. After lime stabilization of the subgrade, Runway 17R was left unpaved for approximately one year to allow one season of weathering to reach equilibrium of shrinking and swelling. We believe that the surface roughness profile is remarkably smooth considering the traffic and swelling potential of the clay subgrade. Because of roughness concerns, we recommend the airport authority consider using the same subgrade construction practice used in the original construction of Runway 17R and Taxiway L for future construction.

5. There is a distinct pattern of corner spalling and joint spalling that has been repaired with very small patches (most less than 2 ft. long) which mostly occurs outside the trafficked portion of the runway. Much of this distress is associated with the free longitudinal joint restricted only with a keyway. Some of this corner spalling at 50 ft. intervals continues into Runway 17R extension which is only two years old. There will continue to be joint spalling even in the untrafficked slabs due to environmental forces. The longitudinal joint spalling may be a result of insufficient course aggregate in the corner of the slipform paver.

6. Subsurface deterioration could be a problem in the future. Figure 7.2 also shows the percent reduction in the runway and taxiway due to aircraft trafficking as measured by comparative cross-hole seismic testing. Cross-hole seismic testing indicated that the base and subgrade layers under the joints were approximately 50 percent lower in stiffness than those under the midslab. If the loss of stiffness of the total layer were compared to the untrafficked sections, it would theoretically account for 50 to 70 percent greater reduction in pavement life.

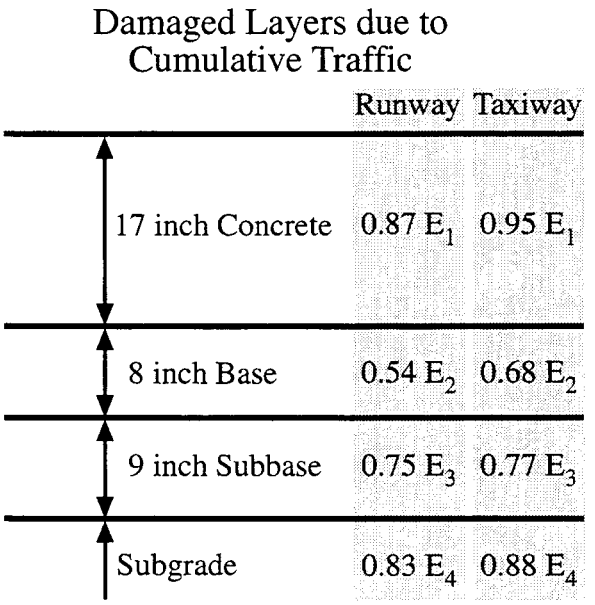

Figure 7.2. Loss of Stiffness in Layers

From the cross-hole seismic analysis the average in-situ modulus values where calculated for the runway and taxiway in certain locations both in the trafficked area and adjacent to the trafficked area. Comparison of the results shows that the loss of stiffness (reduction in modulus) is most pronounced in the cement treated base layer. As shown in Figure 7.2, both the runway and taxiway had reduced stiffness in all layers due to trafficking. This data represents midslab measurements and even greater reductions are evident in the subsurface layers when measured across a joint. The significance is that combined loss of stiffness for all layers results in higher stress due to load and therefore a reduced service life.

RECOMMENDATIONS FOR EVALUATING DFW AIRPORT PAVEMENTS

One of the objectives of this report is to make recommendations on how the remaining runways and taxiways should be evaluated. This research project employed a test plan which was based upon applying new technology developed for the highway sector that had not yet been applied to airport pavements. During the proposal phase, we suggested some testing which we later decided was not feasible or necessary. SASW testing was one proposed test that was abandoned because the thickness of the concrete pavements would not allow adequate information of the subsurface materials to be collected. The cross-hole seismic test was used to measure directly the required parameter. Dynamic Cone Penetrometer tests were also deemed not useful. The success of the RDD testing and the lack of success with the heavyweight deflectometer has lead us to conclude that future HWD testing would be pointless.

For the evaluation of the remaining runways and taxiways we recommend a two phase program of data collection and analysis as described in the following sections.

Data Collection

We recommend that a data collection effort be developed for all pavements that encompass the rolling dynamic deflectometer (RDD), cross-hole seismic testing, fatigue cracking inspection, and mapping of pavement distress. In areas where runway roughness is apparent, profilometer measurements should be obtained. In the following subsections a brief description is provided for the recommended testing.

Rolling Dynamic Deflectometer (RDD)

The use of the RDD for evaluating thick concrete pavement systems proved to be invaluable. Our initial test results on Runway 17R/35L were quite revealing, especially when comparing the new construction of Runway 17L/35R with the heavily trafficked Runway 17R/35L. Our findings indicate that the influence of the joint affects the deflection profile as much as 8 ft. away. As a result of our analysis, we would move our longitudinal test line closer to the center of the slab for future evaluations. We have only begun to fully appreciate the wealth of information that the RDD can provide for nondestructive analyses of airport pavements. We would strongly recommend that the RDD be used to evaluate the remaining runways and taxiways and aircraft parking aprons by collecting the following data:

1. Longitudinal deflection profiles along the runway or taxiway, one in the trafficked area and one in the non-trafficked area.

2. Many more transverse profiles based on areas of major differences derived from the longitudinal deflection profiles to better evaluate the relative effect that trafficking has had on the pavement.
3. The RDD be configured with sensors at several spacings to permit back calculations of layer moduli using a deflection basin.

Cores and Cross-hole Seismic Testing

Cross-hole seismic testing was very successful in the application to DFW airport pavements. Its use permitted detailed evaluations of the individual layers and the damage beneath joints. It may be feasible in the future to reduce the amount of cores which are taken and to rely more heavily on the cross-hole test. It is also possible that these results may be compared with the RDD results so that fewer cross-hole seismic tests will be need to be performed. We would, however, recommend that a limited number of cores be taken and some cross-hole seismic tests be conducted for each major area of the airport. The cross-hole testing locations should be determined after a review of the deflection data. The cross-hole locations would be selected using the following guidelines:

1. A set of cross-holes would be located in the wheel path and in a non-trafficked area along the same transverse line.
2. Several sets would be located longitudinally along the runway at areas of highest and lowest deflections as well as in any other unusual areas.

Fatigue Cracking Inspection

The results of the analysis is that concrete fatigue is the critical mode of failure of Runway 17R/35L and Taxiway L. We would expect this to be consistent with the remaining runways and taxiways. The PCI method of distress identification and recording is not sensitive to fatigue cracking for analysis of remaining life. Therefore we would recommend changing the PCI method for future inspections. The change needs to be formally defined, but in the absence of a better standard, the procedures developed for this project have proven adequate.

Fatigue cracking will present the most significant inspection problem for operations and maintenance personnel for Runway 17R/35L and Taxiway L. Currently the north half of the runway has slabs with more than five cracks extending the length of the slab. In the future, as cracking becomes more closely spaced, transverse cracking will occur between the longitudinal cracks, and eventually punchouts may result. Fortunately, the increased design slab thickness of

17 in. over the original FAA recommended thickness of 14 in. has extended the expected 20 year life and the steel reinforcement is keeping the fatigue crack widths small. Without reinforcement, the concrete would most probably already have failed due to punchouts.

Mapping of Pavement Distress and Test Data

We would recommend a method of fatigue cracking inspection which records in a graphical format all cracking that was found. We would suggest the development of a MicroStation based database of cracking, patching and other distress that can be updated in the field from daily inspections rather than using either the videotape system or hiring a consultant every five years. The University of Texas has proposed the development of a differentially corrected global positioning system (D-GPS) for field use in Operations and Maintenance vehicles to collect this information. A proposal was submitted to the Airport in June 1996 but has not yet been approved.

DATA ANALYSIS

The data collected will be analyzed to develop the following output from a network planning and design guidelines standpoint.

Network Planning

1. A plan of predicted times including when deterioration will start, approach failure, and require major repair will be developed for each runway and taxiway.
2. The information from item 1 will be compiled for a twenty year projected plan of major rehabilitation for all pavements on the airside of the airport.
3. The plan can be periodically updated.

Design Guidelines

1. The load transfer capabilities of all joints will be ascertained along with the deterioration rates. This information can be used to revise the design details.
2. Determination of the proper amount of longitudinal and transverse reinforcement to provide 100 percent level transfer as originally intended.
3. Longitudinal joints that provide excellent load transfer, thus eliminating the problems being experienced at some longitudinal joints.

REFERENCES

1. Gervais, Edward L., "Runway Roughness Measurement, Quantification and Application; The Boeing Approach," *Aircraft/Pavement Interaction - An Integrated System,* Conference Proceedings, ASCE, September 4-6, 1991, Edited by Paul Foxworthy, pp. 121-131.
2. Nair, Sukumar K., W. Ronald Hudson, and Clyde E. Lee, "Realistic Pavement Serviceability Equations Using the 690D Surface Dynamics Profilometer," Research Report 354-1F, Center for Transportation Research, The University of Texas at Austin, August, 1985.
3. Richart, Jr., F., E., R.D. Woods and J.R. Hall, Jr. (1970), "Vibrations of Soils and Foundations," Prentice-Hall, pp. 414.
4. Graff, K.I. (1975), "Wave Motion in Elastic Solids," Ohio State University Press, Columbus, Ohio.
5. Yimprasert, P., and B. Frank McCullough, "Fatigue and Stress Analysis for Modifying the Rigid Pavement Design System," Center for Highway Research, CFHR Report 123-16, Austin, Texas, 1973.